POTENTIAL OF THE OSTEOCLAST'S PROTON PUMP AS A DRUG TARGET IN OSTEOPOROSIS

by

Jonas Nyman

From the Department of Cell Biology and Anatomy, Institute of Biomedicine, University of Turku, Turku, Finland, and the Drug Discovery Graduate School

Supervised by
Professor Kalervo Väänänen, M.D., Ph.D.
Department of Cell Biology and Anatomy
Institute of Biomedicine
University of Turku
Turku, Finland

Reviewed by
Professor Juha Tuukkanen, D.D.S., Ph.D.
Department of Anatomy and Cell Biology
Institute of Biomedicine
University of Oulu
Oulu, Finland

and

Professor Karl Åkerman, M.D., Ph.D.
Department of Physiology
Institute of Biomedicine
University of Helsinki
Helsinki, Finland

Opponent:
Professor Seppo Parkkila, M.D., Ph.D.
Department of Anatomy
School of Medicine
University of Tampere
Tampere, Finland

To Ester and Matias

Jonas Nyman
POTENTIAL OF THE OSTEOCLAST'S PROTON PUMP AS A DRUG TARGET IN OSTEOPOROSIS
Institute of Biomedicine, Department of Cell Biology and Anatomy, University of Turku
Annales Universitatis Turkuensis, Medica-Odontologica, Turku, Finland, 2011

ABSTRACT

Decreasing bone mass during aging predisposes to fractures and it is estimated that every second woman and one in five men will suffer osteoporotic fractures during their lifetime. Bone is an adaptive tissue undergoing continuous remodeling in response to physical and metabolic stimuli. Bone mass decreases through a net negative balance in the bone remodeling process of bone, in which the new bone incompletely replaces the resorbed bone mass. Bone resorption is carried out by the osteoclasts; the bone mineral is solubilized by acidification and the organic matrix is subsequently degraded by proteases. Several classes of drugs are available for prevention of osteoporotic fractures. They act by different mechanisms to increase bone mass, and some of them act mainly as antiresorptives by inhibition of osteoclast formation or their function.

Optimally, a drug should act selectively on a specific process, since other processes affected usually result in adverse effects. The purpose of this study was to evaluate whether the osteoclastic vacuolar adenosine trisphosphatases (V-ATPase), which drives the solubilization of bone mineral, can be selectively inhibited despite its ubiquitous cellular functions. The V-ATPase is a multimeric protein composed of 13 subunits of which six possesses two or more isoforms. Selectivity for the osteoclastic V-ATPase could be provided if it has some structural uniqueness, such as a unique isoform combination. The a3 isoform of the 116kDa subunit is inevitable for bone resorption; however, it is also present in, and mainly limited to, the lysosomes of other cells. No evidence of a structural uniqueness of the osteoclastic V-ATPase compared to the lysosomal V-ATPase was found, although this can not yet be excluded. Thus, an inhibitor selective for the a3 isoform would target the lysosomal V-ATPase as well. However, the results suggest that selectivity for bone resorption over lysosomal function can be obtained by two other mechanisms, suggesting that isoform a3 is a valid target. The first is differential compensation; bone resorption depends on the high level of a3 expression, and is not compensated for by other isoforms, while the lower level of a3 in lysosomes of other cells may be partly compensated for. The second mechanism is because the bone resorption process itself is fundamentally different from lysosomal acidification because of the chemistry of bone dissolution and the anatomy of the resorbing osteoclast. By this mechanism, full inhibition of bone resorption is obtained with more than tenfold lower inhibitor concentration than those needed to fully inhibit lysosomal acidification. The two mechanisms are additive.

Based on the results, we suggest that bone resorption can be selectively inhibited if V-ATPase inhibitors that are sufficiently selective for the a3 isoform over the other isoforms are developed.

Keywords: osteoclast, V-ATPase, osteoporosis, drug target

Jonas Nyman
OSTEOKLASTIN VAKUOLAARINEN PROTONIPUMPPU OSTEOPOROOSILÄÄKEKEHITYKSEN KOHTEENA
Biolääketieteen laitos, Solubiologia ja Anatomia, Turun Yliopisto

YHTEENVETO

Ikääntymisen myötä luukudoksen määrä vähenee, minkä seurauksena luusto altistuu murtumille. On arvioitu, että noin puolet naisista ja viidennes miehistä saa osteoporoottisia luunmurtumia. Luun mikrorakenne muuttuu jatkuvasti muun muassa siihen kohdistuvan rasituksen mukaan. Osteoklastit hajottavat luuta ja osteoblastit muodostavat tilalle uudisluuta. Luumassa vähenee saman mekanismin kautta, mutta tällöin uudisluun kokonaismäärä on jatkuvasti pienempi kuin hajoitetun luun kokonaismäärä. Osteoklastit hajottavat luuta erittämällä luun mineraaliainesta liuottavaa happoa sekä orgaanista ainesta hajottavia proteaaseja luun pinnalle.

Osteoporoosiin liittyvän murtumariskin pienentämiseen on käytettävissä vaikutus-mekanismeiltaan erilaisia lääkkeitä, jotka kaikki lisäävät luumassaa. Osa lääkkeistä vaikuttaa pääsosin estämällä osteoklastien muodostumista tai niiden toimintaa. Vaikka useita lääkkeitä luukatoon on olemassa, tavoitellaan yhä parempia lääkkeitä. Hyvä lääkeaine on riittävän selektiivinen, jolloin sen vaikutus rajoittuu tietyn solun tai proteiiniin toimintaan ja haittavaikutukset vähenevät.

Tässä tutkimuksessa tarkasteltiin osteoklastin vakuolaarisen adenosiinitrisfosfataasi-entsyymin (V-ATPaasi) soveltuvuutta lääkekehityksen kohteeksi. Tällä entsyymillä osteoklasti erittää happoa, joka liuottaa luun mineraliaineksen. Työssä tarkasteltiin, onko sen selektiivinen estäminen mahdollista siitä huolimatta, että V-ATPaaseja tarvitaan kaikissa soluissa. Entsyymi koostuu kolmestatoista alayksiköstä, joista kuudesta on olemassa isoformeja. Osteoklastin V-ATPaasin selektiivinen estäminen olisi mahdollista jos sen isoformikoostumus olisi ainutlaatuinen. 116 kDa alayksikön isoformeista yksi, a3, on välttämätön luun hajotukselle, mutta se ei vaikuta solujen elinkykyyn. Tätä isoformia löytyy myös muiden solujen lysosomeista. Tutkimuksessa ei löydetty viitteitä siitä, että osteoklastin V-ATPaasi eroaisi lysosomalisesta V-ATPaasista. Näin ollen a3-selektiivinen inhibiittori estäisi myös lysosomalista V-ATPaasia. Tutkimuksen perusteella luun hajotus voi kuitenkin olla lysosomien toimintaa herkempi inhibiitoreille ainakin kahden eri mekanismin kautta.

Ensimmäinen mekanismi perustuu isoformien kompensaatioon, eli kykyyn korvata estetyn isoformin toimintaa. Luun hajotus on riippuvainen osteoklastin korkeasta a3-tasosta, jolloin kompensaatio on riittämätön, kun taas lysosomikalvon matalampi a3-taso mahdollistaa riittävän kompensaation lysosomalisen toiminnan ylläpitämiseen. Toinen mekanismi perustuu siihen, että matalan pH:n ylläpitämimen lysosomeissa ja luun hajotus ovat kemiallisesti hyvin erilaisia toimintoja luun mineralin liukoisuudesta ja luuta hajottavan osteoklastin anatomiasta johtuen. Siksi luun hajotuksen täydelliseen estoon tarvitaan vain kymmenesosan siitä V-ATPaasin inhibiitorikonsentraatiosta, jolla lysosomien happamoittuminen pystytään estämään täysin.

Tulosten perusteella luun hajotusta pystyttäisiin selektiivisesti estämään kehittämällä riittävän a3-selektiivisiä V-ATPaasi inhibiittoreita.

Avainsanat: osteoklasti, V-ATPaasi, osteoporoosi, lääkekohde

TABLE OF CONTENTS

ABBREVIATIONS

BMD   bone mineral density
BMI   body mass index
BMU   basic multicellular unit
CaR   calcium-sensing receptor
ClC7   chloride channel 7
CTX   carboxy-terminal cross-linked telopeptide of type I collagen
DMSO   dimethylsulphoxide
EMA   European Medicines Agency
FDA   Food and Drug Administration (in the United States)
HEPES   4-(2-hydroxyethyl)-1-piperazineethanesulfonic acid
HRT   hormone replacement therapy
IAP   ionic activity product
IP   ionic concentration product
LAMP   lysosome-associated membrane protein
OPG   osteoprotegerin
PTH   parathyroid hormone
RANK   receptor activator of nuclear factor kappa B
RANKL   ligand for receptor activator of nuclear factor kappa B
SERM   selective estrogen receptor modulator
siRNA   small interfering ribonucleic acid
V-ATPase vacuolar H^+ adenosinetrisphosphatase

LIST OF ORIGINAL PUBLICATIONS

This thesis is based on the following articles, which are referred to in the text by the Roman numerals (I-IV)

I   Hu Y, Nyman J, Muhonen P, Väänänen HK, Laitala-Leinonen T. (2005) Inhibition of the osteoclast V-ATPase by small interfering RNAs. **FEBS Lett.** 579:4937-42.

II   Nyman JK and Väänänen HK. (2010) A rationale for osteoclast selectivity of inhibiting the lysosomal V-ATPase a3 isoform. **Calcif Tissue Int.** 87:273-83.

III   Nyman JK and Väänänen HK. The unique anatomy and function of the resorbing osteoclast render bone resorption hypersensitive to V-ATPase inhibition. **Submitted manuscript.**

IV   Dixon N, Páli T, Kee TP, Ball S, Harrison MA, Findlay JB, Nyman J, Väänänen K, Finbow ME, Marsh D. (2008) Interaction of spin-labeled inhibitors of the vacuolar H+-ATPase with the transmembrane Vo-sector. **Biophys J.** 94:506-14.

The original publications have been reproduced with the permission of the copyright holders

1   INTRODUCTION

Bone loss starts in the early midlife and continues throughout life, it affects everybody and may thus be considered a natural process of aging. In addition, bone loss may be secondary to other diseases and their medication. It is well established that loss of bone tissue increases the susceptibility to fractures; therefore its prevention by medication is well justified. Several drugs that increase bone mass exist and these clearly reduce the number of fractures. On the other hand, bone mass is clearly affected by lifestyle choices, and most osteoporotic fractures are caused by falls, so reducing the number of falls among the elderly is clearly another option to reduce fractures.

The mechanism by which bone mass is reduced is fairly well understood. Bone loss occurs through remodeling by basic multicellular units, in which osteoclasts resorb a small volume of bone tissue, which osteoblasts subsequently fill with new bone. Bone is lost when the new bone incompletely replaces the bone mass resorbed. Osteoclasts resorb bone mineral by acididifying the surface of the bone, and this process is dependent on the vacuolar ATPase, a multisubunit protein that acidifies many other organelles. The aim of this study was to determine whether the osteoclast V-ATPase and thus bone resorption can be selectively inhibited.

A few words about the structure of the thesis may be in place, and especially how the review of the literature is written. I tried to put special emphasis on putting this work into its context. In the first place, I think of this work as a target validation, an early phase of drug development, against bone loss. In fact, it is more of a re-validation, since the V-ATPase was recognized as target for inhibiting bone loss more than 20 years ago, and inhibitors that are effective in pre-clinical models of osteoporosis were published already 10 years ago.

Another part of the context is that several good drugs exist. Any potential new drug will be compared against the existing ones with respect to efficacy and adverse effects. These drugs act on different components on the bone remodeling unit. I therefore found it relevant to include rather short chapters of the mechanisms of actions of these drugs, together with the efficacies to indicate what is expected from a new drug. I also included one section in the discussion about how a potential V-ATPase inhibitor would be similar or dissimilar to the existing osteoporosis drugs.

Having read some of Harold Frost's publications, I think that the principles of biomechanics of bone must be included. I believe that most of the bone loss can be explained by adaptation to the decreased use of bone upon aging, rather than some disease process *per se*. Finally, to make this thesis easy to read, I tried to avoid sticking it full with details, and some topics are overviewed rather than reviewed.

2   REVIEW OF THE LITERATURE

2.1   BONE TISSUE

2.1.1   *Overview of bone structure and function*

The skeleton, consisting of 206 bones in adults, confers rigidity to the body and together with the muscles it forms the locomotor system, protects many organs and serves as a reservoir of minerals. Each bone, or pair of bones, is unique regarding anatomical structure (i.e. shape, articulations and muscle insertions) and function. For instance, the long bones of the appendicular skeleton act as lever arms, while the long bones of the legs are in addition weight bearing. The tarsal bones in the foot act as a unit that together with the metatarsal bones forms the transverse and longitudinal arches of the foot. The arches act as shock absorbers allowing distribution of the downward forces during walking on uneven ground. The main function of the bones of the scull is to protect the brain while the spinal cord is protected by the spinal canal formed by the vertebral bones, the bodies of which also are weight bearing.

Bone tissue can be **macroscopically** divided into compact and cancellous, or trabecular, bone. All bones have a cortex of compact bone with varying amounts of cancellous bone inside. Compact and trabecular bone are strategically distributed within bones in a way that they accommodate the loads encountered. Long weight-bearing bones, such as the femur and tibia, have thick cortices composed of compact bone and lack cancellous bone in their diaphyses, i.e. middle parts. The cancellous bone in such bones is limited to the epiphyses where it appears to distribute the loads and forces from the joints to the cortical bone (Figure 1).

Figure 1. Illustration showing the distribution of cortical and trabecular bone in the femur.

The vertebral bodies resist axial compression within a limited angle, have thin cortices with a tight network of trabeculae inside, which constitutes up to 75% of the total bone mass of a vertebral body. Although referred to as spongy, the plates and rods of bone tissue that constitute trabecular bone, are not randomly arranged, but provide an architecture that apparently best resists the forces it encounters. This is evident from analysis of the microarchitecture of the talus, the bone in the foot through which weight-bearing load is distributed to the heel and the arches of the foot (Pal and Routal 1998). Likewise, in the vertebral bodies, the trabeculae in the direction of the axial load are thicker, and more numerous, than the trabeculi in the transverse or horizontal planes. Cortical bone is most prominent in the diaphyses of long bones where the forces conduct primarily unidirectionally. Trabecular bone appears to be favored close to the joints, where

it transmits and distributes the load applied on the joint to the cortical bone (in the case of long bones) or to the other joint (for instance in the vertebral bodies).

At the **microscopical** level, several differences and similarities between compact and trabecular bone are evident. The compact bone contains entities called osteons, composed of concentric lamellae, with blood vessels in their central channel, the Haversian canals. In the long weight-bearing bones, the osteons run in longitudinal direction. Typically, the osteons are 200-250 µm in diameter, and contain 7-8 concentric lamellae. Comparisons between species revealed that osteon size scales with body size up to about the size of 10 kg after which it remains stable around the size seen in humans (Jowsey 1966). Volkman's canals run perpendicular to the osteons and connect neighbouring Haversian canals, allowing connections of blood vessels. In addition to Haversian and Volkman's canals, bone also contains a minute but extensive channel system composed of lacuna and canaliculi, of sufficient size to encompass resident bone cells and their processes, respectively, and a small volume of interstitial fluid. Trabecular bone is also lamellar, but the lamelli do not form osteons. Accordingly, trabecular bone lacks internal blood vessels but contain osteocytes inside the lacunae and canaliculi. The trabeculi, which have an average thickness of 120-140 µm, and the endocortex are lined by bone marrow, while a fibrous sheet containing fibroblastic cells with the capacity to develop into osteoblasts covers the periosteum.

Chemically, bone is composed of 25% organic matrix, including 2-5% cells, 5% water, and 70% inorganic mineral. Type 1 collagen is the main protein in bone, it constitutes up to 90% of the protein contents of bone. Molecules of type 1 collagen are composed of two α1 chains and one α2 chain coiled around each other, and collagen molecules assemble parallel to each other to form collagen fibrils. The lamellar appearance of osteons comes from the periodic spiral arrangement of collagen fibrils. Within a lamelli, the innermost layers of fibrils run in the direction of the osteon axis and subsequent fibril layers are gradually more tilted to reach some 60º (Wagermaier *et al.* 2006). Collagen fibrils have great tensile strength but little resistance to compressive and shear forces. The mineral component of bone provides the mechanical rigidity and resistance to compression. In addition to type I collagen, small amounts of other collagens are also present in bone. The non-collagenous proteins in bone is usually subdivided into four groups; proteoglycans, glycoproteins containing RGD-motifs, non-RGD-containing glycoproteins, and gammacarboxylated proteins. Some examples of these are introduced later.

Bone mineral is present in the form of plate-like crystals, 20-80 nm in length and 2-5 nm thick. The main component is hydroxyapatite, however, carbonate is present at about 5% (weight percent), and the mineral contains small amounts of sodium and divalent cations such as magnesium, strontium and cadmium. Compared to pure hydroxyapatite crystals, the crystals in bone are smaller and more soluble. The precise localization of the crystals with respect to the collagen fibrils is not known. However, during mineralization, the first crystals are formed in the gap-regions of end-to-end aligned collagen molecules in a fibril, and subsequently most of the interfibrillar space is filled with crystals (Rey et al. 2009). The detailed mechanism for mineralization of the extracellular matrix is unknown; the theories are presented in chapter 2.2.6.

2.1.2   *Solubility of bone hydroxyapatite*

In order to meet up with the functional roles of the skeleton, the mineral crystals deposited in the bone should be stable in the organism and dissolvable only in a controllable fashion. The hydroxyapatite crystals fulfill this criterion; they are sparingly soluble in the solution that surrounds them, because the solution is supersaturated with respect to the ions that comprise the mineral. Because it is essential to the thesis, the chemical basis of the stability of calcium hydroxyapatite in physiological conditions is overviewed, and the chemical principle of its dissolution in acid pH is described. This includes the concepts of **solubility product constant** and the **ionic product**.

The solubilization of bone crystals in water is a thermodynamic process that obeys the laws of mass action. When a solid compound, such as bone hydroxyapatite, dissolves in water, there is a limit how much can be dissolved. This is the thermodynamic equilibrium between the solid and liquid phase. The solubility product constant describes the concentrations of the constituent ions at which the solid is in equilibrium with the liquid and indicates the degree to which a compound dissociates in water. In principle, the solubility product constants can be empirically determined, but for bone mineral, it is clear that no single solubility product constant can describe its solubility behavior, however, the approximate values reported, $2,3 \times 10^{-55}$ are about 10^4 times higher than for pure hydroxyapatite (Brown 1976; Baig et al. 1999).

In water, calcium hydroxyapatite dissolves into its constituent ions:

$$\left[Ca_5(PO_4)_3OH\right]_{SOLID} \rightarrow 5(Ca^{2+}) + 3(PO_4^{3-}) + (OH^-)$$

The ionic product for hydroxyapatite (IP_{HAP}) is:

$$IP_{HAP} = (Ca^{2+})^5 (PO_4^{3-})^3 (OH^-)$$

Correctly, in describing the solubility characteristics, one should use the ionic activity product (IAP_{HAP}):

$$IAP_{HAP} = (a_{Ca})^5 (a_{PO_4})^3 (a_{OH})$$

in which *a* denotes activity of the ions in solution. Ionic activity is a dimensionless quantity, not identical to the ionic concentration, but in addition dependent on some other factors, such as the presence of other ions. However, to describe the principle of bone dissolution by acid, I use IP_{HAP} here analogously to IAP_{HAP}.

In practical terms, for the dissolution of hydroxyapatite the concentration of Ca^{2+}, phosphate and hydroxyl ions in solution need to be low enough, so that the product of their concentrations is less than the solubility product constant. If the ionic product is higher than the solubility constant, the solution is supersaturated and mineral crystals will not dissolve, but they can potentially grow.

By homeostatic mechanisms, the pH and the Ca^{2+} and phosphate levels in the interstitial fluid are kept relatively stable. The reference levels for both inorganic phosphate and free Ca^{2+} in plasma is 1 mM and the interstitial fluid concentrations are considered similar. However, phosphate is a triprotic acid that is present in four molecular species, of which

the important phosphate ion species is the PO_4^{3-} ion. The pKa values for the protonation reactions are 12.2, 7.2 and 2.1. Because of the buffer system, the PO_4^{3-} ion constitutes only a small fraction of the total phosphate at physiological pH.

The concentration of the phosphate ion species at a given pH can be calculated from the Henderson-Hasselbalch equation, here the molar fractions of PO_4^{3-} were obtained from a table (CurTiPot freeware).

At pH 7.2, the molar fraction of PO_4^{3-} is $10^{-5.45}$, and at pH 5.2 it is $10^{-9.15}$. Accordingly, if the total phosphate ion concentration is 1 mM (0.001 M) the concentration of PO_4^{3-} is 10^{-3} M x $10^{-5.45}= 10^{-8.45}$ M (~3.5 nM), and at pH 5.2, analogously, $10^{-12.15}$ M (~0.7 pM).

At pH 7.2, the IP_{HAP} in 1 mM calcium and 1 mM phosphate is thus:

$$(10^{-3})^5 \times (10^{-8,45})^3 \times (10^{-6,8}) = 10^{-47,15}$$

which is considerably higher than the approximate bone hydroxyapatite solubility constants reported. Thus in physiological conditions, plasma and interstitial fluid is supersaturated with respect to the bone mineral ions.

Let us consider what happens to the IP_{HAP} if the pH decreases to 5.2, a pH value easily reached in lysosomes. At pH 5.2 the concentration of OH^- is decreased to $10^{-8.8}$ M and the concentration of PO_4^{3-} is $10^{-12.15}$ M. The IP_{HAP} is then

$$(10^{-3})^5 \times (10^{-12.15})^3 \times (10^{-8.8}) = 10^{-60.25}$$

This is significantly less than the solubility constant for bone hydroxyapatite and bone mineral can dissolve.

Thus, in summary, the bone mineral crystals in bone are stable in physiological conditions, because the interstitial fluid is supersaturated with respect to the constituent ions of bone mineral. By reducing the pH, the concentrations of the OH^- and PO_4^{3-} ions decrease so that the IAP_{HAP} of the hydroxyapatite constituent ions can be less than the solubility product constant of bone hydroxyapatite allowing bone to be dissolved. A practical consequence is that there is a pH-threshold, or a critical pH value, which must be reached before bone mineral can be dissolved.

2.1.3 Bone cells

The bone cells include four histologically different cell-types (Figure 2). Osteoclasts are of hematopoietic origin, while osteoblasts, osteocytes and bone lining cells are of mesenchymal origin.
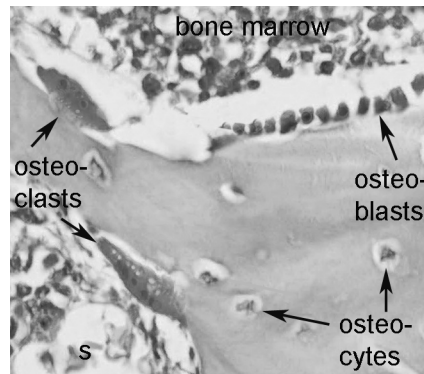
Figure 2. Micrograph of a histologic section showing two osteoclasts and a row of osteoblasts on the surface of trabecular bone. Osteocytes are visible inside lacuna. Bone lining cells are not present in this image. A sinusoid (s) containing erythrocytes is visible.

Osteoclasts are multinucleated cells formed by the fusion of mononuclear precursors. They resorb bone. Bone lining cells are flat cells on the endocortical and trabecular surface of bone that is not undergoing turnover. Many consider them simply nonactive osteoblasts. Osteoblasts are actively bone-forming cells that are cuboid or polyhedral in shape. They synthesize bone by laying down osteoid, the organic component of bone, which subsequently mineralizes. During bone formation, a fraction of the osteoblasts become embedded in bone and become osteocytes. Osteocytes are the most abundant cell-type. The cell bodies reside in lacunas and they possess extensive cell processes that radiate out from the lacuna in canaliculi. Osteocytes in human cortical bone have some 20-100 of these processes (Beno *et al.* 2006). Through gap junctions in the processes, the cytoplasm of neighboring osteocytes are in contact (Doty 1981; Taylor *et al.* 2007). Thus, osteocytes constitute a true syncytium, i.e. network of connected interacting cells.

Together, the bone cells are responsible for the modeling and remodeling of bone, the reshaping of bone during growth, and the adaptation of bone structure to increased or decreased load.

2.2   BONE AS AN ADAPTIVE ORGAN

Bone has the capacity to adapt to the load it encounters. During the evolution, bone strength may have been optimized to withstand voluntary physical load without fracturing. In addition to being rigid, bone tissue is also heavy, so excess bone mass may have been evolutionary unfavorable by increasing energy expenditure and reducing running speed. Thus, the evolutionary pressure may have been to use a minimal amount of bone tissue to achieve sufficient bone strength.

When a load or force applies to bone, the bone will deform, and the amount of deformation relative to the original length is the bone strain. The three types of deformation or strain, into which all forces can be resolved, are compressive, tensile and shear (Rubin 1999). In practice, any skeletal muscular activity will produce a complex combination of strains on the bones involved. For instance, long bones acting as lever arms will experience tension at one side of the bone and compression at the other side. Vigorous exercise cause 0.35% strain in compression, while two-fold higher strain will cause material damage (i.e. microcracks in bone). The notation that peak strains are very

similar across a spectrum of vertebrates, ranging from turkeys (7 kg) to elephants (2500 kg), suggests that the adaptation of bones is linked to the peak strain (Rubin and Lanyon 1984).

In addition to the intrinsic (material) properties of bone and bone mass, bone strength is highly determined by the bone geometry. Important geometrical parameters include the long-bone curvature, and the perimeter and shape of the cross-sectional area (Rubin 1999). In the case of hollow tube-like bones, resistance to bending and torsion increases if the diameter of the tube increases.

Adaptation of the bone architecture and mass is observable in, for instance, individuals subjected to ”vigorous” use of bones and in bone disuse. For instance, professional male soccer players of a first division team had 18% higher bone mineral content than age- and body mass index (BMI)-matched controls performing less than 3 hours of recreational sport activities per week (Wittich *et al.* 1998). The difference was due to both a 5.2% increase in bone size and a 12.3% increase in bone mineral density (BMD) in the bones of the legs and pelvis. On the other extreme, disuse of bone caused by spinal cord injury-mediated paralysis cause rapid bone loss; the BMD of the epiphyses of the femur and tibia decreased 50% and 60%, respectively, while the BMD of the femoral and tibial diaphyses decreased 35% and 25%, respectively (Eser *et al.* 2004).

Bones that act as lever arms have to resist the combined action of gravity and muscle force. Muscle forces generate the largest loads on such bones. It is becoming evident that lean mass is associated with bone strength parameters of the proximal femur, while BMI and fat mass is not associated after controlling for lean mass (Travison *et al.* 2008). In the adaptation of bone, two processes, bone modeling and bone remodeling are distinguishable and introduced next.

2.2.1   *Bone modeling and remodeling*

Bones grow in diameter by appositional growth. This is referred to as modeling, in which bone is added to an existing structure. In remodeling, bone resorption and formation are spatiotemporally coupled so that bone formation always follows bone resorption. Remodeling of bone takes place on the trabecular and endocortical surfaces, and to a lesser extent, intracortically. In intracortical remodeling, new osteons replace the old bone. In addition, microfractures in cortical bone heal by remodeling. The remodeling cycle occurs continuously at distinct sites throughout the skeleton in response to mechanical and metabolic influences, so that in healthy adults, up to 10% of the bone mass is remodeled annually. At any time, some 15% of the cancellous bone surface remodels. The remodeling cycle commences with osteoclast formation, followed by osteoclast-mediated bone resorption, a reversal period, and then a long period of bone matrix formation mediated by osteoblasts, followed by mineralization of the organic matrix (Figure 3). Bone mass and architecture is modified through remodeling; if the eroded bone is incompletely refilled with bone the bone mass will decrease.
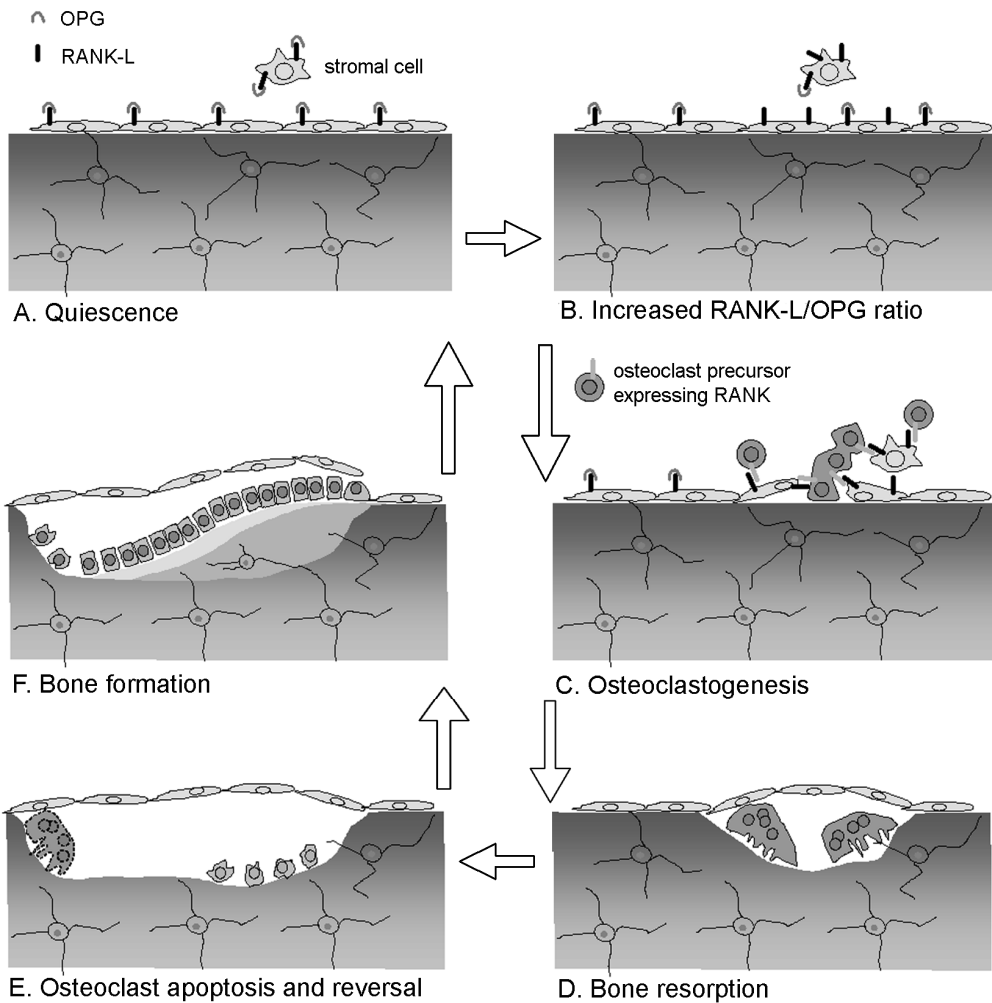
Figure 3. The bone remodeling cycle. See text for explanation.

2.2.2   *The mechanostat*

Harold Frost first introduced the mechanostat theory (Frost 1987), in which he postulated how load-bearing bones adapt to changes in mechanical environment. According to this theory, the bone tissue acts as a mechanostat that recognizes the strain, so that below a certain threshold of mechanical load, bone is resorbed, and above another threshold bone is formed on existing structures to meet up with the increased load. The existence of a mechanostat is well accepted although the mechanisms behind the mechanostat are not yet well understood. It is thought that osteocytes sense the strain on bone at a particular site and signal, potentially through the bone lining cells, to the effector cells at the surface of the bone. Three key proteins involved are the ligand for receptor activator of nuclear factor kappa B (RANK-L), osteoprotegerin (OPG) and sclerostin. The nature of the mechanical

signal and the molecular mechanism, by which osteocytes sense it, remains to be elucidated. However, it is well recognized that strain causes pressure gradients on the interstitial fluid in the lacunas and canalicular system, and movement of fluid from sites of high pressure toward sites of low pressure will impose fluid shear stress on the osteocytes (Bonewald 2006). Several signaling molecules are reported to be induced within minutes of mechanical stimulation of cultured osteocyte-like cells, including nitric oxide, prostaglandins, and adenosine trisphosphate (Ajubi *et al.* 1999; Bacabac *et al.* 2004).

Furthermore, there is substantial evidence that osteocytes require mechanical stimulation for their survival and viability (Bakker *et al.* 2004; Mann *et al.* 2006; Tan *et al.* 2008). In addition, lack of mechanical stimulus will lead to apoptosis of the osteocytes in regions where bone resorption is subsequently initiated (Aguirre *et al.* 2006; Emerton *et al.* 2010). There is some evidence that the load-induced fluid flow is needed to provide the osteocytes with high molecular weight compounds like proteins, while small molecular weight compounds may diffuse at a rate sufficient to reach all osteocytes without loading (Knothe Tate *et al.* 1998).

While osteocyte apoptosis, for instance due to microfractures, at least in part may determine where remodeling should take place, it does not explain the fine-tuning of the mechanostat; the mechanostat should also regulate how much new bone is deposited. The mechanical stimulus must be integrated with regard to its magnitude, frequency and duration, and this information must be translated to the surface of the bone, telling the osteoblasts how much bone should be deposited. One gene, SOST, has been reported to be regulated by mechanical loading, so that expression of its product, sclerostin, is decreased by mechanical loading (Robling *et al.* 2008). Sclerostin has an antagonistic effect on WNT/β-catenin signaling, which is an important signaling pathway in osteoblast differentiation. It was recently shown that even short mechanical stimulations of long bones in mice are able to reduce the expression of sclerostin and increase bone formation at the same time (Robling *et al.* 2008; Moustafa *et al.* 2009). The effect of sclerostin is evident from a rare genetic disease called sclerosteosis, caused by the loss of sclerostin. It is characterized by progressive bone thickening producing an "overgrown" skeleton (Vanhoenacker et al. 2003; Wergedal et al. 2003). Deletion of the SOST gene in mice results in a similar phenotype (Li *et al.* 2008).

2.2.3 *RANK-L and osteoclastogenesis*

During the recent decade, it has become evident that osteoclast formation and, thus, the bone turnover rate, is regulated through the RANK-L activation of RANK in osteoclast progenitor cells (Figures 3B and 3C). OPG is a soluble RANK-L receptor and acts as a decoy receptor. Thus, the RANK-L/OPG ratio at the local microenvironment is important. The central roles of RANKL, RANK and OPG in determining the level of bone resorption were demonstrated through the generation of transgenic mice: RANKL$^{-/-}$ and RANK$^{-/-}$ mice were osteopetrotic due to an absence of osteoclasts; OPG$^{-/-}$ mice were severely osteoporotic and had increased numbers of osteoclasts (reviewed in Blair *et al.* 2006). RANK-L and OPG are co-expressed in the same cells, which, by immunohistochemistry and in situ hybridization, have been shown to include active osteoblasts, early osteocytes, bone lining cells, maturative and hypertrophic chondrocytes, some bone marrow cells and sinusoid lining cells (Ikeda *et al.* 2001; Silvestrini *et al.* 2005). In osteoblastic cells RANK-L have been detected on the plasma membrane but also in the lysosomes, and there

is data to suggest that RANK-L and OPG form a complex in the Golgi apparatus, and OPG is essential to target the complex to secretory lysosomes (Aoki *et al.* 2010; Kariya *et al.* 2011). Considering that bone resorption precedes bone formation, the role of RANK-L expression in active osteoblasts appears irrational. In vitro, mechanical stimulation of osteoblastic cells potently reduces RANK-L expression (Rubin *et al.* 2000). The osteoclast progenitor cells could be recruited either from the circulation or directly from the bone marrow; this has not been conclusively studied. However, RANK-positive monocytic cells fuse on the very close vicinity of the bone surface. Some authors have provided evidence for the existence of a bone remodeling compartment, i.e. a space between the bone surface and an intact layer of bone lining cells, that is in close contact with blood vessels (Hauge *et al.* 2001; Eriksen *et al.* 2007; Andersen *et al.* 2009).

2.2.4   *Resorption and osteoclast physiology*

Once osteoclasts are formed, they start to resorb bone (Figure 3D) this phase takes place over a 6-12 day period (Eriksen *et al.* 1984) during which also new osteoclasts are formed. Resorbing osteoclasts form a specialized resorption space in between the bone surface and the osteoclast itself (Figure 4). This space is limited by a sealing zone, formed by ring-like arrangement of podosomes (Kanehisa *et al.* 1990), and dependent on integrin $\alpha_v\beta_3$-mediated attachment to the RGD-sequence containing proteins of the bone matrix (McHugh *et al.* 2000).
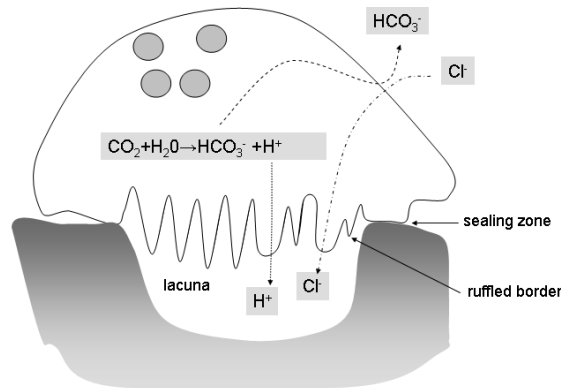
Figure 4. Schematic illustration of a resorbing osteoclast and the essential ion transport mechanisms leading to acidification of the resorption lacuna and dissolution of bone mineral.

By reducing the pH of the resorption lacuna, the bone mineral dissolves and organic matrix is exposed and made accessible to proteases, which the osteoclast also secretes into the resorption lacuna. Due to the numerous extensions and invaginations of the plasma membrane inside the sealing zone, it is called the ruffled border membrane (Figure 4). It is the resorptive organ of the osteoclast. Across this ruffled border membrane protons are transported into the resorption lacuna by a V-ATPase (Blair *et al.* 1989; Sundquist *et al.* 1990; Väänänen *et al.* 1990), accompanied by Cl- flow that allows electroneutral secretion (Kornak *et al.* 2001). Inactivating mutations of the genes for the V-ATPase a3 subunit or chloride channel 7 (ClC7) render the osteoclasts essentially incapable of bone resorption; in humans such gene defects cause different forms of osteopetrosis (Del Fattore *et al.*

2008). While it is clear that the ClC7 is essential for bone resorption and, additionally, for lysosomal function, its action is not well understood. ClC7 is a voltage-dependent $2Cl^-/H^+$ exchanger (Graves *et al.* 2008). It differs from other characterized Cl^-/H^+ exchangers of the ClC family inthat it activates and deactivates sluggishly, and this sluggishness appears of physiologic significance, since some of the mutations that cause osteopetrosis accelerate its gating (Leisle *et al.* 2011).

Protons are generated by carbonic anhydrase activity (Hall and Kenny 1987). Bicarbonate accumulation is counteracted by Cl^-/bicarbonate exchange on the basolateral membrane (Teti *et al.* 1989), (Figure 4). Osteoclasts are motile on the bone surface. Collagen fragments resulting from cathepsin K activity, called carboxy-terminal cross-linked telopeptides of type I collagen (CTX), are released into the circulation and their serum concentrations are used as markers of the resorption activity. The mineral phase is resorbed to a deeper aspect than the organic phase, since the resorption phase leaves lacunas covered with irregular bundles of collagen fibrils (Ren *et al.* 2005).

2.2.5   *Reversal and recruitment of osteoblastic cells*

After osteoclast apoptosis, mononuclear cells populate the eroded bone surface (Figure 3E). These cells degrade the remaining collagen fragments, and lay down a histologically differentiable cement line, which marks the border between new and old bone. These events can be mimicked in vitro by addition of osteoblastic cells onto preformed resorption lacunas (Mulari *et al.* 2004), suggesting that these cells are of osteoblastic origin, possibly bone lining cells (Everts *et al.* 2002). The reversal phase may last for several weeks (Eriksen *et al.* 1984). It is well established that bone formation always follows resorption, except for in some pathological conditions such as myeloma. The coupling involves the attraction of cells of the mesenchymal origin, their proliferation, differentiation to osteoblast precursors, and maturation. Complex interactions of local growth factors in the bone marrow microenvironment, transcriptional factors, as well as systemic hormones govern the differentiation of osteoblasts from the mesenchymal progenitors. The differentation depends on the WNT-signaling pathway which leads to the translocation of β-catenin to the nucleus and its transcriptional activity (Milat and Ng 2009), and involves two other subsequent transcription factors, Runx2 and osterix (Marie 2008). It is unknown how cells of the osteoblastic lineage are recruited to the resorption lacuna. Some have identified platelet-derived growth factor secretion by mature osteoclasts as a chemotactic agent (Sanchez-Fernandez *et al.* 2008; Kreja *et al.* 2010). There is also data to suggest that growth factors, such as transforming growth factor-β and bone morphogenetic proteins, released from the bone matrix by osteoclast activity may fulfill some of the coupling functions (Martin and Sims 2005).

2.2.6   *Bone formation*

Mature osteoblasts, some 100-400 per BMU (Figure. 3F), synthesize and secrete collagen and other bone matrix proteins, which together are referred to as osteoid. After a time lag of approximately 10 days, during which the osteoid self-arranges, the osteoid is mineralized subsequently at a rate of about 0.55 μm per day. This time lag results in a transient osteoid seam of about 10 μm.

Mineralization of the osteoid starts with nucleation, i.e. formation of an initial crystal, which may contain a few unit cells in size. Three principally different but not mutually exclusive modes of nucleation have been proposed. According to the first theory crystals are actively nucleated from solution by charged proteins in the collagen gap zones without any intervention of cellular processes (Veis and Perry 1967; Glimcher 1984). Another theory suggest that the initial nucleation takes place in matrix vesicles budding from the plasma membrane of the osteoblasts, followed by propagation of the mineral out of the vesicles into the matrix (Ali *et al.* 1970; Orimo 2010). Matrix vesicles have been observed and isolated from woven bone and mineralizing cartilage (Väänänen *et al.* 1983; Schwartz *et al.* 1989). A third more recent theory, in part based on the observation that amorphous, phosphate-rich material is found in vesicles in osteoblasts, suggests that amorphous precursor material is formed intracellularly, exocytosed and deposited in the gap zone, where it is crystallized (Mahamid *et al.* 2011).

After nucleation, the initial crystals grow rapidly to reach about 70% of the final density. This primary mineralization is followed by a secondary mineralization lasting for months, during which impurities are exchanged and mineral crystals become more perfectly arranged. Several proteins secreted by osteoblasts are required for proper mineralization. These include tissue non-specific alkaline phosphatase, the ablation of which results in hypomineralization of the skeleton and in disordered alignment of the mineral crystal (Tesch *et al.* 2003), and osteocalcin, the ablation of which results in slightly impaired mineral maturation (Boskey *et al.* 1998). Alkaline phosphatase, preferably the bone-specific post-translationally modified form of it, procollagen type I N-terminal propeptide (PINP), and osteocalcin are used as serum markers of osteoblastic activity.

2.3   BONE LOSS AND OSTEOPOROSIS

2.3.1   *Age-and menopause-related bone loss*

During a normal lifespan, women may lose 50% of the trabecular bone mass and 30% of the cortical bone mass, the corresponding numbers for men are 30% and 20%, respectively. For both genders, bone loss typically starts during the fourth decade and trabecular bone loss starts before cortical bone loss starts; about 40% of the total trabecular bone loss occurs before the age of 50, while very little cortical bone is lost by this age. For women, bone loss is accelerated for a period of time following the menopause, at which the BMD at the total hip and the lumbar spine is lost at an annual rate of 1.6% and 2%, respectively (Finkelstein *et al.* 2008). For diagnosis of osteoporosis, the BMD T-score is used; the actual BMD of a person is measured by dual energy x-ray absorptiometry. The value is compared against the mean BMD of a reference population consisting of young healthy adults and the standard deviation thereof. Osteoporosis is diagnosed when the BMD value is more than 2.5 standard deviations less than the mean BMD.

The pattern of age-related bone loss is by no means tissue-specific; for instance, muscle mass and strength is also declining in a similar time of onset and magnitude. In cross-sectional studies comparing young normal subjects in the 20–40-year age range to healthy subjects in the 70–80-year age range, declines in knee extensor torque and power have ranged from 20% to 50% (Larsson *et al.* 1979; Murray *et al.* 1980; Young *et al.* 1984; Murray *et al.* 1985; Young *et al.* 1985). To what extent the age-related decline in bone mass is purely adaptation to the reduced bone strain stimulus during aging, for instance,

due to loss of muscle strength, remains to be studied. The outcome of successive bone loss is more dramatic than successive loss of muscle strength, since bone loss will potentially result in fractures.

2.3.2 Other causes of bone loss

Bone loss can also be secondary to a number of primary diseases or their treatment including osteolytic bone metastasis, hyperparathyroidism and rheumatoid arthritis. It is estimated that secondary osteoporosis accounts for 20-30% and 50% of the cases in women and men, respectively (Fitzpatrick 2002). The mechanisms behind these causes of bone loss are partly different from those of age and- menopause related bone loss, and though important, the reviewing is beyond the scope of this thesis.

2.3.3 Anatomical differences of bone loss

The available data on non-load bearing bones, such as the parietal bone of the skull, show that very little bone is lost with age from parietal bone (Hwang *et al.* 2000; Torres-Lagares *et al.* 2010). This is very different when compared to another flat bone, the ilium, the trabecular bone volume of which is reduced to 50% in 90 year old subjects compared to young adults (Thomsen *et al.* 2002). In addition to the different load-bearing characteristics of the parietal bone and the ilium, they have a different embryological origin (the parietal bone forms by intramembraneus ossification, while the ilium forms by endochondral ossification).

In the diaphyses of long bones, bone is selectively lost from the endocortical surface. The reason for this may be biomechanical in origin; the endosteal surface, which is closest to the axis of the bone, is subject to the smallest bending and torsional strains. Another interesting fact is that there is no negative balance in intracortical bone remodeling, i.e. the Haversian canal areas do not increase with age (Qiu *et al.* 2010), as could be expected if there was a general age- or menopause linked defect in osteoblast differentiation and function.

2.3.4 Histopathology of osteoporosis

The age-related loss of bone tissue has been shown, by dynamic histomorphometry, to be due to the following mechanism. Bone formation is reduced in the BMUs, so that the resorbed bone is bone is incompletely replaced by new bone, in fact there is an inverse correlation between bone volume formed in the BMU and age (Lips *et al.* 1978; Vedi *et al.* 1984; Eriksen 1986). The bone erosion depth and the volume of eroded bone in the BMU is not increased with age, rather it remains unchanged or it decreases (Eriksen 1986; Croucher *et al.* 1991). Furthermore, analysis of femur midshaft osteons from 88 human cadavers shows that osteon diameter, which is dependent on osteoclast activity, decrease with age, and female osteons are smaller than male, with no observable effect of the reproductive status (Britz *et al.* 2009). However, some have reported a small increase in erosion depth during the early postmenopausal years (Eriksen *et al.* 1999). The accelerated bone loss following the menopause is caused mainly by an increase in the number of BMUs, i.e. within one year, the BMU activation frequency is doubled, and this higher turnover rate continues throughout life (Recker *et al.* 2004). However, compared to the rate at menopause, the net bone loss a few years after the menopause is somewhat decreased, when the new steady state at the higher bone turnover rate is reached.

The higher turnover rate induced by the menopause may explain some of the differences between bone loss in women and men; in men the trabeculi become thinner, while in women the trabecular connectivity may be lost and individual trabeculi completely resorbed (Aaron *et al.* 1987). Because of the higher remodeling rate in postmenopausal women, the porosity of cortical bone is higher. Another difference is that the periosteal apposition of bone is greater in men than in women, and thus it more efficiently compensates for the endosteal bone resorption.

2.3.5   *Incidence of osteoporotic fractures*

A bone is likely to fracture when the loads imposed are similar to, or greater than, its strength. Thus, the consequence of bone loss is an increased susceptibility to fractures. One in every two white women suffers an osteoporosis-related fracture during their lifetime (Kanis *et al.* 2002a; Kanis *et al.* 2002b). Fractures of the spine are most common but may be asymptomatic and thus subclinical. Hip fractures receive most attention because they are associated with the greatest morbidity and healthcare costs. More than 90 % of the hip fractures are caused by falls (Youm *et al.* 1999). For the spine fractures, 25% is caused by a fall (Cooper *et al.* 1992) and about 50% of the cases are precipitated by non-traumatic events, which may include lifting rather light objects non-ergonomically (Silva 2007).

Because of the high impact of osteoporotic fractures on morbidity of individual patients, and the medical costs for the society, the prevention of fractures is well justified (Harvey *et al.* 2010). Treatment of bone loss by medication is an obvious approach to reduce the risk of fractures. On the other hand, more attention should be paid on preventing falls, as argued by Järvinen and colleagues (Järvinen *et al.* 2008).

2.4   OVERVIEW OF CURRENT OSTEOPOROSIS MEDICATION

Osteoporosis differs from many other diseases in that bone loss by itself is asymptomatic until a fracture eventually occurs, and many osteoporotic subjects does not suffer any fractures at all during their lifetime. This puts special requirements on the medication; essentially no adverse effects induced by the medication itself are ethically acceptable for prevention of osteoporotic fractures. For treatment of established osteoporosis, only minor adverse effects are acceptable.

The current drugs classes are nitrogen-containing bisphosphonates, selective estrogen receptor modulators (SERMs), parathyroid hormone (PTH) and a neutralizing antibody. Strontium ranelate is an odd drug, since it consists simply of strontium ions (Sr^{2+}) and an organic carrier, ranelic acid. The drug classes differ considerably concerning the mechanisms of action, and spectra of adverse effects. Drugs approved for marketing in EU-countries by the European Medicines Agency (EMA) (www.ema.europa.eu) are listed in table 1, together with alendronate, which was on the markets before the EMA was founded.

In addition, hormone replacement therapy (HRT) (estrogen alone or estrogen and progestin) also has antiosteoporotic effects, however, prevention of fractures alone is not a primary indication of HRT; it is considered in recently menopausal women when there are additional menopausal indications. The next sections review the currently available drug classes with respect to their mechanisms of actions, efficacy on fracture prevention and on

the BMD. The review of the efficacies is limited to data on the dose approved for treating postmenopausal osteoporosis. In addition, some unique features are emphasized. Although not reviewed further, one should note that the subindications and contraindications differ significantly among the drugs, and the most appropriate treatment depends on the overall clinical situation.

Active compound	Name	Year of approval	Dosing/Route of administration
Alendronate	Fosamax +generics	1995 (FDA)	One tablet weekly
Raloxifene	Evista, Optruma	1998	One tablet daily
PTH(1-34)	Forsteo	2003	Subcutaneous injection once daily
Ibandronate	Bondenza, Bonviva	2004	One tablet monthly, or one intravenous injection every third month
Strontium ranelate	Protelos, Osseor	2004	Orally daily, one sachet is suspended into one glass of water
Zoledronic acid	Aclasta	2005	Intravenous infusion once yearly
PTH(1-84)	Preotact	2006	Subcutaneous injection once daily
Lasofoxifene	Fablyn	2009	Tablet once daily
Basedoxifene	Conbriza	2009	Tablet once daily
Denosumab	Prolia	2010	Subcutaneous injection twice yearly

Table 1. Drugs approved for treatment of postmenopausal osteoporosis by the European Medicines Agency. FDA, Food and Drug Administration in the Unites States.

2.4.1 The nitrogen-containing bisphosphonates

Pharmacokinetics. Bisphosphonates (alendronate, ibandronate, and zoledronic acid, Figure 5) have high affinity for hydroxyapatite, this feature is essential to their efficacy as antiosteoporotic drugs, and gives them a unique pharmacokinetic profile.
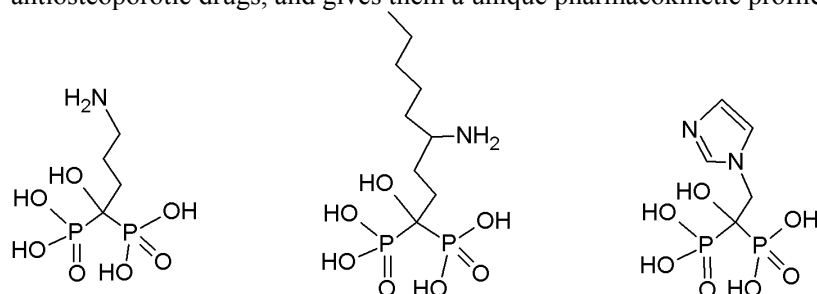
Figure 5. The structure of alendronate (left), ibandronate (middle) and zoledronate (right)

The terminal half-life of alendronate is similar to that of bone mineral, approximately 10.5 years (Rodan *et al.* 2004). Because of the hydrophilicity, after oral administration typically less than 1-2% is absorbed and a fraction of the circulating bisphosphonate is very rapidly taken up by bone tissue, while the remainder is excreted unchanged in the urine within a few hours. After intravenous administration some 40-70 % of the dose is excreted in the urine depending on the bisphosphonate side chains (Conrad and Lee 1981; Khan *et al.* 1997; Mitchell *et al.* 2001; Chen *et al.* 2002). Bisphosphonates are circulating in the plasma only during the administration and they are not metabolized in the liver. Within the

skeleton, bisphosphonates binds to the surface of bone, especially to sites of active mineralization and resorption. After continuous dosing, the bisphosphonates accumulate onto the hydroxyapatite crystals and the cumulative dose is the major determinant of their effects. Accordingly, the dosing regime has shifted toward higher doses less frequently.

Mechanism of action. The selectivity of bisphosphonates for osteoclasts is because upon resorption, bisphosphonates will enter osteoclasts and exert intracellular effects only in osteoclasts. In the cytosol, nitrogen-containing bisphosphonates inhibit the farnesyl pyrophosphate synthase, an enzyme in the mevalonate biosyntetic pathway, which is needed for prenylation of members of the small guanosine triphosphatases (GTPase) including the Ras, Rho and Rab families. Prenylation, i.e. addition of an isoprenoid lipid chain, is essential for the correct subcellular membrane localization of these small GTPases. The prenylated small GTPases act as molecular switches, the regulation capacity of which appears be lost in the absence of a prenylation so that downstream effectors are inappropriately, probably constitutively, activated (Dunford *et al.* 2006). Recent data, reviewed by (Coxon *et al.* 2006) suggest that the bisphosphonates compete directly for binding with the natural substrates. This binding is followed by conformational changes that promote the binding of the second substrate, which itself stabilizes the final complex of bisphosphonate-bound enzyme resulting in essentially irreversible inhibition. Anyhow, the essential outcome is that osteoclasts lose the capacity to resorb bone. As measured by serum markers of bone resorption, bisphosphonate medication decreases bone resorption to low premenopausal levels. However, after a delay, also bone formation marker levels decrease.

Long-term alendronate treatment is associated with an increase in the number of osteoclasts, which include distinctive giant, hypernucleated, detached osteoclasts that are undergoing protracted apoptosis adjacent to superficial resorption cavities (Weinstein *et al.* 2009). The number of osteoclasts increased by a factor of 2.6 in patients receiving alendronate for 3 years as compared with the placebo group. Moreover, the number of osteoclasts increased as the cumulative dose of the drug increased (Weinstein *et al.* 2009).

Efficacy. A meta-analysis demonstrated the efficacy of alendronate against hip fractures in postmenopausal women with osteoporosis (Papapoulos *et al.* 2005). This analysis included 6,804 women with a BMD T-score of −2.5 or less from six randomized placebo-controlled trials. The relative risk of having a hip fracture when taking alendronate was 0.45 and it was consistent across all studies. Alendronate also reduced the relative risk of vertebral fractures among women with osteopenia to 0.40 (Quandt *et al.* 2005). The long-term (10-year) efficacy and safety of alendronate has been examined in extensions of the clinical trials; reductions in bone turnover markers remain stable throughout 10 years of alendronate treatment and are associated with continued gains in lumbar spine and hip BMD (Bone *et al.* 2004).

Alendronate increased BMD at all sites studied (Cummings *et al.* 1998). The effect on BMD is biphasic; following the onset of effect, the BMD increases rapidly, then the rate attenuates to a very slow increase in BMD, which may continue as long as the treatment continues. The rapid increase in BMD is considered to be due to the completion of existing bone multicellular units while excavation of pits is inhibited, and the slow phase is considered to be due to the secondary mineralization of preformed bone.

Discontinuation. Even five years after discontinuation of alendronate treatment, serum levels of bone turnover marker are still suppressed, and the BMD is decreasing only slowly (Bone *et al.* 2004; Black *et al.* 2006). This sustained effect may be due to the long terminal half-life of alendronate, and the fact that bisphosphonates detach from bone into the interstitial fluid and a fraction of this pool may attach anew to the bone being remodeled.

2.4.2 Parathyroid hormone

Parathyroid hormone is a peptide hormone involved in the homeostasis of the Ca^{2+} concentration in plasma. Low plasma Ca^{2+} induces PTH secretion. Circulating PTH then binds to its receptor expressed on cells of the osteoblastic lineage, renal tubular cells and intestine. PTH induces increased uptake of Ca^{2+} from the intestine, reduces Ca^{2+}-excretion by the kidney and induces release of Ca^{2+} from bone by increasing bone resorption. Continuous infusion of PTH results in increased resorption as soon as 6 hours after start, and the osteoprotegerin mRNA level is decreased and the RANK-L mRNA level is increased within hours (Ma *et al.* 2001). However, somewhat paradoxically, intermittently administered low dosage of PTH has anabolic properties on bone. It appears that the duration at which PTH is above a serum threshold level determines whether an anabolic or a catabolic bone effect is the outcome (Frolik *et al.* 2003). Like other peptide hormones, the half-life of PTH is short, 75-90 minutes (Lindsay *et al.* 1993). There are several contraindications to PTH treatment, including disorders of Ca^{2+} homeostasis, and, because of the anabolic effect on bone cells, bone metastasis and osteosarcoma.

Mechanism of action. Although the potential positive effect of PTH on bone volume and microarchitecture has been known for several decades, the molecular mechanism is not known in detail. PTH and its analogues mediate their biological effect via a specific, G-protein-dependent, high-affinity membrane cell surface receptor. Ligand binding activates multiple intracellular signaling cascades, including cyclic AMP, protein kinase C and phospholipase C (Dunlay and Hruska 1990; Mahon *et al.* 2006). The activation of these pathways results in an increase in the number of active osteoblasts, probably by inducing differentiation of bone-lining cells to osteoblasts (Dobnig and Turner 1995; Schmidt *et al.* 1995) and by decreasing osteoblast apoptosis (Jilka *et al.* 2009). Part of the effect may be due to reduction of sclerostin expression by osteocytes (Bellido *et al.* 2005; Keller and Kneissel 2005), thus promoting osteoblast differentiation. Upon start of the daily injections, bone formation markers increase rapidly to reach a mean threefold increase within 3 months, while the markers of bone resorption also increase, but do so more slowly (Lindsay *et al.* 1997; Hodsman *et al.* 2003; Bauer *et al.* 2006). Thus, there is an "anabolic window" a period of time when PTH acts as an anabolic skeletal agent, which has been utilized to increase bone mass. Bone histomorphometry after 18 months of treatment show that both trabecular number and thickness is increased and that bone turnover is upregulated (Recker *et al.* 2009). Trabecular connectivity density was high, indicating that the new bone forms at relevant sites and contributes to increased bone strength.

Efficacy. In a large study with postmenopausal women with prior vertebral fractures, PTH(1-34) treatment reduced the relative risk of new vertebral fractures to 0.31 and nonvertebral fractures to 0.46, compared to the placebo group (Neer *et al.* 2001;

Greenspan *et al.* 2007). The average time of treatment was 18 months and that of observation was 21 months. The overall outcome for PTH(1-84) was quite similar. In a phase III trial comprising women with osteoporosis, in which the incidence of new or worsening pre-existing vertebral fractures was the primary outcome the relative risk of such fractures during 18 month treatment with PTH(1–84) was 0.42 compared to placebo (Greenspan *et al.* 2007).

Measured by BMD, there appears to be anatomical differences on the response to PTH. During 18 months of PTH(1-84) treatment, the lumbar spine BMD increased continuously by 6.5% compared to baseline (Greenspan *et al.* 2007). In the total hip, BMD was decreased at 6 months, but increased thereafter, and by month 18 hip BMD was 1% higher than baseline and significantly higher than for placebo (-1.1% relative to baseline) (Greenspan *et al.* 2007). In an open-label extension of this trial, completed by 61 patients, the lumbar spine BMD increased by 8.5% above baseline at 36 months of PTH(1–84) treatment, remaining essentially stable during the last 12 months of treatment (Zanchetta *et al.* 2010). The increases in total hip and femoral neck BMD occurred more slowly, reaching 3.2% and 3.4%, respectively, above baseline at 36 months (Zanchetta *et al.* 2010).

However, the BMD of the radius decreased for both PTH(1-34) and (1-84) (Neer *et al.* 2001; Greenspan *et al.* 2007; Stroup *et al.* 2007). A cross-sectional study including peripheral quantitative computerized tomography analysis of the distal radius, suggests that treatment with PTH(1-34) induces periosteal mineral apposition and increased endocortical bone resorption, resulting in higher axial and polar cross-sectional moments of inertia (Zanchetta *et al.* 2003). This pattern is also seen in hyperparathyroidism (Chen *et al.* 2003). Thus, it is possible that the decreased BMD at the radius represents an improvement of bone strength by geometrical parameters, not detectable with dual emission x-ray absorptiometry.

Discontinuation of PTH treatment leads to a rapid decline in BMD; the bone mass gained during one year of treatment is essentially lost within one year, unless followed by alendronate treatment, which seems to further increase the BMD (Black *et al.* 2005). Combination therapy of alendronate and PTH(1-34) results in an attenuation of the anabolic effect of PTH, which is also well seen by bone formation markers (Finkelstein *et al.* 2010).

2.4.3   Denosumab

Mechanism of action. Denosumab is a human antibody that binds to RANK-L and prevents its binding to its receptor. As an effect, osteoclast maturation and survival is inhibited. By histomorphometric evaluation of iliac crest biopsies from patients in a clinical trial, the median eroded surface was reduced by >80% and osteoclasts were absent from >50% of biopsies in the Denosumab group (Reid *et al.* 2010). However, the median bone formation rate was also reduced by 97%, and while double labeling in trabecular bone was observed in 94% of placebo bone biopsies, it was observed in only 19% of the biopsies from those treated with Denosumab.

Efficacy. The clinical trial included 7868 women between the ages of 60 and 90 years who had a bone mineral density T-score of less than –2.5 at the lumbar spine or total hip.

Compared to placebo, subcutaneous administration of Denosumab twice yearly for 36 months reduced the relative risk of new radiographic vertebral fracture to 0.32. For hip fractures and nonvertebral fractures the risk ratios were 0.60 and 0.80, respectively, in the Denosumab treated group (Cummings *et al.* 2009). In a phase 3 trial, Denosumab was compared against alendronate (Brown *et al.* 2009). In this trial 1189 postmenopausal women with a T score less than -2.0 at the lumbar spine or total hip were randomized 1:1 to receive subcutaneous Denosumab injections every 6 months plus oral placebo weekly, or oral alendronate weekly plus subcutaneous placebo injections. Compared with alendronate, Denosumab treatment resulted in significantly greater increases in BMD at all measured skeletal sites. At the total hip, Denosumab significantly increased BMD compared with alendronate at month 12 (3.5% versus 2.6%). Serum markers of bone turnover were also reduced more by the Denosumab treatment than with alendronate.

Discontinuation of Denosumab treatment results in a rapid decrease of BMD, and most of the BMD gained during two years of treatment is lost during the following year (Miller *et al.* 2008). This period of rapid bone loss is mirrored by an increase of serum bone resorption markers to levels above both baseline and placebo and slightly above for bone-specific alkaline phosphatase. Two years after discontinuation, the BMDs appeared to plateau to levels slightly above the levels for placebo, and serum markers of bone turnover levels returned close to those of placebo (Miller *et al.* 2008).

2.4.4   *Hormone replacement therapy*

Mechanism of action. The postmenopausal increase in bone turnover and accelerated bone loss is complex and the mechanism poorly understood, however, HRT counteracts it. By histomorphometry, HRT reduces bone turnover in elderly seen as a 50% reduction in activation frequency (Steiniche *et al.* 1989). In early postmenopausal women, HRT was reported to reduce the resorption rate (Eriksen *et al.* 1999). The inhibition of turnover is also seen as a reduction of both bone formation and resorption markers (Prestwood *et al.* 1994; Marcus *et al.* 1999), but less than with alendronate (Evio *et al.* 2004).

Efficacy. Women's Health Initiative trial, a massive randomized placebo-controlled trial in which 16 608 postmenopausal women aged 50 to 79 years either receiving HRT or placebo were followed up for an average of 5.6 years, a hazard ratio of 0.76 for fractures, which was a secondary outcome of the trial, was reported (Cauley *et al.* 2003). Total hip BMD, as measured in 1024 of these women, increased 3.7% after 3 years of treatment with HRT compared with 0.14% in the placebo group. However, this trial produced evidence against the cardioprotective effect of HRT in older postmenopausal women and highlighted an increased risk of breast cancer associated with extended use (Rossouw *et al.* 2002). This trial resulted in a global discussion of use of HRT concerning its overall benefits and risks, and the number of HRT prescriptions has declined.

Discontinuation of HRT was followed by marked increases of serum bone turnover markers. Osteocalcin, bone alkaline phosphatase, and serum CTX levels increased by 36 %, 23% and 120%, respectively, six months after discontinuation (Sornay-Rendu *et al.* 2003). Thus, withdrawal of HRT reproduces the accelerated bone loss observed immediately following menopause.

2.4.5   SERMs

Raloxifene and the two recently approved drugs Lasofoxifene and Bazedoxifene are selective estrogen receptor modulators. They were developed to favour estrogen agonism in bone, but lack agonism in the uterus and breast. The differential effect of SERMs in different tissues is not completely understood, however, it may be mediated at least through the genomic action of estrogen receptors (Nilsson and Koehler 2005). The ligand-activated estrogen receptors interact with transcription factors, thus modulating gene expression. By definition, different genes are activated in different cell types, so both the genes available for transcription, and the levels of co-activators and co-repressors of transcription, as well as the estrogen receptor levels themselves are different. The SERMs are thought to alter the conformation of the estrogen receptor complex, with the outcome that in some cell type, a SERM is agonistic, while in the other cell type the context is different, so the same conformation of the receptor is not active.

Mechanism of action. Raloxifene induces increased levels of osteoprotegerin in serum (Messalli *et al.* 2007). By histomorphometry analyses of paired iliac crest biopsies, raloxifene was shown to have similar effects to HRT; a reduction in the activation frequency and the bone formation rate compared to the baseline biopsy (Ott *et al.* 2002; Weinstein *et al.* 2003). Raloxifene treatment for one year decreases the levels of bone alkaline phosphatase and NTx, especially among those that had high-baseline levels of these markers (Majima *et al.* 2008), and serum osteocalcin levels were decreased from baseline by mean 28% (Sarkar *et al.* 2004).

Efficacy. In the clinical trials with postmenopausal women with osteoporosis, Raloxifene, Bazedoxifene and Lasofoxifene were shown to reduce the relative risk of new vertebral fractures to 0.6-0.7 relative to placebo, and increased BMD in the spine by 2-3% and less in the femoral neck (Ettinger *et al.* 1999; Silverman *et al.* 2008; Cummings *et al.* 2010). However, the reduction of nonvertebral fractures was not statistically significant for Raloxifene and Basedoxifene (Silverman *et al.* 2008), while statistical significance was reached for Lasofoxifene (Cummings *et al.* 2010). In an extension of the Raloxifene trial, administration for 8 years had no significant effect on the risk of new nonvertebral fractures compared with placebo, except for some high-fracture risk subgroups (Siris *et al.* 2005). The gains of femoral neck BMD and spine BMD reached by 3 years of treatment were maintained or slightly increased at the 7 years time point. Women receiving SERMs had increased relative risk of venous thromboembolus but reduced risk for breast cancer (Ettinger *et al.* 1999; Lippman *et al.* 2006; Cummings *et al.* 2010).

2.4.6   Strontium ranelate

A beneficial effect of low doses of stable strontium in the treatment of osteoporosis was reported almost 60 years ago. Currently, the EMA, but not by the FDA, has approved strontium ranelate.

Pharmacokinetics. The body handles Sr^{2+} in a similar way to Ca^{2+} in that it is absorbed from the intestine, concentrated in bone, and excreted mainly in the urine. The ionic radius size of a Sr^{2+} ion (1.13 Angstrom) is greater than that of a Ca^{2+} ion (0.99 Angstrom). Sr^{2+} is present on the bone mineral substance with an heterogeneous bone distribution (i.e.,

higher concentrations in new than in old bone) (Boivin *et al.* 1996; Dahl *et al.* 2001; Farlay *et al.* 2005; Roschger *et al.* 2010). Sr^{2+} is mainly incorporated by exchange onto the crystal surface, and it appears that very little Sr^{2+} is stably incorporated into the crystals (Farlay *et al.* 2005). After treatment withdrawal, Sr^{2+} exchanged onto the crystal surface is rapidly eliminated, which leads to a rapid decrease in total bone Sr^{2+} levels. In the clinical trials, the median serum Sr^{2+} concentration rose from 0.3 µM to a plateau level of 117.9 µM within 3 months (Meunier *et al.* 2004).

Mechanism of action. At the third month of therapy, the serum concentration of bone-specific alkaline phosphatase was slightly higher in the strontium ranelate group than in the placebo group (a treatment-related increase of 8.1 percent), and this difference persisted at each evaluation during the three years (Meunier *et al.* 2004). The concentration of serum CTX was lower in the strontium ranelate group than in the placebo group at month 3 (a treatment-related difference of 12.2%) and at each subsequent evaluation during the three years. This suggests that strontium ranelate modestly increases bone formation and decreases bone resorption. Histomorphometry data from a small number of samples from the clinical trials indicate that osteoid thickness, mineralization lag time, and the mineral apposition rate were not altered by the treatment (Meunier *et al.* 2004). In vitro, submillimolar concentrations of Sr^{2+} enhances bone cell replication and bone formation in vitro and inhibits osteoclastogenesis (Canalis *et al.* 1996; Bonnelye *et al.* 2008). Interestingly, Sr^{2+} enhances osteoprotegerin expression and down-regulates RANKL expression in human osteoblastic cells *in vitro* (Atkins *et al.* 2009; Brennan *et al.* 2009).

The molecular mechanism of Sr^{2+} action is not fully elucidated. However, Ca^{2+} stimulates osteoblastic functions through receptors (Yamaguchi 2008). There is evidence that the anabolic effect of Sr^{2+} could be mediated by agonism on the extracellular Ca^{2+}-sensing receptor (CaR) that is expressed at all stages of osteoblast development and exerts several actions on bone cells *in vitro* (Chattopadhyay *et al.* 2004; Dvorak *et al.* 2004; Caudrillier *et al.* 2010). In human embryonic kidney 293 cells transfected with the bovine CaR, Ca^{2+} and Sr^{2+} concentration-dependently activated the CaR, and within physiologic Ca^{2+} concentrations Sr^{2+} induced further CaR activation (Chattopadhyay *et al.* 2007). Interestingly, Sr^{2+} was less potent than Ca^{2+} in stimulating inositol phosphate accumulation but was comparable with Ca^{2+} in stimulating extracellular signal-regulated kinase phosphorylation, indicating that Sr^{2+} and Ca^{2+} differ in their agonistic characteristics (Chattopadhyay *et al.* 2007).

Efficacy. In a three year trial comprising 1649 postmenopausal women with osteoporosis and at least one vertebral fracture, the relative risk of new vertebral fractures in the strontium ranelate treated group was 0.59 compared to the placebo group. Strontium ranelate increased the BMD by 14.4% at the lumbar spine and by 8.3% at the femoral neck (Meunier *et al.* 2004). In another double-blinded, placebo-controlled trial, with non-vertebral fractures as the primary outcome, the relative risk for the strontium ranelate group was 0.81 for major nonvertebral fractures compared to placebo (Reginster *et al.* 2005). In an open-label, non-controlled extension of this study, including 893 women, the strontium treatment for 8 years resulted in further continuous increase in BMD of the spine, femoral neck and total hip, so that by 8 years the BMDs at these sites had increased by 26.7%, 10.3% and 10.7%, respectively, from the baseline levels (Reginster *et al.* 2009).

However, strontium interferes with the bone density scan, thus, the BMD values may be somewhat overestimated (Blake and Fogelman 2007).

In summary, there are several options for treating bone loss; the spectrum includes peptide hormones, one biological drug, more traditional chemical drugs, some of which utilize a non-conventional tissue-selectivity and even an ion. BMD may increase by several mechanisms including bone anabolic agents, but also by reducing bone resorption or bone turnover. It is also evident that increased bone mass obtained by medication reduces the fracture risk. Medication reduces the risk for vertebral fractures of the spine by up to 70% and the risk of hip fractures by up to 50%. Another apparent phenomenon is that the BMD gained by the medication is rapidly lost when the effective concentration of the drug is decreased suggesting that the bone mass tends to return to the level set by the mechanostat.

2.5   THE V-ATPase

2.5.1   *Structure*

The V-ATPase is clearly different from the common ion pumps (P-type), which form a covalently phosphorylated enzyme intermediate and are sensitive to vanadate inhibition. The V-ATPase has structural similarity to the mitochondrial ATP synthase, which, powered by an electrochemical H^+ gradient, in the inner mitochondrial membrane, generates ATP. The knowledge on the structure of the V-ATPase comes from a variety of methods including electron microscopy, two hybrid screening, biochemical crosslinking, and mutational studies. No crystal structure has been obtained for the holoenzyme, and the structure of only two yeast subunits, C and H, have been resolved to high resolution by X-ray crystallography. However, the crystal structure and NMR data of the mitochondrial ATPase F1-sector (Abrahams *et al.* 1994) and the holoenzyme, respectively, and the solved crystal structure of a Na^+-transporting vacuolar-type ATPase from the bacterium *Enterococcus hirae* (Murata *et al.* 2005) have provided useful working models for understanding the V-ATPase structure. Most of the functional studies on eukaryotic V-ATPase have been conducted with the yeast *Sacharomyces cerevisiae* and fungus *Neurospora crassa* because they can grow without V-ATPase activity at pH 5.5 but not at pH 7.

The V-ATPase holoenzyme consists of a cytosolic catalytic sector, V1, and a membrane sector Vo (Figure 6).
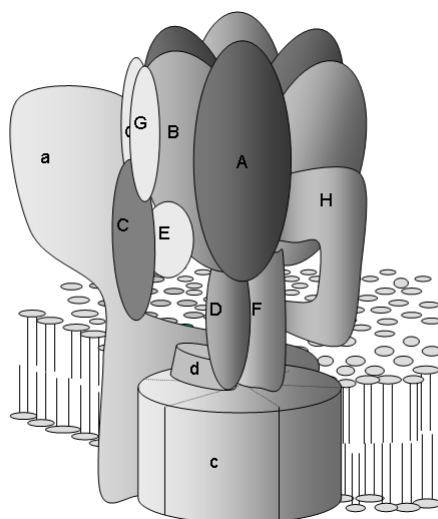
Figure 6. Schematic illustration showing the V-ATPase and its subunits in the membrane. The subunits constituting the cytosolic sector are indicated by capital letters A-H. The membrane sector is composed of subunits a and d, and a hexamer of c and c'' subunits. Two additional integral membrane proteins, which are not illustrated here are associated with the V-ATPase.

The Vo-sector consists of a six different subunits, a, c, c'', d, e, and Ac45 in mammals (and a, c, c', c'', d, and e in yeast). The proteolipid subunits c and c'' are essentially composed of four and five transmembrane helices, respectively (Flannery *et al.* 2004). Presumably five copies of c and one c'' subunit constitute a highly ordered proteolipid hexamer ring (Wang *et al.* 2007). Each proteolipid subunit contains a single essential buried glutamic acid residue that undergoes reversible protonation during proton transport (Hirata *et al.* 1997). Subunit a is a large 116 kDa protein with a cytosolic N-terminal domain, and a carboxy-terminal half containing several (6-9) putative membrane-spanning helices. Situated at the periphery of the proteolipid hexamer, the a subunit is thought to constitute two hemichannels, one facing the cytosolic side and one facing the lumenal side, that allows protons to reach and leave, respectively, these buried glutamate residues in the proteolipid (Forgac 2007). In addition, a peripheral membrane 42 kDa subunit (d) is tightly associated with the Vo-sector on its cytosolic side. Subunits e and Ac45 are integral membrane proteins associated with the Vo sector (Getlawi *et al.* 1996; Sambade and Kane 2004).

The catalytic, cytosolic sector V1 consists of at least eight different subunits (denoted with capital letters A-H), out of which subunits A and B are present in three copies each. The interphase between A and B contains the ATP-catalytic site, most out of which is contributed by subunit A (Liu *et al.* 1996; Liu *et al.* 1997; MacLeod *et al.* 1998). The other interphase between A and B contains a non-catalytic nucleotide binding site that may regulate activity (MacLeod *et al.* 1998; Vasilyeva *et al.* 2000). Thus, one V-ATPase enzyme has three catalytic sites and three noncatalytic ATP binding sites. The catalytic sector is connected to the proteolipid ring through a central stalk composed of subunits d, D and F (Arata *et al.* 2002a; Iwata *et al.* 2004). In addition, there exist peripheral stalks, composed of subunits C, E, and G subunits (Arata *et al.* 2002b). All subunits are required

for enzyme activity, and all subunits except subunit H are required for its assembly (Rizzo *et al.* 2003).

2.5.2   *Mechanism*

The V-ATPase is one of a few proteins in nature proven to operate by rotation (Hirata *et al.* 2003; Yokoyama *et al.* 2003). Rotation occurs in 120º steps, which matches the three catalytic sites per turn. The detailed mechanism of rotation is not solved. With analogy to the F-ATPase, it has been suggested that hydrolysis of ATP drives the rotation of the central stalk and the attached proteolipid ring (i.e. the $DFc_5c"d$ rotor complex) relative to the other subunits which is the stator complex (Forgac 2007), (Figure 7).
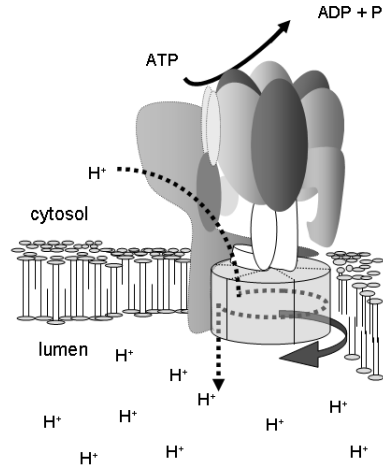
Figure 7. The proposed mechanism of proton translocation and rotation. Upon hydrolysis of ATP the rotor part of the V-ATPase, consisting of the subunits indicated with solid lines, rotates around its axis. See text for further explanation.

The peripheral stalks may connect and stabilize the stator parts of the V1 and the Vo-sectors. In the plane of the lipid membrane, the ring of proteolipid hexamer is thought to rotate around its axis and on the surface of the protein a subunit. The transmembrane segments of a and c' can be crosslinked (Kawasaki-Nishi *et al.* 2003). When exposed to the hemichannel facing the cytosol during rotation, the glutamic acid residue on the proteolipid subunit is protonated. When the protonated glutamic acid residue accesses the hemichannel facing the lumenal side, it is deprotonated. The different environments of the two hemichannels may cause different pKa values of the glutamic acid residue in the proteolipid (Forgac 2007). In this respect, a conserved arginine residue in one of the putative transmembrane helices of subunit a is critical for proton transport, and is thought to act by stabilizing the glutamic acid residue favouring deprotonation in the lumenal hemichannel (Kawasaki-Nishi *et al.* 2001a).

Because a single proton-transporting glutamic acid residue is found in each of the c and c" subunits (and c' in yeast) which form the transmembrane rotor ring, rotation of the $c_5c"$ ring likely translocates six protons per 360° rotation. Therefore, the V-ATPase basicly translocates two protons per one molecule of ATP hydrolyzed. However, there is evidence

that the coupling efficiency may differ significantly between the two yeast isoforms (Kawasaki-Nishi *et al.* 2001b).

2.5.3   Subunit isoforms

In mammals, several of the subunits are represented by different isoforms and splice variants that are differentially expressed (summarized in table. 2).

subunit	kDa	isoforms	aa identity	expression pattern
A	70			
B	56	B1, B2	83%	B2 is ubiquitous, B1 in renal intercalated cells, lung (Nelson *et al.* 1992) and epididymis (Miller *et al.* 2005)
C	42	C1, C2	62%	C1 is ubiquitous, C2-a contains an 46 aa insertion, is in type II pneumocytes, C2-b is in renal intercalated cells (Sun-Wada *et al.* 2003a; Sun-Wada *et al.* 2003b)
D	34			
E	31	E1,E2	77%	E2 ubiquitous, E1 in sperm, epididymis (Imai-Senga *et al.* 2002)
F	14			
G	13	G1, G2	53-64%	G1 is ubiquitous, G2 is expressed in neurons (Murata *et al.* 2002) G3 in kidney (Sun-Wada *et al.* 2003b)
		G3		
H	50			
a	>100	a1-a4	47-61%	see text for expression pattern and further data
c	17			
c"	21			
d		d1	68%	d1 is ubiquitous, d2 is expressed in kidney, osteoclasts and at lower levels in heart, spleen, skeletal muscle, and testis (Nishi *et al.* 2003; Sun-Wada *et al.* 2003b; Smith *et al.* 2005)
		d2		
ac45	29			
e				

Table 2. The mammalian V-ATPase subunits and their isoforms, aa, amino acid.

However, little is known about the functions of the different isoforms. The 116kDa a subunit has been ascribed two roles; subcellular targeting and coupling efficiency of ATP hydrolysis and proton transport, the latter is described in the next section. The four subunit a isoforms have a lower degree of amino acid identity than the other isoforms, especially in the cytosolic amino terminal half of the protein. The two a isoforms found in yeast are targeted differentially; one to the Golgi apparatus and the other to the vacuole (Manolson *et al.* 1994; Kawasaki-Nishi *et al.* 2001b). With chimera of these isoforms it was shown that the targeting signal resides in the amino-terminal cytoplasmic domain (Kawasaki-Nishi *et al.* 2001c). There is evidence that the mammalian isoforms of subunit a localize differentially, although the picture is incomplete. However, a1 has been detected in synaptic vesicles (Morel *et al.* 2003) and the endosomal/phagosomal vesicles (Peri and Nusslein-Volhard 2008). Isoform a2 was found to localize to the early endosomes of proximal tubule cells (Hurtado-Lorenzo *et al.* 2006) and to colocalize with a marker for

the Golgi apparatus (Toyomura *et al.* 2003). Isoform a3 colocalizes with lysosomal markers in macrophages (Toyomura *et al.* 2003). In addition, it localizes to a subset of secretory vesicles of endocrine cells including those of the Langerhans islets, the adrenal, parathyroid, thyroid and pituitary glands (Sun-Wada *et al.* 2006; Sun-Wada *et al.* 2007). There is evidence that the a1, a2, and a3 isoforms are ubiquitously but differentially expressed in different tissues. As assayed by semiquantitative RT-PCR, isoform a1 shows highest expression in brain, isoform a2 in lung, while a3 is highly expressed in bone (osteoclasts) (Toyomura *et al.* 2003). Isoform a4 is prominently expressed in the intercalated cells of the distal tubules and collecting duct, but also detected in heart, lung, skeletal muscle and testis (Kawasaki-Nishi *et al.* 2007). To add to the complexity, splice variants have been detected for isoforms a1, a3 and a4 (Nishi and Forgac 2000; Poea-Guyon *et al.* 2006; Kawasaki-Nishi *et al.* 2007)

2.5.4　Regulation of the V-ATPase activity

Coupling efficiency. Potentially, the isoforms could alter the enzymatic properties of the V-ATPase. There is evidence that the two yeast subunit a isoforms differ with respect to the coupling efficiency, i.e. how efficiently protons are transported during the rotation. The V-ATPase targeted to the Golgi apparatus has a coupling efficiency that is 4-5 fold lower than the V-ATPase of the vacuole. By analysis of chimera of the yeast a subunits it was shown that the coupling efficiency is determined by the carboxyterminal hydrophobic half of the a subunit (Kawasaki-Nishi *et al.* 2001c). Analogous data for the mammalian a isoforms is missing due to the lack of suitable model systems and the inability to obtain isoform-pure preparations. Although in principle the intraorganellar pH could be regulated by such mechanisms, direct evidence for this is lacking, and several other mechanism may be more suitable for regulating intraorganellar pH. As evident from the Nernst equation, any ion pump or ion channel affecting the membrane potential will be as good a regulator of pH as is the proton pump itself.

Reversible dissociation. Following glucose deprivation of yeast, the holoenzyme is inactivated by reversible dissociation of V1 from Vo (Kane 1995). Dissociation also occurs in insect cells during molting (Beyenbach and Wieczorek 2006). Dissociation may function to minimize cellular ATP consumption during periods of limited nutrient supply. There is some evidence that the V-ATPase of renal cells also dissociate in response to low glucose levels (Sautin *et al.* 2005), although the physiological significance is not as evident, since the plasma glucose levels in mammals are kept relatively constant. However, the Vo-sector appears to be expressed in excess relative to V1. This was found to be the case in vesicles derived from chicken osteoclasts (Mattsson and Keeling 1996). Furthermore, in attempts to purify the proton pump from lung, only Vo was found (Peng *et al.* 1999). These findings possibly support that the assembly and dissociation of V1 and Vo is dynamic and regulated also in higher eukaryotes, or that the Vo has another function apart from proton translocation.

V-ATPase dissociation in yeast occurs rapidly, and the ATPase activity of V1 is inactivated and the Vo does not leak protons (Kane 1995). Subunit C is released from the rest of the V1 complex, and subunit H is important for inactivating the ATPase activity of the V1-sector when it is dissociated from the Vo-sector (Parra *et al.* 2000). This inactivation involves conformational changes (Diab *et al.* 2009), possibly direct bridging of the central and peripheral stalks (Jefferies and Forgac 2008). Dissociation does not

require protein synthesis (Kane 1995; Qi and Forgac 2007), but it requires an intact microtubular network (Xu and Forgac 2001). Assembly, on the other hand, requires a protein complex named RAVE (Seol *et al.* 2001), composed of three proteins, that appears to bind to subunits E, G, and C. In yeast deprived of glucose, reassembly of V-ATPase by restoration of glucose levels is dependent on the cAMP-protein kinase A pathway (Bond and Forgac 2008). Also in insect cells, protein kinase A has been shown to stimulate assembly of the holoenzyme, and to phosphorylate subunit C, although it is not phosphorylated in the assembled complex (Voss *et al.* 2007). Recently, also subunit A was found to be phosphorylated by protein kinase A (Alzamora *et al.* 2010). Another observation supporting a tight link between energy metabolism and V-ATPase activity is that subunit E directly interacts with the glycolytic enzyme aldolase; mutations in aldolase that prevents this interaction also prevents the assembly of the holoenzyme (Lu *et al.* 2007). Furthermore, subunit a was reported to interact with phosphofructokinase-1 (Su *et al.* 2008).

2.5.5 Functions of the V-ATPase

Acidification of organelles. The V-ATPase is the enzyme responsible for the acidification of intracellular organelles. Many intracellular organelles are acid to variable extents by V-ATPase action. Due to the unlimited supply of protons in aqueous environment, it is not surprising that proton concentration gradients are utilized in a number of different settings (Nishi and Forgac 2002). Along the endocytic pathway, the pH sinks from slightly acidic pH in early endosomes to pH less than 5 in lysosomes. The sorting and processing of endocytosed substances is highly dependent on this pH gradient; a well-studied example of this is the cellular uptake of iron through the transferrin receptor. Iron loaded transferrin binds to the receptor on the plasma membrane and is endocytosed. The slightly acidified pH in the endosome causes release of iron from transferrin, and the transferrin molecule and receptor are recycled to the plasma membrane, where they dissociate. In an analogous way, the mannose-6-phosphate receptor mediates transport of lysosomal proteins from the trans-Golgi network to lysosomes; the release of ligands similarly depends on the more acidic pH in the destination compartment. Hydrolytic enzymes in the highly acidified lysosomes usually have a pH-optimum around 5. As with other charged molecules, active proton transport across a membrane generates an electrochemical gradient, the energy of which can be used to import and store other molecules. For instance, Ca^{2+} storage in catecholamine storage vesicles (Terland and Flatmark 2000), adrenalin uptake into chromaffin granules (Johnson *et al*. 1982), and uptake of 5-hydroxytryptamine (serotonin) into parafollicular granules (Cidon *et al*. 1991) are powered by the proton gradient.

Acidification of extracellular spaces. In addition to acidifying intracellular organelles, certain cells need the V-ATPase activity for transporting protons into extracellular spaces. The most well understood functions are bone resorption by osteoclasts, as presented in section 2.2.4, plasma acid-base homeostasis by intercalated cells of the distal convoluted tubules and collecting ducts of the kidney, and maintenance of an appropriately low pH in the lumen of the epididymus and vas Deferens.

In response to acidosis, α-intercalated cells in the nephron respond by increasing the number of V-ATPases in the apical membrane (Wagner *et al.* 2004). This is conducted by fusion of subapical V-ATPase containing vesicles with the apical membrane, and the a4 isoform is responsible for plasma membrane localization (Smith *et al.* 2000). Mutations in

the a4 and B1 isoforms, cause renal tubular acidosis, which is associated with deafness in the case of B1-mutations (Karet *et al.* 1999; Smith *et al.* 2000). The a4 isoform is also expressed in β-intercalated cells, which has the opposite polarization compared to α-intercalated cells, and possibly in other cells of the nephron (Stehberger *et al.* 2003).

In the epididymis and vas deferens, sperm development depends on a slightly acidic luminal pH. Analogous to the intercalated cells in the kidney, epithelial clear cells maintain the lumen acidic. These cells respond to elevated cytoplasmic levels of HCO_3^- by increasing the V-ATPase density in the apical membrane by exocytosis of V-ATPase containing organelles. By immunohistochemistry, subunit a4 was detected also in these cells (Smith *et al.* 2001).

Non-enzymatic functions of the V-ATPase. Based on the observation that Vo subunits on the docking membranes *in vitro* can be coimmunoprecipitated, Peters et al. suggested a role for Vo in the fusion of vesicles (Peters *et al.* 2001), in the process of which the hydrophobic nature of the proteolipid could guide the actual fusion of docking lipid bilayers. In support of this function is the observation that a1 is present in both synaptic vesicles and in the presynaptic membranes of nerve terminals (Morel *et al.* 2003). In *Drosophila melanogaster* the a1 analogue is needed for the exocytosis and fusion of vesicles (Hiesinger *et al.* 2005). Here, the fusion of membranes is independent of the proton transport activity of the V-ATPase, since a mutation in the a1 analogue that inhibits proton transport does not inhibit fusion (Williamson *et al.* 2010). Interestingly, when the gene encoding for the d2 subunit in mice is disrupted, the fusion of osteoclast precursor to form multinucleated osteoclasts is severely inhibited (Lee *et al.* 2006). There are some interesting findings regarding the proteolipid protein itself. In the arthropod *Nephrops norvegicus*, the proteolipid functions as gap junctions (Finbow *et al.* 1993).

2.5.6   *The V-ATPases of the osteoclast*

Isoforms a1, a2 and a3 isoforms are expressed in the osteoclast, however, during osteoclast differentiation the levels of a3 mRNA is dramatically upregulated (Toyomura *et al.* 2003). By *in situ* hybridization of sections from bone marrow it was shown that osteoclasts contain 30-fold more a3 mRNA per nucleus than mononuclear cells do, while the a1 mRNA levels does not differ (Manolson *et al.* 2003). Roughly half of the osteopetrosis cases are caused by mutations of the TCIRG-gene encoding for a3, resulting in a clinical picture including high bone density, propensity to fractures, no marrow cavity, and pancytopenia with extramedullary hematopoiesis causing hepatosplenomegaly and anemia (Villa *et al.* 2009). Neurological defects including blindness and deafness due to compression of the cranial nerves and hydrocephalus, due to skull deformities, are also observed. However, the neurological deficits are considered secondary to the bone defects (Villa *et al.* 2009). A number of mutations in the gene encoding the a3 isoform have been identified, these include splice site mutations, and point mutations introducing preterminal stop codons, insertions and deletions causing frameshifts, and two missense mutations of conserved aminoacid residues (G405R and R444L) (Kornak *et al.* 2000; Sobacchi *et al.* 2001; Scimeca *et al.* 2003).

The spontaneously evolved oc/oc mouse has a gross deletion in the corresponding gene (Scimeca *et al.* 2000). The *oc/oc* homozygote mice usually die around 3 weeks of age, and the *oc*/+ heterozygote do not display any particular phenotype. Affected animals (*oc/oc*)

exhibit the characteristic radiologic and histologic features of osteopetrosis, including a generalized increase in skeletal density and absence of marrow cavities. In contrast to ClC7 deficient mice, oc/oc mice display neither lysosomal storage disease nor neuronal degeneration (Kasper *et al.* 2005).

2.5.7 Specific inhibitors of the V-ATPase

Several classes of highly potent V-ATPase inhibitors have been identified. However, due to lack of structure information of the V-ATPase, the precise interactions of the inhibitors with the target are only beginning to be understood.

Plecomacrolides. The plecomacrolides Bafilomycin A1 and Concanamycin A (Figure 8) produced by bacteria of the species *Streptomyces* are potent and specific inhibitors of V-ATPases with IC50 values in the low nanomolar or subnanomolar range, and can be considered the prototype V-ATPase inhibitors.
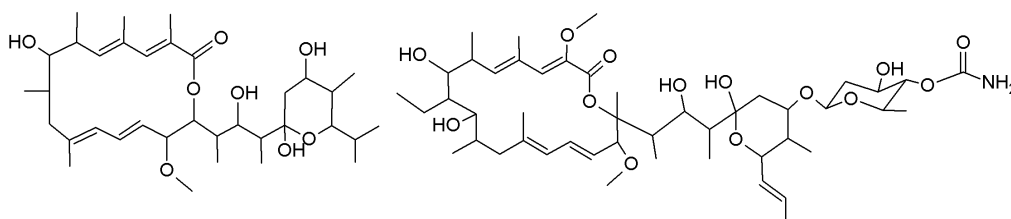

Figure 8. Structure of Bafilomycin A1 (left) and Concanamycin A (right).

Accumulating evidence speaks in favor of the fact that Bafilomycins and Concanamycins bind to the c subunit, with a small contribution by the a subunit. Early on, using affinity chromatography with Bafilomycin columns, last protein to be eluted was subunit c (Rautiala *et al.* 1993). Subsequently, the long-term culture of the fungus *Neurospora Crassa* in the presence of Bafilomycin generated Bafilomycin-resistant clones with mutations in the gene encoding the c subunit (Bowman and Bowman 2002), and a semisynthetic reactive derivative of Concanamycin A was shown to specifically bind to subunit c.

Recently, the crystal structure of the bacterial Na^+ V-ATPase was utilized to model the proteolipid ring of the V-ATPase (Bowman *et al.* 2006). In this model, the mutations, which affect Bafilomycin and Concanamycin binding most strongly, cluster in the interphase between transmembrane helices 1 and 2 in one subunit, and helix 4 in the neighbouring c subunit in the cytosolic half of the membrane bilayer, suggesting that these inhibitors intercalate between neighbouring c subunits in the proteolipid ring. However, point mutations in subunit a also has an influence on binding (Wang *et al.* 2005). It has been suggested that plecomacrolides block rotation of the proteolipid ring relative to subunit a, or prevent internal torsion of the transmembrane helices within the proteolipid ring (Bowman *et al.* 2004; Forgac 2007).

Archazolides. Archazolides (Figure 9) are produced by the myxobacteria *Archangium gephyra* and *Cystobacter violaceus* (Sasse *et al.* 2003; Menche *et al.* 2007). They inhibit V-ATPases with IC50 values in the nanomolar range (Huss *et al.* 2005). The amino acid

residues that affect archazolid binding are partly different from those affecting Bafilomycin and Concanamycin, and by modeling archazolid A was suggested to bind to single c subunits at the outer aspect of the proteolipid ring, and more equatorially than the plecomacrolides (Bockelmann *et al.* 2010).
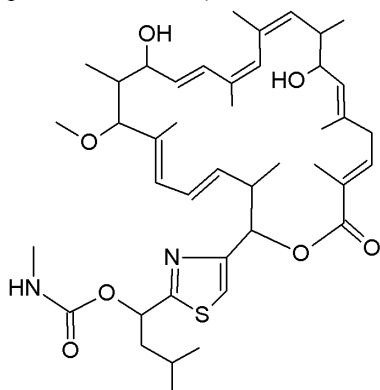

Figure 9. The structure of archazolid A.

Benzolactone enamides. The benzolactone enamides, which includes the salicyli-halamides, lobatamides (Figure 10), oximidines and apicularens, were isolated from the sponge *Haliclona sp*, the tunicate *Aplidium lobatum*, the gram-negative bacterium *Pseudomonas sp* and the myxobacterium *Chondromyces sp.*, respectively (Erickson *et al.* 1997; Kunze *et al.* 1998; Kim *et al.* 1999). However, the benzolactone enamides isolated from sponges and tunicates are assumed to be metabolites from microbial symbionts (Boyd *et al.* 2001). They were identified as V-ATPase inhibitors in screening for antiproliferative cancer drugs (Boyd *et al.* 2001).
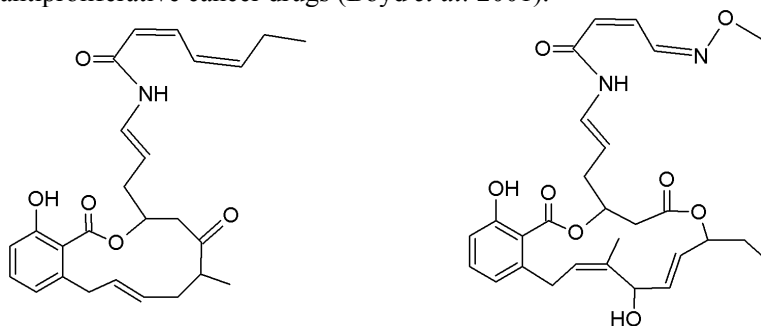
Figure 10. The structure of salicylihalamide A (left) and lobatamide A.

When compared for the potency against V-ATPase activity from osteoclastic tumor cells, kidney and liver, the benzolactone enamides showed some differential inhibition, with salicylihalamide A showing about tenfold higher selectivity for the osteoclast V-ATPase. This observation has not been followed up. A unique feature of this class of compounds is that fungal i.e. *Neurospora crassa* and yeast *Streptomyces cerevisiae* V-ATPases are not inhibited (Boyd *et al.* 2001). The reason for this species selectivity is still unknown. There is evidence that the binding site of at least salicylihalamide A is also in the Vo-sector (Xie *et al.* 2004), but different from that of the plecomacrolides, since salicylihalamide A and apicularen do not prevent binding of a reactive Concanamycin derivative to the c subunit (Huss *et al.* 2005).

SB242784. Studies on the structure-activity relationship of Bafilomycin identified the structural elements that were needed for inhibition and led to the design of synthetic compounds with a indolyl pentadienamide backbone (Gagliardi *et al.* 1998a). This lead was optimized with respect to potency and selectivity between V-ATPase from different tissues such as osteoclast-rich chicken bone and adrenal gland-derived vesicles (Gagliardi *et al.* 1998b). The resulting, most selective and potent compound, SB242784 (Figure 11) shows a 10-fold selectivity for the V-ATPase activity from osteoclastoma in *in vitro* assays (Nadler *et al.* 1998b), and in the rat it was effective in preventing osteoporosis induced by ovariectomy or thyroparathyroidectomy (Visentin *et al.* 2000). The *in vivo* data is reviewed in detail in the next section. The binding sites of these compounds are mostly contributed by the c subunit, because mutations in the c subunits that decrease the affinity of Concanamycin also prevented binding of SB242784 (Whyteside *et al.* 2005). However, it is reasonable that the selectivity is conferred through interaction with the a subunit (Whyteside *et al.* 2005).
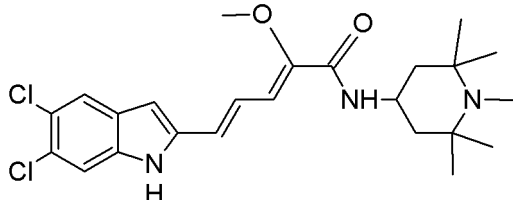
Figure 11. Structure of SB242784.

FR167356 and FR177995. In a screening assay based on acidification, an iminidazopyridine hit was found and optimized; the resulting compounds FR167356 and FR177995 (Figure 12) have an IC50 around 200 nM in *in vitro* assays and are less potent than the other inhibitors presented here (Niikura *et al.* 2004; Niikura *et al.* 2007). However, FR167356 was shown to inhibit membrane preparations of osteoclast V-ATPase tenfold more potently than the preparations of liver V-ATPase (Niikura *et al.* 2004), and it has been tested in rat models of osteoporosis, as presented in the next section. Another related compound developed by the same authors is FR177995, which effectively reduced retinoic acid-induced hypercalcemia and adjuvant-induced arthritis in the rat (Niikura *et al.* 2007).
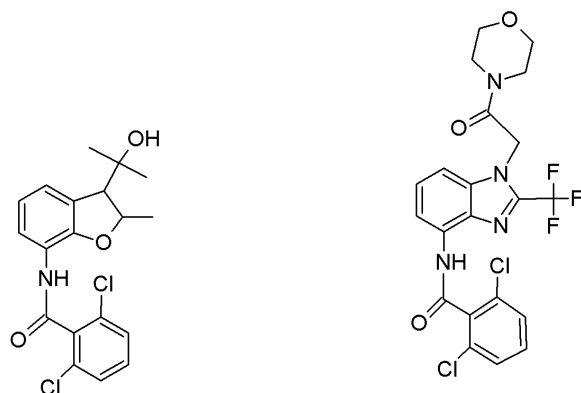
Figure 12. Structure of FR167356 (left) and FR177995 (right).

Diphyllin. In screening of natural compounds in an acidification assay, diphyllin (Figure 13) was identified as a potent V-ATPase inhibitor. In nanomolar concentrations it inhibits V-ATPase activity and osteoclasts resorption, while it does not inhibit bone formation and osteoblast viability at concentrations up to 100 nM (Sorensen *et al.* 2007).
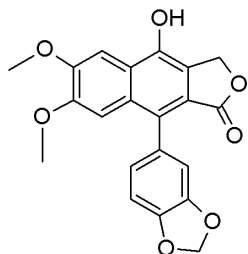
Figure 13. Structure of diphyllin.

2.5.8   *V-ATPase inhibitors in preclinical experiments*

Bafilomycin A1, SB242784 and FR167356 have been tested for their effects on bone in growing or ovariectomized rats. Because these studies are the only ones that give some clue about the efficacy/safety profile of V-ATPase inhibitors, they are reviewed in more detail.

Intravenous doses of Bafilomycin A1 higher than 0.3 µmol/kg caused acute toxicity signs, however, injection of this dose twice daily reduced bone resorption in growing rats as monitored by urinary excretion of ^{3}H-tetracycline (Keeling *et al.* 1997). The toxicity signs were disturbances in locomotor control and piloerection (5 minutes after dosing) and, with intravenous doses of 1 µmol/kg and above, signs of cyanosis and convulsions (10–15 minutes after dosing). Somewhat higher doses, 1.4 µmol/kg/day, could be administered subcutaneously without toxic symptoms, and this treatment for 14 days resulted in increased bone density in growing rats (Keeling *et al.* 1997).

SB242784 was administered by gavage, i.e. forced feeding, for six months, starting the day following ovariectomy, and BMD was measured by dual-photon absorptiometry of the distal femur metaphysis and lumbar vertebrae each month (Visentin *et al.* 2000). Ten mg/kg/day fully prevented the ovariectomy-induced loss of BMD on both sites and the effect was similar to that of estrogen, which raised the BMD to higher values than those of sham-operated rats. The level of urinary deoxypyridinoline cross-links, a marker for bone collagen degradation, was also reduced to half of the levels in ovariectomized animals, in samples taken at 1, 2 and 3 months time points. As shown by histomorphometry of the proximal tibia, 10mg/kg/day SB242784 totally counteracted the 50 % reduction of trabecular number and area induced by ovariectomy. Compared to ovariectomized rats, the percent of eroded perimeter/trabecular bone perimeter was reduced by 67% and similar to that of sham-operated animals. The osteoid perimeter was lower in the SB242784-group than that of both sham and ovariectomy-group, but this change was not statistically significant. Treatment with 10 mg/kg/day had no effect on the urine pH and urine total acid concentration. However, the ovariectomy-induced weight gain decreased by the SB242784 treatment to a level similar to that of sham-operated animals.

In the study on FR167356, it was partly compared with SB242784 (Niikura *et al.* 2005). This study included static histomorphometry and measurement of some blood parameters

to assay adverse effects. Following ovariectomy, FR167356 or SB242784 was administered to the rats by gavage once daily for 27 days. By the end of the experiment, the highest doses reported (FR167356 at 100 mg/kg/day or SB242784 at 10 mg/kg/day) inhibited 75% of the ovariectomy-induced loss of BMD at the distal femur metaphysis. Both compounds also slightly reduced the ovariectomy-induced weight-gain. Among the plasma parameters assessed, blood urea nitrogen, creatinine, (which are renal parameters) glutamic oxaloacetate transaminase, glutamic pyruvic transaminase (which are hepatic parameters) and triglyceride levels did not significantly change when compared to animals that received vehicle. However, total cholesterol was increased and glucose levels were reduced in mice treated with SB242784. Histomorphometric parameters were reported only for FR167356; the ovariectomy-induced decreases in bone volume per tissue volume and trabecular thickness were both abolished by FR167356. Osteoblast and osteoclast surfaces per bone surface were also reduced to the levels of sham-operated rats. FR167356 for 27 days also increased the BMD in non-ovariectomized 5-week-old rats. FR167356 did not cause any changes in the acid-base balance.

In summary, two structurally non-related V-ATPase inhibitors appeared to be well tolerated in that no signs of toxicity were evident and they prevented ovariectomy-induced bone loss, and neither caused any side effects on kidney function, which was examined in detail in both studies.

3   AIMS OF THE PRESENT STUDY

The study started as a European Commission-supported research project "*New therapeutic approaches to osteoporosis: targeting the osteoclast V-ATPase*" (acromym MIVase, contract No. QLG-CT-2000-01801). The consortium consisted of contributors from University of Leeds, Wageningen University, Max-Plank-Institute Göttingen, Glasgow Caledonian University, and the University of Turku. The general aims of the consortium included "*novel chemical synthesis, analysis of the functional effects of chemical agents and antibodies, structural analysis of the targeted subunits of the complex to determine drug interactions and testing of potential leads in in-vivo animal systems*". In practice, the role of ours in the research consortium was to validate the role of isoform a3 in bone resorption (I) and characterize the novel modified inhibitors in assay systems (IV).

During the MIVase project, the following specific questions emerged and were subsequently addressed:

-Does the osteoclast V-ATPase harbour any unique structural properties that would allow its selective targeting?

-Does the unique function of the osteoclastic V-ATPase, bone resorption, confer increased sensitivity to V-ATPase inhibition compared to other V-ATPase-mediated functions?

4 MATERIALS AND METHODS

4.1 REAGENTS

Bafilomycin A1 was from Sigma-Aldrich, Concanamycin A was obtained from Fluka (Buchs, Switzerland). The inhibitor (2Z,4E)-5-(5,6-dichloro-2-indolyl)-2-methoxy-*N*-(1,2,2,6,6-pentamethylpiperidin-4-yl)-2,4-pentadienamide commonly referred to as SB 242784, or INDOL0 in (IV) was synthesized according to the literature by Terrence Kee, Leeds UK). Spin-labeled 5-(5,6-dichloro-2-indolyl)-2,4-pentadienoyl inhibitors INDOL6 and INDOL5 were synthesized as described (Dixon *et al.* 2004) by Neil Dixon and Terrence Kee, Leeds UK. Dimyristoyl phosphatidylcholine was from Avanti Polar Lipids (Alabaster, AL).

4.2 ANTIBODIES (II,III)

Two different human V-ATPase isoform a3 peptide-specific antisera were used in this study. One, provided by Professor John Findlay (Leeds UK), was raised against a peptide corresponding to amino acids 661–691 and the other, raised against a peptide corresponding to the carboxy terminus (amino acids 811–829), was provided by Dr. Jan Mattsson, as was the antibody against subunit A (Frattini *et al.* 2000). Mouse monoclonal antibodies used in the immunocytostaining experiments were against lysosome-associated membrane protein-2 (LAMP-2) (Research Diagnostics, Minneapolis, MN), cathepsin K (Fuji Chemicals, Tokyo, Japan), early endosomal antigen-1 (Transduction Laboratories, Lexington, KY), Rab11 (Transduction Laboratories), matrix metalloproteinase-9 (NeoMarkers, Fremont, CA), and osteocalcin (3H9, 3H8, 8H12) (Hellman *et al.* 1996). The rabbit polyclonal antibody against type I collagen was from Research Diagnostics (Minneapolis, MN). Secondary antibodies used in the immunocytostaining studies were either fluorescein isothiocyanate- or tetramethylrhodamine isothiocyanate-conjugated donkey anti-mouse or donkey anti-rabbit (Jackson ImmunoResearch Laboratories, West Grove, PA). The antibodies recognizing V-ATPase a1 and Rab7 were purchased from Santa Cruz Biotechnology (Santa Cruz, CA). The production of antisera against cytoplasmic carbonic anhydrase II (Väänänen and Parvinen 1983) and mitochondrial carbonic anhydrase V (Väänänen *et al.* 1991) has been described. The horseradish peroxidase-conjugated secondary antibodies used in immunoblotting were purchased from Zymed (San Francisco, CA).

4.3 CELL CULTURES

All cultures were incubated at 37ºC in an atmosphere composed of 5% CO_2 and 95% air. Osteoclasts have different morphology depending on the substrate. In vivo and when cultured on bone slices in vitro most osteoclast form a ruffled border and resorb bone. When cultured on plastic or glass coverlips the osteoclasts do not form a ruffled border, and the cytoplasm contain a high number of lysosomes, which in resorbing osteoclast may form the bulk of the ruffled border. This experimental setting is utilized in articles I, II, and III. The terms inactive or nonresorbing osteoclasts refer to osteoclasts cultured on glass or plastic, not to osteoclasts cultured on bone that are not actually resorbing.

4.3.1   Rat primary osteoclasts (I)

To obtain rat osteoclasts, 1-2-day-old rat pups were decapitated and femuri, tibiae and humeri were isolated, briefly rinsed in 70% ethanol and transferred to cell culture dishes containing α-Minimal essential medium supplemented with 20mM HEPES; 10% heat-inactivated fetal bovine serum; 100 IU/ml penicillin, and 100 µM/ml streptomycin (pH 6,9), in which they were split longitudinally. To release osteoclasts, the inner aspects of the bone were scraped with a scalpell blade. After concentration of the cells by centrifugation, aliquots of the resulting cell suspension was seeded on glass coverslips or bovine bone slices, after 30 min incubation the coverslips or bone slices were gently rinsed in PBS to remove non-attached cells. Experiments were performed in the medium descibed above.

4.3.2   Human osteoclasts (II, III)

Human osteoclasts were cultured from peripheral blood monocytes from male blood donors. The monocyte- and lymphocyte-rich fraction was separated from erythrocytes and polymorphonuclear cells by Ficoll centrifugation. The monocyte- and lymphocyte-rich fraction was washed by four sequential centrifugations in PBS. In (III) the monocytes were purified by Magnetic Cell Sorting (Miltenyi) with a CD14 antibody according to the manufacturer's instructions, and 100.000 and 200.000 cells were plated onto cortical bone slices, or into 8-well chambers with a coverslipbottom for live cell imaging, respectively.

In (II), the monocyte- and lymphocyte-rich fraction was suspended to 20 million/ml α-MEM and plated at a density of 20,000/mm^2 either on slices of bovine cortical bone, glass coverslips, or tissue culture wells, depending on the experiment. After 2 h, nonadherent lymphocytes were removed by gentle swirling of the plate, and adherent cells were induced to differentiate to osteoclasts by culturing in α-MEM supplemented with 10% inactivated fetal bovine serum, 20 ng/ml RANK-L (PeproTech, Rocky Hill, NJ), 10 ng/ml macrophage-colony stimulating factor (PeproTech), and 10 nM dexamethasone (II) and 100 IU/ml penicillin, and 100 µM/ml streptomycin.
Half of the medium was changed every third or fourth day. This protocol generated multinucleated osteoclasts with varying portions of non-osteoclastic mononuclear cells. Before performing the experiments with latex beads (II), the purity of osteoclast cultures was increased by trypsin treatment to detach mononuclear cells, and the resulting purity of these osteoclast cultures was >95% (osteoclast nuclei/nuclei of mononuclear cells).

4.3.3   THP.1 Cell line (II)

The THP.1 monocyte cell line was cultured in RPMI-1640 supplemented with 10% inactivated fetal bovine serum, 5 mM HEPES, 1 mM sodium pyruvate and 100 IU/ml penicillin, and 100 µM/ml streptomycin. In all experiments, THP.1 cells were induced to more actively phagocytosing macrophages by treatment with 10 ng/ml phorbol-12-myristate-13-acetate (PMA) for 16 h and cultured for additional 24 h in the absence of PMA and HEPES before use in the experiments with latex beads. Where indicated, THP.1 cells were treated with 20 µM cytochalasin D.

4.4 RNA EXPERIMENTS (I)

4.4.1 Design and syntesis of siRNA molecules

Three small interfering RNA (siRNA) molecules targeting rat a3 (NM 199089) were designed with Ambion's design system (www.ambion.com). The siRNA molecules (shown in Table 3) were synthesized from DNA templates with the Silencer siRNA construction kit according to the suggested protocol (Ambion, USA). To analyze uptake and intracellular distribution of siRNA molecules, Cyanine 3 labeling with Silencer siRNA labeling kit was used (Ambion, USA).

siRNA-1 sense	5'-CAAGUUCUAUUCAGGGACCUU-3'
siRNA-1 antisense	5'-GGUCCCUGAAUAGAACUUGUU-3'
siRNA-2 sense	5'-UGGGACAGGAAUAAAAAGCUU-3'
siRNA-2 antisense	5'-CUUUUUAUUCCUGUCCCAUU-3'
siRNA-3 sense	5'-UAAAAAGCUGGCUGGCCCAUU-3'
siRNA-3 antisense	5'-UGGGCCAGCCAGCUUUUUAUU-3'
Scrambled control sense	5'-GCACCUAUGAGAGACUGACUU-3'
Scrambled control antisense	5'-UUGCCAUUAGCUGCAGCGUUU-3'

Table 3. siRNA molecules targeted against rat a3.

4.4.2 Transfection of siRNA

30 U of prime RNAse inhibitor (Eppendorf, Germany) was added to each 300 µl of culture medium 15 min before siRNA additions to inhibit RNAse activity in the medium. All siRNA molecules were used at 100 nM concentrations. Uptake of labeled siRNA-molecules into osteoclasts was monitored in samples incubated with siRNA-duplexes at +4 °C; control samples were kept at room temperature. After 45 min, cells were washed in PBS and transferred into fresh, warm culture medium. Endocytosis of membrane-bound siRNA-molecules was allowed to proceed for 0, 1, 2, 4 or 12 h prior to microscopical evaluation. The effects of siRNA-molecules on osteoclast cytoskeleton were monitored by incubating cells in the presence of siRNA-molecules for 48 h, rinsed and incubated in fresh medium for another 24 h.

4.4.3 RNA extraction and RT-PCR

Total RNA was extracted from siRNA-treated cells using GenElute mammalian total RNA kit (Sigma, USA) and genomic DNA was removed with DNAse (Ambion, USA). Quantitative RT-PCR was performed using the Opticon DNA Engine (MJ Research, USA) and DyNAmo SYBR Green 2-step qRT-PCR system according to the suggested protocol (Finnzymes, Finland). The primer sequences (5' to 3') are shown in table 4. Cycle thresholds were determined and a1 and a3 fluorescence was normalized with the GAPDH reference gene fluorescence. All primers were used at 0.5 µM concentrations and the annealing temperature was +61 °C.

	Forward	Reverse	
rat a1:	ACGACCTCCAAATGGTTCTG	ACTTCTGCGATCAGGCACTT	172bp product
rat a3:	ATGAAGGCCGTGTACCTGAC	AGCCACAGCACTCACTCCTT	153bp product
rat GAPDH:	CAGCAATGCATCCTGCAC	TGGCATGGACTGTGGTCA	101bp product

Table 4. Primers for quantitative RT-PCR.

4.5   CELL ASSAYS

4.5.1   *Bone resorption (I, II)*
Bone resorption was measured using the CrossLaps for culture kit (Nordic Biosciences, Denmark) according to the manufacturer's instructions.

4.5.2   *Cell viability (I)*
To monitor cell viability, Live/Dead-system was used according to manufacturer's protocol (Molecular Probes, USA). 0.8% sodium azide-treated samples were included in the assay as a death control group. Cells were incubated with dyes for 45 min, followed by fluorescence intensity measurements using exitation/emission filter sets of 495/520 nm (for Calcein) and 530/642 nm (for Ethidium). Viability indexes were counted by dividing live cell fluorescence by dead cell fluorescence.

4.6   STAININGS AND MICROSCOPY

4.6.1   *Live cell imaging (I ,III)*
To evaluate the effect of siRNA treatment on organellar acidification (I), Acridine orange was added to the medium of treated or control cells 48h after start of the experiment, bone slices and coverslips containing V-ATPase were analysed by fluorescence microscopy.

To analyse the effect of V-ATPase inhibitors on lysosomal pH (III), FITC-TRITC conjugated dextran (MW 70.000) was added to wells containing osteoclasts at a final concentration of 0.5 mg/ml, and incubated for 20h. Following four washes with fresh medium, the inhibitor was added and the cells were incubated 4-6 hours before analysis of FITC-TRITC fluorescence ratios by live cell microscopy at 37º C and CO_2-supply (Olympus MT microscope equipped with CellR software).

4.6.2   *Immunocytostaining protocol (I, II, III)*
Cells were briefly rinsed in PBS, fixed for 20 min in 3% paraformaldehyde and permeabilized in ice-cold acetone for 30 seconds. Cells were incubated in PBS containing 2% bovine serum albumin for 30 min to block unspecific binding. Staining was performed by sequential one hour incubations with primary and fluorochrome-conjugated secondary antibodies diluted in PBS containing 0.5% bovine serum albumin, separated by four washes with PBS, 5 min each. When fluorochrome-conjugated phalloidin was used to stain filamentous actin, it was included in the solution containing the secondary antibody. After counterstaining of nuclei with Hoechst (Molecular Probes, USA) and three 5-min

washes, samples were mounted on microscope slides and viewed under a Leica TCS-SP confocal microscope equipped with Argon-Crypton laser (Leica Microsystems GmbH, Germany) or an Olympus (Tokyo, Japan) fluorescence microscope.

4.6.3   Other stainings

Bone resorption was evaluated by counting WGA-lectin stained resorption pits (I). For quantification of osteoclast numbers (I), cells were stained for using Leukocyte acid phosphatase kit (Sigma, USA) and osteoclasts were counted as tartrate-resistant acid phosphatase-positive cells with at least 3 nuclei.

4.7   IMMUNOBLOTTING (II)

For whole-cell lysates, THP.1 cells and osteoclasts were collected into lysis buffer (1% Triton X-100, 10 mM Tris–HCl [pH 7.5], 1 mM EDTA, 50 mM NaCl, protease inhibitor cocktail [Complete Mini; Roche, Indianapolis, IN]) and briefly sonicated to fragment DNA. The protein concentration was determined using Bradford reagent, and a $5\times$ sample buffer (10% SDS, 300 mM TrisCl [pH 6.8] 0.4% bromophenol blue, 50% glycerol) was added to the samples before 10 μg protein per sample were separated with SDS-PAGE. For immunoblotting of the latex bead-containing phagolysosomes from osteoclasts and THP.1 cells, isolated phagolysosomes were collected by centrifugation and $5\times$ sample buffer was added to the pellets. Out of these samples, aliquots that contained approximately as much LAMP-2 as did 10 μg of the parental whole-cell lysates were loaded. After SDS-PAGE, the separated peptides were transferred to nitrocellulose membrane (Bio-Rad, Richmond, CA) with a semidry transfer system. Unspecific binding was blocked by incubating the membrane for 1 h in PBS containing 5% skim milk. Primary antibodies, diluted in PBS containing 3% skim milk and 0.3% Tween-20, were incubated overnight at 4°C. On the next day, membranes were washed four times for 5 min each time with PBS containing 0.3% Tween-20 and incubated for 1 h with PBS containing secondary antibody, 2% skim milk, and 0.3% Tween-20. After four washes, 5 min each, in PBS containing 0.3% Tween-20, bands were detected with Immun-Star reagents (Bio-Rad) and X-ray film (Kodak, Rochester, NY).

4.8   ACIDIFICATION AND V-ATPase ASSAYS

4.8.1   Isolation of Chicken Bone and Brain Microsomes (II, IV)

Regular egg-laying hens, housed by the University of Turku, were killed and the medullary bone from the femora and tibiae was collected into an isolation buffer (250 mM sucrose, 1 mM EGTA, 1 mM NaHCO$_3$, 10 mM Tris–HCl [pH 7.0], 1 mM dithiothreitol, and protease inhibitor cocktail [Complete Mini]). After brief homogenization in Ultra Turrax, the tissue was further homogenized with a glass–glass dounce homogenizator. Pieces of bone, unbroken cells, mitochondria, and nuclei were pelleted by centrifugation of the homogenate for 15 min at $10,000\times g$, and the resulting supernatant was subjected to ultracentrifugation at $100,000\times g$ for 45 min. The final pellet was dissolved in isolation buffer and frozen at −70°C until used. Brain microsomes were prepared according to the same protocol, except that chicken cerebrum and cerebellum were used as the starting material.

4.8.2   Isolation of phagolysosomes from osteoclasts and THP.1 cells (II)

The protocol was essentially adapted from a previously described one (Desjardins *et al.* 1994) with some modifications. Blue-colored latex beads, 0.8 μm in diameter (Sigma-Aldrich), were diluted 1:100 in the appropriate medium just enough to cover the cells for the 4-h pulse time. Nonphagocytosed latex beads were removed by rinsing the cells with PBS until few free-floating beads were visible under the microscope. After the chase time, the medium was exchanged for ice-cold isolation buffer, and the cells were scraped off the plates and homogenized in a glass–glass dounce homogenizator. By adding isolation buffer containing 60% sucrose, the sucrose content of the homogenized solution was adjusted to 34% (w/w) and loaded under a sucrose gradient of 10, 20, 25, and 30% (top to bottom). After ultracentrifugation at $100,000 \times g$ for 90 min, phagolysosomes were collected from the 10–20% interphase. The sucrose content was readjusted to <10% and the phagolysosomes concentrated by ultracentrifugation at $20,000 \times g$ for 20 min, resuspended in isolation buffer, and frozen in aliquots.

4.8.3   Proton Transport Assays (II, IV)

Microsome acidification was assayed by measuring fluorescence quench of acridine orange (excitation at 485 nm and emission at 535 nm). Assays were performed in 96-well plates and measured with a Cameleon microplate reader (Hidex OY, Turku, Finland). The microplate reader was programmed to take fluorescence readings of the wells at 20-, 30-, or 120-second intervals. The assay mix consisted of 150 mM KCl, 5 mM $MgSO_4$, 1.5 μM acridine orange, 1 μM valinomycin, and 5 mM Tris/HEPES (pH 7.4). Inhibitors were added 20–30 min before the start of the assay in 2 μl DMSO, and control contained only DMSO. To start the tissue vesicle acidification, ATP was added to 5 mM from a 250-mM stock buffered to pH 7.4 with Tris. To dissipate the proton gradient at the end of the experiment, nigericin was added to a final concentration of 10 μg/ml. Phagolysosomes were acidified as with the tissue-derived microsomes, except that the assay volume was scaled down to 50 μl, the inhibitor was added in 1 μl DMSO, and the reaction was started with 2 mM ATP. We noted that the amount of microsomes and phagolysosomes affected the IC_{50} values therefore, we used amounts of microsomes and phagolysosomes that gave a clear quench of fluorescence and were partly inhibited by 0.3 nM Bafilomycin A1, which was used as a reference inhibitor. Moreover, since at room temperature the acidification activity of all preparations decreased with time, the experiments were performed with both inhibitors simultaneously, and representative results are presented.

4.8.4   Measurement of V-ATPase activity in yeast (IV)

The *Saccharomyces cerevisiae* W303-1B vatc cells (*MATα ade2*, *ura3*, *leu2 his3*, *trp1*, Δ*vma3*∷*LEU2*) were a kind gift of Nathan Nelson, University of Tel-Aviv. V-ATPase was purified from yeast vacuolar membranes solubilized in dodecyl maltoside on discontinuous glycerol gradients. ATPase activity was assayed at 30°C by colorimetric development of phosphate release using ammonium molybdate.

4.9 SPIN-LABEL STUDIES (IV)

4.9.1 *Isolation of 16-kDa membranes and vacuolar membranes*

Endogenous membranes containing the 16-kDa channel proteolipid were prepared from the hepatopancreas of the decapod *Nephrops norvegicus* by extraction with *n*-lauryl sarcosine, or with 20 mM NaOH, according to the procedures in the literature ((Finbow *et al.* 1984) and (Hertzberg 1984), respectively). These membranous preparations contain the endogenous lipids, but the amount of lipid is strongly reduced in the preparations extracted with *N*-lauroyl sarcosine (Pali *et al.* 1995). EDTA-washed yeast vacuolar membranes transfected with *Nephrops* 16-kDa proteolipid were prepared as described (Uchida *et al.* 1985).

4.9.2 *Spin-labeling*

Membranes, either *Nephrops* 16-kDa membranes or yeast vacuolar membranes, were suspended in 50 mM borate buffer with 10 mM NaCl, pH 9.0, or in 50 mM HEPES buffer with 10 mM NaCl and 10 mM EDTA, at pH 7.8, respectively. Spin-labeled inhibitors were added to membranes (~1 mg membrane protein) in 500 μl of buffer from concentrated solutions in <10 μl dimethyl sulfoxide (DMSO). Nominal spin-labeled inhibitor to protein mole ratio was 1:1 or less (for 16-kDa membranes). When required, Concanamycin A was added similarly in concentrated DMSO solution. After incubation for 30 min, membranes were packed in 1-mm (internal diameter) glass capillaries by pelleting in a benchtop centrifuge. Sample length was trimmed to 5 mm, excess supernatant was removed, and the capillary was flame-sealed.

4.9.3 *EPR spectroscopy*

EPR spectra were recorded on a Bruker EMX 9-GHz spectrometer (Rheinstetten, Germany). Sample capillaries were accommodated in standard quartz EPR tubes that contained light silicone oil for thermal stability. Temperature was regulated by thermostated nitrogen gas-flow, and measured with a fine-wire thermocouple situated in the silicone oil at the top of the microwave cavity. Analysis of two-component EPR spectra was performed as described (Pali *et al.* 1995). In spectral addition, the whole of the two-component experimental spectrum was fitted first, and then the relative weights of the two components were optimized on the low-field hyperfine lines.

4.10 SEQUENCE ALIGNMENTS (IV)

Amino-acid sequences were taken from the PIR Database. Sequence alignments were performed with CLUSTAL W and displayed with the PIR alignment viewer.

4.11 STATISTICAL ANALYSIS

Analysis of variance (ANOVA) followed by Student's *t* test was used for statistical analysis. Means and standard deviations (S.D.) were calculated and are shown in the Figures. $P < 0.05$ was considered statistically significant.

5   RESULTS

5.1   INHIBITION OF BONE RESORPTION BY siRNA-MEDIATED KNOCK-DOWN OF ISOFORM a3 (I)

5.1.1   *Isoform a3 mRNA can be down-regulated by siRNA*

The critical role of isoform a3 in bone resorption was confirmed by knock-down experiments in primary rat osteoclast cultures. Following addition of Cyanine-3 labelled siRNA molecules into the osteoclast medium Cyanine-3 fluorescence could clearly be detected intracellularly in a significant fraction (8-16%) of the osteoclasts. This method of detecting siRNA uptake is rather insensitive and another fraction of the osteoclasts may have taken up siRNA molecules at levels below the detection limit.

siRNA molecules targeted to the coding region of a3 mRNA down-regulated the relative a3 mRNA levels, as detected by quantitative RT-PCR at timepoints 24, 48 and 72 hours posttransfection. The effect was time dependent and increasing with time for up to 72 hours for the most efficient siRNA molecule. Normalized to a housekeeping gene, the siRNA treatment increased the cycle threshold for a3 cDNA 3.5-6 fold, implying an approximate 12 to 64-fold decrease in a3 mRNA levels at timepoints 12-72 hours post transfection. Importantly, the effect was sequence-dependent, since it was not seen with siRNA of scrambled nonsense sequence. Equally important, the isoform a1 mRNA level was unaffected by siRNAs targeted against a3. Furthermore, treatment with 5 nM Bafilomycin A1 had no effect on the a3 mRNA level.

5.1.2   *Reduction of a3 mRNA results in reduced resorption*

The down-regulation of a3 mRNA was associated with a reduction of bone resorption as assayed by two methods. First, the number of pits formed per osteoclast, was significantly reduced at 48 hours post transfection by the two siRNA molecules that reduced a3 mRNA most. Secondly, the same siRNA treatment reduced the release of CTX into the medium. The onset of effect on the resorption may be delayed compared to the effect on a3 mRNA reduction depending on the half-life of the a3-containing V-ATPase in the osteoclasts. Morphologically, the inhibition of resorption was associated with an increased fraction of osteoclasts with disrupted actin rings.

5.1.3   *The siRNA effect is not due to cytotoxicity*

The siRNA-mediated reduction of bone resorption was not due to cytotoxicity, since the treatment did not significantly reduce the number of osteoclasts at 48 hours and the cell viability index was not increased. Furthermore, the siRNA-induced increase in the fraction of osteoclasts with disrupted actin rings appeared to be transient.

5.2   SUBCELLULAR LOCALIZATION OF V-ATPase a3 (II)

5.2.1   *Localization in resorbing osteoclasts*

Assayed by immunofluorescence staining of in vitro differentiated human osteoclasts on bone, a3 localized mainly within the actin ring. Co-immunostaining of a3 and osteocalcin, a bone matrix protein, showed that a3 is polarized toward the leading edge of the pit. This staining pattern suggests a ruffled border localization, with additional sub-ruffled border vesicular localisation. Only multinucleated cells were heavily a3-positive while no or weak staining was detected in nondifferentiated mononuclear cells, showing that a3 expression is highly induced during osteoclast differentiation.

5.2.2   *Localization in nonresorbing osteoclasts*

In osteoclasts cultured on glass coverslips a3 clearly localized to intracellular vesicular structures. a3 colocalized almost perfectly with LAMP-2, a transmembrane glycoprotein used as a marker protein of lysosomes and late endosomes, and it colocalized with cathepsin K, a lysosomal cystein proteinase. a3 did not colocalize with matrix metalloproteinase-9, a nonlysosomal collagenase or early endosomal antigen-1, indicating that a3 localization is limited to the late endosomal/lysosomal compartment in nonresorbing osteoclasts.

5.2.3   *Phagolysosomal localization of a3*

By immunoblotting, we detected a3 in phagolysosomes isolated from osteoclasts and from a monocyte/macrophage cell line. However, osteoclast phagolysosomes contained more a3 than THP.1 phagosomes did. The isolated phagolysosomes contained LAMP-2 and Rab7, a small GTPase involved in lysosomal biogenesis. Both phagosomal fractions were essentially depleted of the nonlysosomal proteins assayed: Rab11, which is a small GTPase located to recycling endosomes; cytosolic carbonic anhydrase II; mitochondrial carbonic anhydrase V; and the clathrin heavy chain, which is a component of coated pits and vesicles budding from the plasma membrane and the *trans*-Golgi network.

5.3   PHAGOLYSOSOMES CONTAIN MULTIPLE a ISOFORMS (II)

By immunoblotting, we found that the phagosomes were positive for a1 in addition to a3. The a3/a1 ratio was 3.8 to 11.2-fold higher in osteoclast phagolysosomes (mean 6.9) than in THP.1 phagolysosomes. The protein levels of subunit A, a member of the V1-sector of V-ATPase, mirror a3 levels rather than a1 levels, indicating that the increased a3 levels on osteoclast phagolysosomes represent assembled V-ATPase, not only the Vo-sector.

5.4   PHAGOLYSOSOMES LOCALIZE TO SITES OF OSTEOCLAST-
BONE CONTACT (II)

To prove the relevance of using phagolysosomal V-ATPase as ruffled border V-ATPase, we expected that the phagocytosed latex beads would localise to the ruffled border area in resorbing osteoclasts. However, this could not be confirmed because resorbing osteoclasts on bone did not phagocytose latex beads. However, when we added bone particles to osteoclasts on coverslips that already had phagocytosed latex beads, the phagolysosomes relocalized and concentrated to the vicinity of the bone particle in many osteoclasts. This

event appeared to be actin-dependent since it was not observed in osteoclasts where bone particles were without associated actin-filament staining.

5.5   ACIDIFICATION AND INHIBITOR SENSITIVITY OF ISOLATED PHAGOLYSOSOMES (II)

The phagolysosomes isolated from both osteoclasts and THP.1 cells acidified by a Bafilomycin A1 sensitive V-ATPase. After adjusting the amounts of phagolysosomes so that 0.3 nM Bafilomycin A1 inhibited approximately 50% of the acidification-mediated fluorescence quench, SB242784 at concentrations of 3, 10, and 30 nM inhibited both sources of phagolysosomes very similarly, although the relative sensitivity of osteoclast phagolysosomes to SB242784 appeared to be very slightly higher (Fig. 6, II). This result shows that phagolysosomal acidification is very sensitive to SB242784 and indicates that there is very little, if any, selectivity of SB242784 for the V-ATPase of osteoclast phagolysosomes over that of THP.1 phagolysosomes. However, phagolysosomes from osteoclasts appeared to acidify more rapidly than those of THP.1 cells did.

5.6   BONE RESORPTION AND LYSOSOMAL ACIDIFICATION ARE DIFFERENTIALLY SENSITIVE TO V-ATPase INHIBITION (III)

5.6.1   *Inhibition of bone resorption by Bafilomycin A1 and SB242784*

As assayed by the CTX concentration in the culture medium of human osteoclasts after 3 day incubations, both inhibitors dose-dependently inhibited bone resorption and 3 nM Bafilomycin A1 completely inhibited the release of CTX. For SB242784, 100 nM CTX almost completely inhibited CTX release. The inhibition of resorption was not due to cytotoxicity, since the osteoclast numbers were unaltered by Bafilomycin A1 up to 10 nM and SB242784 up to 300 nM (not shown).

5.6.2   *Dose-response of Bafilomycin A1 and SB242784 on lysosomal pH in osteoclasts*

Bafilomycin A1 concentrations lower than 30 nM did not raise the lysosomal pH above pH 5.5 and 30 nM raised the lysosomal pH to about 6.3. For SB242784, the highest concentration that we were able to use, 1000 nM, did not raise the pH above 5.5. Since SB242784 is a colored compound, we were concerned that the lack of effect was due to some interference with the FITC-TRITC signal. However neutral osteoclasts were present, and when cells were treated with both 30 nM Bafilomycin A1 and 1000 nM SB242784, the effect was additive compared to 30 nM Bafilomycin A1, showing that the V-ATPase inhibitory effect of 1000 nM SB242784 was not blocked by interference with the FITC-TRITC signal.

5.7   INTRACELLULAR AND EXTRACELLULAR DEGRADATION OF BONE ARE DIFFERENTIALLY SENSITIVE TO V-ATPase INHIBITION (III)

We hypothesized that the anatomy of the resorbing osteoclast contributes to the hypersensitivity of bone resorption to V-ATPase inhibition compared with other lysosomal functions. We tested this hypothesis by examining whether osteoclasts are able to degrade

phagocytosed bone in the presence of SB242784 at a concentration at which extracellular bone is inhibited.

5.7.1 600 nM SB242784 inhibits extracellular dissolution of bone mineral

Two days after the addition of 600 nM SB242784 to osteoclasts on bone slices very few of the osteoclasts were associated with pits as evidenced by lack of exposed collagen staining, while the in the control, most of the actin rings of the osteoclasts were associated with extensive collagen staining.

5.7.2 600 nM SB242784 does not inhibit degradation of phagocytosed bone fragments

We added small (less than five micrometer in diameter) bone particles to osteoclasts on coverslips and transferred the coverslips to medium with or without 600 nM SB242784. The phagocytosis and degradation of bone was evaluated on samples fixed at timepoints 1h, 24h and 72h, and stained. At the one-hour timepoint there were large bone particle-accumulations associated with, but not necessarily phagocytosed by the osteoclasts. 24 hours later, most of the bone particle-accumulations were replaced by discrete intracellular localization of the bone particles. In both treated and untreated samples from the 72 hours timepoint, most of the osteoclasts were devoid of collagen staining, and no particulate matter was observable. Thus, osteoclasts efficiently phagocytosed and degraded bone particles in both control and SB242784-treated cells.

Furthermore, from the staining intensities of the samples treated with 600 nM SB242784 at the 1 and 24 hours timepoints it was apparent that upon phagocytosis particles lost calcein fluorescence and gained collagen-staining, indicating that bone mineral is dissolved and more collagen is exposed. Thus, osteoclasts are capable of degrading bone particles intracellularly in the presence of 600 nM SB242784.

5.8 STRUCTURE-ACTIVITY RELATIONSHIP OF SPIN-LABELLED SB242784 ANALOGUES (IV)

We characterized the spin-labelled analogues (Figure 14) of SB242784 with respect to potency and selectivity in acidification assays with microsome preparations from chicken brain and bone. The SB242784 (INDOL0) showed a 5-fold selectivity for bone microsome acidification. The INDOL6, which closely mimics SB242784, was equally potent, but the tissue selectivity was essentially lost. The INDOL5 derivative optimized for electron paramagnetic resonance spectroscopy studies was more than two orders of magnitude less potent than the parental compound. Despite the decreased inhibitor potency, INDOL5 bound to the subunit c analogue of Nephrops norvegicus (which has 80% amino acid identity with the human c subunit), as assayed by electron paramagnetic resonance spectroscopy.
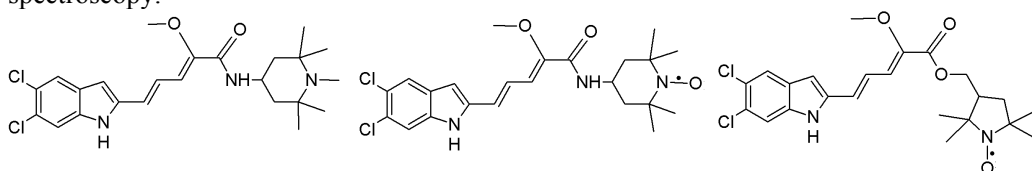

Figure 14. The structure of SB242784 (left), INDOL6 (middle) and INDOL5 (right).

6   DISCUSSION

6.1   DOWNREGULATION OF a3 BY siRNA

Our paper (I) was one of the very first to show that gene expression in osteoclast can be downregulated by siRNA molecules, although osteoclasts are considered resistant to conventional plasmid transfections. Since year 2005, the number of articles utilizing siRNA-mediated knockdown of different targets in osteoclasts has been increasing. Our results support the reported phenotype resulting from nonfunctional a3; a3 is essential for efficient resorption, but not for cell viability. However, compared to inhibition of V-ATPase activity by inhibitors, there was a differential outcome of siRNA-mediated inhibition: a fraction of the osteoclasts showed apparently disrupted actin rings.

RNA interference as a therapeutic treatment of diseases has progressed rapidly into early stage clinical testing of siRNAs for a variety of diseases. There are, however, problems to be solved concerning the delivery and uptake; currently the siRNA approach may be considered promising (Tiemann and Rossi 2009). The V-ATPase may be rate limiting for bone resorption, as discussed later. Thus, a partial down-regulation of a3 may be sufficient to obtain a beneficial effect on bone resorption.

6.2   SUBCELLULAR LOCALIZATION OF SUBUNIT a3

The results concering the subcellular distibution of a3 are in agreement with previous studies showing an lysosomal localization of a3 in macrophages, and ruffled border localization of a3 in resorbing osteoclasts (Toyomura *et al.* 2003). However, in pancreatic β-cells, a3 has been demonstrated in the membrane of insulin-containing secretory granules, with less perfect colocalization of a3 with LAMP-2 in these cells (Sun-Wada *et al.* 2006). Among the five anterior pituitary cell types expressing different hormones, a3 appeared to colocalize with growth hormone (but not with other hormones) (Sun-Wada *et al.* 2007), indicating that a3 may not be strictly lysosomal. We observed no colocalization of a3 with early endosome antigen-1 or with matrix metalloproteinase-9 (II, Fig. 2c, d). This does not exclude low levels of a3 in these nonlysosomal organelles. However, we can conclude that the bulk of the a3 protein in osteoclasts is localized to lysosomes/late endosomes in human osteoclasts. Furthermore, our finding that two a isoforms are present on phagolysosomes isolated from both osteoclasts and THP.1 cells, suggest that isoforms may overlap.

6.3   PHAGOLYSOSOMAL V-ATPASE MAY WELL REPRESENT
THE RUFFLED BORDER V-ATPase

The ruffled border has long been considered the analogue of the lysosomes and late endosomes, and it is thought to mainly be formed by exocytosis and fusion of lysosomes with the plasma membrane facing the bone surface (Stenbeck 2002). The only previous study on isolated phagolysosomes from osteoclasts demonstrated that osteoclast phagolysosomes contain cathepsin K (Sakai *et al.* 2001), which is secreted into the resorption lacuna. Encouraged by this study, we speculated that phagolysosomes may carry the ruffled border V-ATPase, and that the ruffled border acid transport mechanism is represented by isolated phagosomes

Three independent facts suggest that the phagolysosomal V-ATPase represents the ruffled border V-ATPase. First, the high level of a3 expression in the osteoclast was represented on the isolated phagolysosomes (II, Fig. 4). Second, in living osteoclasts, the latex bead-containing phagolysosomes relocalized to the close vicinity of subsequently added bone particles (II Fig. 3b, c), mimicking the polarization of a3 in the resorbing osteoclast. Third, acidification of isolated phagolysosomes was highly sensitive to the SB242784 compound; in fact, the relative sensitivity to SB242784 was higher for osteoclast phagolysosomes than for microsomes derived from chicken bone.

6.4 LACK OF EVIDENCE FOR A STRUCTURALLY UNIQUE OSTEOCLAST V-ATPase

One of the main aims of this study was to find out whether the osteoclast V-ATPase is structurally unique in some aspect. Such a structural uniqueness, if "drugable", would permit selective inhibition of bone resorption without affecting other V-ATPase-mediated functions. However, if the ruffled border forms by the fusion of lysosomes with the plasma membrane, it may contain a common lysosomal V-ATPase that is only quantitatively upregulated, or it may possess a qualitatively unique subunit composition. The methodology we used allowed us to compare the a3-positive compartment from osteoclasts with the corresponding compartment from monocytic THP.1 cells. In this comparison, we found that phagolysosomes from THP.1 cells also contained the a3 isoform (II, Fig. 4), although significantly less than did osteoclast phagolysosomes, and that the SB242784 compound inhibited acidification of the isolated phagolysosomes from both sources at similar concentrations (II, Fig. 6.). We believe that the small difference in relative sensitivity to SB242784 between osteoclasts and THP.1 phagolysosomes is due to the differential a3/a1 ratios (II, Fig. 4), rather than representing a true pharmacological difference. Thus, we have no indication of a qualitative difference between the V-ATPases from the two sources. Rather than indicating something unique, the high level of a3 expression in the osteoclast and its phagolysosomes may represent the fact that a high level of lysosomal V-ATPase is needed for efficient bone resorption, while significantly less V-ATPase is needed to maintain lysosomal pH in other cells.

6.5 PHAGOLYSOSOMES CONTAIN a1 IN ADDITION TO a3

We were surprised by the observation that isoform a1, in addition to isoform a3, was detected on phagolysosomal fraction, since a1 was originally found in clathrin-coated vesicles (Perin *et al.* 1991). However, clathrin was abscent from the phagosomal fraction, as were all the nonlysosomal markers tested, so we do not believe that the presence of a1 in the phagolysosomal fraction is a result of contamination. Our finding is supported by a study in which a1 was found as a component of late endosomes by proteomic analysis (Lafourcade *et al.* 2008). Moreover, by immunostaining, there was some colocalization of a1 with LAMP1, although the bulk did not colocalize (Toyomura *et al.* 2003). One should consider that the organelles are not static structures; transient but frequent membrane trafficking events are also represented by the phagolysosomes. A limitation is that we had no tools to detect wheter both isoforms assembled into active holoenzymes. Nonetheless, the identification of a3 and a1 in model phagolysosomes is the first direct piece of evidence that the a isoforms are not mutually exclusive. The observation could explain why the a3 mutations affect bone selectively, and it has impact on the validation of the a3 subunit as a drug target, as discussed next.

6.6   RELEVANCE OF THE FINDING THAT V-ATPase ISOFORMS MAY OVERLAP

If the V-ATPase isoforms are not mutually exclusive, they could compensate for each other. However, because bone resorption is dependent on the very high level expression of a3 in osteoclasts, isoform compensation may be insufficient for proper bone resorption (Manolson *et al.* 2003). Compensation would explain why a3-deficient patients do not have any lysosomal defects (Blair *et al.* 2004), as would be expected if a3 was the only isoform in this compartment. Moreover, the oc/oc mice do not develop lysosomal storage disease, in contrast to ClC7-deficient mice, which have a comparable osteopetrotic phenotype (Kasper *et al.* 2005). Compensation would explain why there is some residual bone resorption left in a3-defective osteoclasts (Taranta *et al.* 2003; Del Fattore *et al.* 2006). Evidence of at least a partial functional compensation of a3 by another V-ATPase comes from macrophages from mice with a disrupted gene for a3, which acidified phagosomes by a Bafilomycin-sensitive mechanism (Sun-Wada *et al.* 2009). Moreover, these cells had normal levels of mature cathepsins and were capable of bacterial killing, albeit at a significantly slower rate than control macrophages (Sun-Wada *et al.* 2009).

 The phenotype of patients with defective a3 function suggests that a3 is a valid target, since except for bone resorption, no other obvious vital V-ATPase a3 mediated functions have been identified. Furthermore, partial inhibition of bone resorption may be sufficient for a beneficial effect on bone. Therefore, one could expect that the adverse effects resulting from partial inhibition with an isoform a3-selective inhibitor would be less severe than the effects resulting from complete lack of a3-protein.

6.7   THE HYPERSENSITIVITY OF BONE RESORPTION TO V-ATPase INHIBITION

When we compared the V-ATPase inhibitor sensitivity of lysosomal acidification and bone resorption, which we believe are mediated by identical V-ATPases, we found that bone resorption is more than tenfold more sensitive as assayed by full inhibition. Our results are consistent with data from similar assays reported in litterature, Sundquist et al. reported that osteoclast resorption was fully inhibited by 3 nM Bafilomycin A1 (Sundquist *et al.* 1990), wheras 100 nM Bafilomycin was needed to block the acidification of intracellular vesicles in osteoclasts as assayed by acridine orange fluorescence (Palokangas *et al.* 1997; Sorensen *et al.* 2007). For SB242784 we are not aware of any previous studies assaying lysosomal acidification.

However, for two other V-ATPase inhibitors, diphyllin and FR167356 there is some data available. Diphyllin inhibited bone resorption with an IC50 of 14 nM, while intravesicular acidification of osteoclasts, as assayed by acridine orange fluorescence, was dose-dependently inhibited at concentrations between 125-1000 nM (Sorensen *et al.* 2007). FR167356 inhibited resorption pit formation at with an IC50 of 190nM, wheras the IC50 of two lysosome-dependent processes, cholesterol ester accumulation in macrophages, and degradation of internalized LDL in hepatocytes were 7800 nM and 5200 nM, respectively (Niikura *et al.* 2004). Thus, in cell culture experiments, four structurally non-related inhibitors with different potencies; Bafilomycin A1, SB242784, FR167367 and diphyllin, all inhibit bone resorption at significantly lower concentrations than they inhibit lysosome acidification or lysosomal functions.

6.8 AN EXPLANATION FOR THE HYPERSENSITIVITY

We could think of several principal differences between bone resorption and lysosomal function, related to the chemical properties of bone mineral and the anatomy of the osteoclast that together may explain this hypersensitivity. The explanation is presented and discussed below.

To start with, the primary role of the ruffled border V-ATPase is to dissolve bone mineral. The main component of bone mineral, calcium hydroxyapatite, is dissolved by acid, according to the equation:

$$[Ca_{10}(PO_4)_6(OH)_2]_{solid} + 14H^+ = 10Ca^{2+} + 6H_2PO_4^- + 2H_2O$$
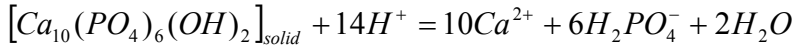
However, as presented in the review of the literature, bone dissolution is governed by the law of mass action, from which follows that the ionic activity product must be lower than the solubility product constant, for bone to dissolve. Reducing the pH dramatically reduces the concentration of PO_4^{3-} in addition to OH^- so that in practice, a pH-threshold exists, below which the pH must be kept for mineral dissolution to proceed. In the rest of the discussion, I refer to this pH-threshold and for simplicity, I anticipate that the quantity of bone dissolved is directly proportional to the quantity of excess protons, according to the above equation.

The primary role of the V-ATPase in the lysosomal membrane is to maintain a proton equilibrium according to (1):

$$K_{eq} = \frac{[H^+_{lysosome}]}{[H^+_{cytosol}]} \quad (1)$$

in which the Keq is empirically known to be in the range of 2,4 pH units (i.e. pH 7,2-7,4 in the cytosol and pH 4,8-5,0 in the lysosome). Proton transport into and out of the lysosome determines the equilibrium according to (2):

$$k_f[H^+_{cytosol}] = k_r[H^+_{lysosome}] \quad (2)$$

in which k_f and k_r represents transport rates in (e.g. V-ATPase activity), and out of the lysosome (e.g. proton leakage), respectively. By rearranging (2) to (3)

$$\frac{k_f}{k_r} = \frac{[H^+_{lysosome}]}{[H^+_{cytosol}]} \quad (3)$$

and combining (3) with (1), we get equation (4), in which the impact of inhibiting the V-ATPase on lysosomal pH can be theoretically calculated.

$$\frac{k_f}{k_r} = K_{eq} \quad (4)$$

One can think of the resorption lacuna as an organelle, in which the proton transport rates in and out maintain the proton gradient at equilibrium. However, the proton transport rates are more complex than for lysosomes, since the resorption space is fundamentally different from lysosomes. The resorption lacuna is hemivacuolar in structure, limited by the bone surface and the osteoclast and its sealing zone.

Thus, we think that, of the total ruffled border V-ATPase activity at a given situation, a certain fraction of the activity maintains the pH threshold, which is opposed by the leakage of protons out of the resorption lacuna. Furthermore, because the pH threshold always must be reached before bone resorption can take place, only the excess V-ATPase activity is used to dissolve bone. Thus, ultimately, the proton leakage rate and the pH threshold, at which the fluid in the resorption lacuna is undersaturated with respect to the bone mineral ion constitients, are important determinants of bone resorption. If the proton diffusion rate out of the resorption lacuna is considerable and the pH threshold is low, i.e. difficult to reach, the excess V-ATPase activity that actually dissolves bone could be considerable small. If, for instance, 50% of the ruffled border V-ATPase activity is needed to maintain the equilibrium, inhibition of the V-ATPase by 50% would result in full inhibition of bone resorption. This is because the remaining activity is only sufficient to maintain the equilibrium and there is no exess V-ATPase activity for actual bone mineral dissolution.
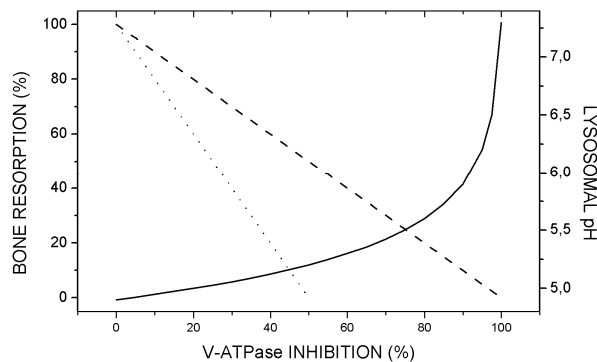

Figure 15. The response of lysosomal pH (solid line) and bone resorption to V-ATPase inhibition in the hypothetical situations where 100% (dashed line) and 50% (dotted line) of the ruffled border V-ATPase activity is used to dissolve bone.

In order to illustrate that V-ATPase inhibition affects bone resorption and lysosomal pH differentially, we have plotted bone resorption and lysosomal pH as functions of the percentage of V-ATPase inhibition in Figure 15. The dashed and dotted lines represent bone resorption in the hypothetical situations where 100% and 50%, respectively, of the ruffled border V-ATPase activity is used to dissolve bone. Lysosomal pH is calculated from equation 4 in a situation where lysosomal and cytosolic pH is 4.9 and 7.3, respectively. Because the pH scale is logarithmic, this curve is exponential. Figure 15 shows that compared to the situation where all the V-ATPase activity would be used for bone dissolution, in the situation where 50% of the V-ATPase activity is consumed in the maintenance of pH threshold, the dose response curve of bone resorption is shifted to the left, i.e. sensitized to V-ATPase inhibition. Furhermore, inhibition of the V-ATPase by 50 % reduces the proton gradient by half, however on the logarithmic pH scale, this results in

an increase in lysosomal pH from 4.9 to 5.2, an increment that may not be too dramatic in terms of consequences on lysosomal function. We suggest that the hypothesis that only a fraction of the total ruffled border V-ATPase is available for bone resorption explains the relative hypersensitivity of bone resorption to V-ATPase inhibition. Furthermore, we suggest that the fraction is determined by the total ruffled border V-ATPase activity, proton diffusion rate and the dissolution properties of bone mineral. However, direct evidence that this is the main mechanism behind the hypersensitivity is difficult to provide, since it would require that the ruffled border V-ATPase activity, proton diffusion rate out of the resorption lacuna could be measured *in situ*.

6.9 ANOTHER DIFFERENCE BETWEEN BONE RESORPTION AND LYSOSOMAL FUNCTION

Another principal difference is that the V-ATPase activity is rate limiting for bone resorption, while the role in the lysosomal membrane is to provide an appropriately low pH for the degradative enzymes. Furthermore, it may be speculated that lysosomal function may possess a reserve capacity, analogous to the overcapacity of the liver at the organ level, where up to 74% of the liver may be removed before the risk of severe hepatic dysfunction increases significantly (Schindl *et al.* 2005). The practical impact of this scenario would be that a small decrease in lysosomal enzyme reaction rate caused by an increase in lysomal pH may have no effect on overall physiology and thus, adverse effects on lysosomal function would not be a problem.

6.10 FUTURE ASPECTS

As presented in the preceeding discussion, we suggest that selectivity for bone resorption could be obtained by developing V-ATPase a3 isoform selective inhibitors. Currently it is hard to imagine any V-ATPase a3-mediated function other than bone resorption that would be particularly sensitive to inhibition. However, for many drugs, adverse effects are not identified until clinical trials are performed.

The V-ATPase is very "drugable", as shown by the rather high number of inhibitors identified, and the data indicating different binding sites for these inhibitors. Is it possible to achieve highly isoform a3-selective inhibitors? The development of isoform-selective synthetic inhibitors has been hampered by the lack of detailed structural information on the V-ATPase, especially concerning the a subunit. Furthermore, the natural inhibitors may not have evolved to inhibit a particular V-ATPase isoform. However, the tissue selectivity of SB242784 is likely to be mediated through the a isoform. It was developed based on structure-activity studies of the plecomacrolides, the binding site of which is in the outer aspect the proteolipid ring, allowing interaction with the a subunit. The lack of isoform-pure V-ATPase preparations has hampered the screening of isoform-selective compounds.

Compared to the existing drugs for osteoporosis, a V-ATPase inhibitor would be classified as an antiresorptive agent like the bisphosphonates and Denosumab. A critical question is whether it can be expected that a V-ATPase inhibitor would be a better drug than the existing ones.

6.11 THE V-ATPase INHIBITOR IN OSTEOPOROSIS -COMPARISON TO ESTABLISHED DRUGS

As presented in the review, the current osteoporosis drugs differ considerable with respect to their targets and mechanisms of action. A V-ATPase inhibitor as a drug for preventing osteoporosis would be similar to bisphosphonates and Denosumab in that bone resorption is inhibited. However, significant principal differences are obvious. Denosumab acts mainly by preventing the formation of osteoclasts, i.e. earlier than a V-ATPase inhibitor, which would act on mature resorbing osteoclasts. Bisphosphonates also acts on resorbing osteoclasts, since resorption is needed for the uptake of bisphosphonates. However, the nitrogen-containing bisphosphonates used in osteoporosis inhibit all prenylation-dependent cell functions, not specifically bone resorption. A V-ATPase inhibitor would inhibit only bone resorption, leaving other cell functions intact. It has been shown that inhibiting bone resorption through the V-ATPase or chloride channel actually increases the life span of the osteoclasts in vitro (Nielsen *et al.* 2007). Furthermore, osteoclasts increased their secretion of tartrate resistant acid phosphatase when bone resorption was completely inhibited by V-ATPase inhibitors in vitro (Sorensen *et al.* 2007), while it is clear that plasma levels of tartrate resistant acid phosphatase decrease and correlate with CTX levels in alendronate treated patients (Nenonen *et al.* 2005).

In this respect, there is data indicating that viable osteoclasts are needed to support bone formation (Martin and Sims 2005; Karsdal *et al.* 2007) possibly by secretion of some factors, since osteoclast conditioned media stimulates bone formation by osteoclasts in vitro (Karsdal *et al.* 2008). It is thus possible that a V-ATPase inhibitor would support bone formation more than the bisphosphonates and Denosumab do. If this was the case it is tempting to speculate that V-ATPase inhibitors could be used in combination with the anabolic agents in contrast to alendronate, which attenuated the anabolic action of PTH (Black *et al.* 2005).

A potential problem with the antiresorptive drugs is that the repair of bone microfractures also inhibited, which may predispose to atypical fractures. However, the scope of this potential problem is not yet established (Shane *et al.* 2010). Furthermore, at least in animal models of fracture repair alendronate delays remodeling of the callus of wowen bone (Cao *et al.* 2002). In this sense, a drawback of the long half-lives of Denosumab and especially the bisphosphonates is that the drug effects are not easily adjustable. A V-ATPase inhibitor would probably be more like a traditional drug with respect to terminal half-life, thus the dosing could be rapidly adjusted and the treatment terminated if desired.

7   CONCLUSIONS

The V-ATPase isoform a3 is essential for proper bone resorption. a3 is highly expressed in osteoclasts and in nonresorbing osteoclasts it localized to the lysosomes, which form the bulk of the ruffled border in resorbing osteoclasts. Phagolysosomes isolated from osteoclasts contain high levels of a3 isoform.

Isoform a3 is also present in phagolysosomes of THP.1 cells, and it may be a common lysosomal isoform, since it is ubiquitously expressed. We found no evidence that the acidification of osteoclast phagolysosomes and the acidification of THP phagolysosomes differ with respect to pharmacology, since they were equally sensitive to inhibition with SB242784, an inhibitor that clearly show selectivity between V-ATPase from different tissues. However, one cannot exclude the possibility that the osteoclast V-ATPase would have some unique structural feature(s) that allows its selective inhibition.

We could identify two distinct V-ATPase structure-independent mechanisms by which bone resorption can be selectively inhibited.

The first is **differential compensation**. We observed that isoform a1 is also present in the phagolysosomes, showing that the V-ATPase isoforms are not mutually exclusive. The a isoforms may overlap and, at least partly, compensate for each other. Osteoclasts are dependent on a high level of a3 for bone resorption, this function is therefore very poorly compensated for when a3 is nonfunctional or lacking, while for instance lysosomal pH is sufficiently compensated for, in order to maintain lysosomal function. This scenario remains to be furher elucidated but it would explain why osteopetrosis is the very dominant outcome of inactivating mutations of the gene for a3. In these patients, no other phenotypes than those that are considered secondary to the bone phenotype have yet been identified. Thus, the currently available data suggest that inhibitors selective for the V-ATPase a3 isoform would be very selective for bone resorption for the reason of differential compensation.

The second mechanism is based on **the unique anatomy of the resorbing osteoclast and the solubility of bone mineral**. According to this mechanism, bone resorption is hypersensitive to V-ATPase inhibition compared to the ubiquitous role of V-ATPases, i.e. organellar acidification. This is because for bone mineral dissolution to proceed, a critical pH value must be reached, and only the excess protons are available for bone resorption. At any time, a fraction of the ruffled border V-ATPase activity is actually resorbing bone, while the other fraction is maintaining the pH threshold. To inhibit bone resorption completely, it is sufficient to inhibit the former fraction. The fraction of V-ATPase activity available for actual bone resorption is determined by the critical pH value and the leakage of protons out of the resorption lacuna, which may be considerable. The situation in the resorption lacuna is very different compared to the acidification of organells; here all the V-ATPase activity contributes to the acidification.

The second mechanism explains the differential inhibitory effect on lysosomal acidification and bone resorption by V-ATPase inhibitors, previously observed by others and confirmed in this study. It also explains why it is possible to inhibit bone resorption

with inhibitors having poor selectivity and even lacking selectivity (Bafilomycin A1) in animal models of osteoporosis.

The two mechanisms are, to some extent, additive and suggest that bone resorption can be very selectively inhibited by targeting the isoform a3-containing V-ATPase.

8   ACKNOWLEDGEMENTS

9   REFERENCES

Aaron, J. E., N. B. Makins and K. Sagreiya (1987). The microanatomy of trabecular bone loss in normal aging men and women. Clin Orthop Relat Res(215): 260-71.

Abrahams, J. P., A. G. Leslie, R. Lutter and J. E. Walker (1994). Structure at 2.8 A resolution of F1-ATPase from bovine heart mitochondria. Nature **370**(6491): 621-8.

Aguirre, J. I., L. I. Plotkin, S. A. Stewart, R. S. Weinstein, A. M. Parfitt, S. C. Manolagas and T. Bellido (2006). Osteocyte apoptosis is induced by weightlessness in mice and precedes osteoclast recruitment and bone loss. J Bone Miner Res **21**(4): 605-15.

Ajubi, N. E., J. Klein-Nulend, M. J. Alblas, E. H. Burger and P. J. Nijweide (1999). Signal transduction pathways involved in fluid flow-induced PGE2 production by cultured osteocytes. Am J Physiol **276**(1 Pt 1): E171-8.

Ali, S. Y., S. W. Sajdera and H. C. Anderson (1970). Isolation and characterization of calcifying matrix vesicles from epiphyseal cartilage. Proc Natl Acad Sci U S A **67**(3): 1513-20.

Alzamora, R., R. F. Thali, F. Gong, C. Smolak, H. Li, C. J. Baty, C. A. Bertrand, Y. Auchli, R. A. Brunisholz, D. Neumann, K. R. Hallows and N. M. Pastor-Soler (2010). PKA regulates vacuolar H+-ATPase localization and activity via direct phosphorylation of the a subunit in kidney cells. J Biol Chem **285**(32): 24676-85.

Andersen, T. L., T. E. Sondergaard, K. E. Skorzynska, F. Dagnaes-Hansen, T. L. Plesner, E. M. Hauge, T. Plesner and J. M. Delaisse (2009). A physical mechanism for coupling bone resorption and formation in adult human bone. Am J Pathol **174**(1): 239-47.

Aoki, S., M. Honma, Y. Kariya, Y. Nakamichi, T. Ninomiya, N. Takahashi, N. Udagawa and H. Suzuki (2010). Function of OPG as a traffic regulator for RANKL is crucial for controlled osteoclastogenesis. J Bone Miner Res **25**(9): 1907-21.

Arata, Y., J. D. Baleja and M. Forgac (2002b). Cysteine-directed cross-linking to subunit B suggests that subunit E forms part of the peripheral stalk of the vacuolar H+-ATPase. J Biol Chem **277**(5): 3357-63.

Arata, Y., J. D. Baleja and M. Forgac (2002a). Localization of subunits D, E, and G in the yeast V-ATPase complex using cysteine-mediated cross-linking to subunit B. Biochemistry **41**(37): 11301-7.

Atkins, G. J., K. J. Welldon, P. Halbout and D. M. Findlay (2009). Strontium ranelate treatment of human primary osteoblasts promotes an osteocyte-like phenotype while eliciting an osteoprotegerin response. Osteoporos Int **20**(4): 653-64.

Bacabac, R. G., T. H. Smit, M. G. Mullender, S. J. Dijcks, J. J. Van Loon and J. Klein-Nulend (2004). Nitric oxide production by bone cells is fluid shear stress rate dependent. Biochem Biophys Res Commun **315**(4): 823-9.

Baig, A. A., J. L. Fox, Z. Wang, W. I. Higuchi, S. C. Miller, A. M. Barry and M. Otsuka (1999). Metastable equilibrium solubility behavior of bone mineral. Calcif Tissue Int **64**(4): 329-39.

Bakker, A., J. Klein-Nulend and E. Burger (2004). Shear stress inhibits while disuse promotes osteocyte apoptosis. Biochem Biophys Res Commun **320**(4): 1163-8.

Bauer, D. C., P. Garnero, J. P. Bilezikian, S. L. Greenspan, K. E. Ensrud, C. J. Rosen, L. Palermo and D. M. Black (2006). Short-term changes in bone turnover markers and bone mineral density response to parathyroid hormone in postmenopausal women with osteoporosis. J Clin Endocrinol Metab **91**(4): 1370-5.

Bellido, T., A. A. Ali, I. Gubrij, L. I. Plotkin, Q. Fu, C. A. O'Brien, S. C. Manolagas and R. L. Jilka (2005). Chronic elevation of parathyroid hormone in mice reduces expression of sclerostin by osteocytes: a novel mechanism for hormonal control of osteoblastogenesis. Endocrinology **146**(11): 4577-83.

Beno, T., Y. J. Yoon, S. C. Cowin and S. P. Fritton (2006). Estimation of bone permeability using accurate microstructural measurements. J Biomech **39**(13): 2378-87.

Beyenbach, K. W. and H. Wieczorek (2006). The V-type H+ ATPase: molecular structure and function, physiological roles and regulation. J Exp Biol **209**(Pt 4): 577-89.

Black, D. M., J. P. Bilezikian, K. E. Ensrud, S. L. Greenspan, L. Palermo, T. Hue, T. F. Lang, J. A. McGowan and C. J. Rosen (2005). One year of alendronate after one year of parathyroid hormone (1-84) for osteoporosis. N Engl J Med **353**(6): 555-65.

Black, D. M., A. V. Schwartz, K. E. Ensrud, J. A. Cauley, S. Levis, S. A. Quandt, S. Satterfield, R. B. Wallace, D. C. Bauer, L. Palermo, L. E. Wehren, A. Lombardi, A. C. Santora and S. R. Cummings (2006). Effects of continuing or stopping alendronate after 5 years of treatment: the Fracture Intervention Trial Long-term Extension (FLEX): a randomized trial. Jama **296**(24): 2927-38.

Blair, H. C., C. W. Borysenko, A. Villa, P. H. Schlesinger, S. E. Kalla, B. B. Yaroslavskiy, V. Garcia-Palacios, J. I. Oakley and P. J. Orchard (2004). In vitro differentiation of CD14 cells from osteopetrotic subjects: contrasting phenotypes with TCIRG1, CLCN7, and attachment defects. J Bone Miner Res **19**(8): 1329-38.

Blair, H. C., S. L. Teitelbaum, R. Ghiselli and S. Gluck (1989). Osteoclastic bone resorption by a polarized vacuolar proton pump. Science **245**(4920): 855-7.

Blair, J. M., H. Zhou, M. J. Seibel and C. R. Dunstan (2006). Mechanisms of disease: roles of OPG, RANKL and RANK in the pathophysiology of skeletal metastasis. Nat Clin Pract Oncol **3**(1): 41-9.

Blake, G. M. and I. Fogelman (2007). The role of DXA bone density scans in the diagnosis and treatment of osteoporosis. Postgrad Med J **83**(982): 509-17.

Bockelmann, S., D. Menche, S. Rudolph, T. Bender, S. Grond, P. von Zezschwitz, S. P. Muench, H. Wieczorek and M. Huss (2010). Archazolid A binds to the equatorial region of the c-ring of the vacuolar H+-ATPase. J Biol Chem **285**(49): 38304-14.

Boivin, G., P. Deloffre, B. Perrat, G. Panczer, M. Boudeulle, Y. Mauras, P. Allain, Y. Tsouderos and P. J. Meunier (1996). Strontium distribution and interactions with bone mineral in monkey iliac bone after strontium salt (S 12911) administration. J Bone Miner Res **11**(9): 1302-11.

Bond, S. and M. Forgac (2008). The Ras/cAMP/protein kinase A pathway regulates glucose-dependent assembly of the vacuolar (H+)-ATPase in yeast. J Biol Chem **283**(52): 36513-21.

Bone, H. G., D. Hosking, J. P. Devogelaer, J. R. Tucci, R. D. Emkey, R. P. Tonino, J. A. Rodriguez-Portales, R. W. Downs, J. Gupta, A. C. Santora and U. A. Liberman (2004). Ten years' experience with alendronate for osteoporosis in postmenopausal women. N Engl J Med **350**(12): 1189-99.

Bonewald, L. F. (2006). Mechanosensation and Transduction in Osteocytes. Bonekey Osteovision **3**(10): 7-15.

Bonnelye, E., A. Chabadel, F. Saltel and P. Jurdic (2008). Dual effect of strontium ranelate: stimulation of osteoblast differentiation and inhibition of osteoclast formation and resorption in vitro. Bone **42**(1): 129-38.

Boskey, A. L., S. Gadaleta, C. Gundberg, S. B. Doty, P. Ducy and G. Karsenty (1998). Fourier transform infrared microspectroscopic analysis of bones of osteocalcin-deficient mice provides insight into the function of osteocalcin. Bone **23**(3): 187-96.

Bowman, B. J. and E. J. Bowman (2002). Mutations in subunit C of the vacuolar ATPase confer resistance to bafilomycin and identify a conserved antibiotic binding site. J Biol Chem **277**(6): 3965-72.

Bowman, B. J., M. E. McCall, R. Baertsch and E. J. Bowman (2006). A model for the proteolipid ring and bafilomycin/concanamycin-binding site in the vacuolar ATPase of Neurospora crassa. J Biol Chem **281**(42): 31885-93.

Bowman, E. J., L. A. Graham, T. H. Stevens and B. J. Bowman (2004). The bafilomycin/concanamycin binding site in

subunit c of the V-ATPases from Neurospora crassa and Saccharomyces cerevisiae. J Biol Chem **279**(32): 33131-8.

Boyd, M. R., C. Farina, P. Belfiore, S. Gagliardi, J. W. Kim, Y. Hayakawa, J. A. Beutler, T. C. McKee, B. J. Bowman and E. J. Bowman (2001). Discovery of a novel antitumor benzolactone enamide class that selectively inhibits mammalian vacuolar-type (H+)-atpases. J Pharmacol Exp Ther **297**(1): 114-20.

Brennan, T. C., M. S. Rybchyn, W. Green, S. Atwa, A. D. Conigrave and R. S. Mason (2009). Osteoblasts play key roles in the mechanisms of action of strontium ranelate. Br J Pharmacol **157**(7): 1291-300.

Britz, H. M., C. D. Thomas, J. G. Clement and D. M. Cooper (2009). The relation of femoral osteon geometry to age, sex, height and weight. Bone **45**(1): 77-83.

Brown, J. P., R. L. Prince, C. Deal, R. R. Recker, D. P. Kiel, L. H. de Gregorio, P. Hadji, L. C. Hofbauer, J. M. Alvaro-Gracia, H. Wang, M. Austin, R. B. Wagman, R. Newmark, C. Libanati, J. San Martin and H. G. Bone (2009). Comparison of the effect of denosumab and alendronate on BMD and biochemical markers of bone turnover in postmenopausal women with low bone mass: a randomized, blinded, phase 3 trial. J Bone Miner Res **24**(1): 153-61.

Brown, W. E., Chow, L. C. (1976). Chemical properties of bone mineral. Annu. Rev. Mater. Sci. **6**: 213-236.

Canalis, E., M. Hott, P. Deloffre, Y. Tsouderos and P. J. Marie (1996). The divalent strontium salt S12911 enhances bone cell replication and bone formation in vitro. Bone **18**(6): 517-23.

Cao, Y., S. Mori, T. Mashiba, M. S. Westmore, L. Ma, M. Sato, T. Akiyama, L. Shi, S. Komatsubara, K. Miyamoto and H. Norimatsu (2002). Raloxifene, estrogen, and alendronate affect the processes of fracture repair differently in ovariectomized rats. J Bone Miner Res **17**(12): 2237-46.

Caudrillier, A., A. S. Hurtel-Lemaire, A. Wattel, F. Cournarie, C. Godin, L. Petit, J. P. Petit, E. Terwilliger, S. Kamel, E. M.

Brown, R. Mentaverri and M. Brazier (2010). Strontium ranelate decreases receptor activator of nuclear factor-KappaB ligand-induced osteoclastic differentiation in vitro: involvement of the calcium-sensing receptor. Mol Pharmacol **78**(4): 569-76.

Cauley, J. A., J. Robbins, Z. Chen, S. R. Cummings, R. D. Jackson, A. Z. LaCroix, M. LeBoff, C. E. Lewis, J. McGowan, J. Neuner, M. Pettinger, M. L. Stefanick, J. Wactawski-Wende and N. B. Watts (2003). Effects of estrogen plus progestin on risk of fracture and bone mineral density: the Women's Health Initiative randomized trial. Jama **290**(13): 1729-38.

Chattopadhyay, N., S. J. Quinn, O. Kifor, C. Ye and E. M. Brown (2007). The calcium-sensing receptor (CaR) is involved in strontium ranelate-induced osteoblast proliferation. Biochem Pharmacol **74**(3): 438-47.

Chattopadhyay, N., S. Yano, J. Tfelt-Hansen, P. Rooney, D. Kanuparthi, S. Bandyopadhyay, X. Ren, E. Terwilliger and E. M. Brown (2004). Mitogenic action of calcium-sensing receptor on rat calvarial osteoblasts. Endocrinology **145**(7): 3451-62.

Chen, Q., H. Kaji, M. F. Iu, R. Nomura, H. Sowa, M. Yamauchi, T. Tsukamoto, T. Sugimoto and K. Chihara (2003). Effects of an excess and a deficiency of endogenous parathyroid hormone on volumetric bone mineral density and bone geometry determined by peripheral quantitative computed tomography in female subjects. J Clin Endocrinol Metab **88**(10): 4655-8.

Chen, T., J. Berenson, R. Vescio, R. Swift, A. Gilchick, S. Goodin, P. LoRusso, P. Ma, C. Ravera, F. Deckert, H. Schran, J. Seaman and A. Skerjanec (2002). Pharmacokinetics and pharmacodynamics of zoledronic acid in cancer patients with bone metastases. J Clin Pharmacol **42**(11): 1228-36.

Cidon, S., H. Tamir, E. A. Nunez and M. D. Gershon (1991). ATP-dependent uptake of 5-hydroxytryptamine by secretory granules isolated from thyroid parafollicular cells. J Biol Chem **266**(7): 4392-400.

Conrad, K. A. and S. M. Lee (1981). Clodronate kinetics and dynamics. Clin Pharmacol Ther **30**(1): 114-20.

Cooper, C., E. J. Atkinson, W. M. O'Fallon and L. J. Melton, 3rd (1992). Incidence of clinically diagnosed vertebral fractures: a population-based study in Rochester, Minnesota, 1985-1989. J Bone Miner Res **7**(2): 221-7.

Coxon, F. P., K. Thompson and M. J. Rogers (2006). Recent advances in understanding the mechanism of action of bisphosphonates. Curr Opin Pharmacol **6**(3): 307-12.

Croucher, P. I., N. J. Garrahan, R. W. Mellish and J. E. Compston (1991). Age-related changes in resorption cavity characteristics in human trabecular bone. Osteoporos Int **1**(4): 257-61.

Cummings, S. R., D. M. Black, D. E. Thompson, W. B. Applegate, E. Barrett-Connor, T. A. Musliner, L. Palermo, R. Prineas, S. M. Rubin, J. C. Scott, T. Vogt, R. Wallace, A. J. Yates and A. Z. LaCroix (1998). Effect of alendronate on risk of fracture in women with low bone density but without vertebral fractures: results from the Fracture Intervention Trial. Jama **280**(24): 2077-82.

Cummings, S. R., K. Ensrud, P. D. Delmas, A. Z. LaCroix, S. Vukicevic, D. M. Reid, S. Goldstein, U. Sriram, A. Lee, J. Thompson, R. A. Armstrong, D. D. Thompson, T. Powles, J. Zanchetta, D. Kendler, P. Neven and R. Eastell (2010). Lasofoxifene in postmenopausal women with osteoporosis. N Engl J Med **362**(8): 686-96.

Cummings, S. R., J. San Martin, M. R. McClung, E. S. Siris, R. Eastell, I. R. Reid, P. Delmas, H. B. Zoog, M. Austin, A. Wang, S. Kutilek, S. Adami, J. Zanchetta, C. Libanati, S. Siddhanti and C. Christiansen (2009). Denosumab for prevention of fractures in postmenopausal women with osteoporosis. N Engl J Med **361**(8): 756-65.

Dahl, S. G., P. Allain, P. J. Marie, Y. Mauras, G. Boivin, P. Ammann, Y. Tsouderos, P. D. Delmas and C. Christiansen (2001). Incorporation and distribution of strontium in bone. Bone **28**(4): 446-53.

Del Fattore, A., A. Cappariello and A. Teti (2008). Genetics, pathogenesis and complications of osteopetrosis. Bone **42**(1): 19-29.

Del Fattore, A., B. Peruzzi, N. Rucci, I. Recchia, A. Cappariello, M. Longo, D. Fortunati, P. Ballanti, M. Iacobini, M. Luciani, R. Devito, R. Pinto, M. Caniglia, E. Lanino, C. Messina, S. Cesaro, C. Letizia, G. Bianchini, H. Fryssira, P. Grabowski, N. Shaw, N. Bishop, D. Hughes, R. P. Kapur, H. K. Datta, A. Taranta, R. Fornari, S. Migliaccio and A. Teti (2006). Clinical, genetic, and cellular analysis of 49 osteopetrotic patients: implications for diagnosis and treatment. J Med Genet **43**(4): 315-25.

Desjardins, M., L. A. Huber, R. G. Parton and G. Griffiths (1994). Biogenesis of phagolysosomes proceeds through a sequential series of interactions with the endocytic apparatus. J Cell Biol **124**(5): 677-88.

Diab, H., M. Ohira, M. Liu, E. Cobb and P. M. Kane (2009). Subunit interactions and requirements for inhibition of the yeast V1-ATPase. J Biol Chem **284**(20): 13316-25.

Dixon, N., T. Pali, T. P. Kee and D. Marsh (2004). Spin-labelled vacuolar-ATPase inhibitors in lipid membranes. Biochim Biophys Acta **1665**(1-2): 177-83.

Dobnig, H. and R. T. Turner (1995). Evidence that intermittent treatment with parathyroid hormone increases bone formation in adult rats by activation of bone lining cells. Endocrinology **136**(8): 3632-8.

Doty, S. B. (1981). Morphological evidence of gap junctions between bone cells. Calcif Tissue Int **33**(5): 509-12.

Dunford, J. E., M. J. Rogers, F. H. Ebetino, R. J. Phipps and F. P. Coxon (2006). Inhibition of protein prenylation by bisphosphonates causes sustained activation of Rac, Cdc42, and Rho GTPases. J Bone Miner Res **21**(5): 684-94.

Dunlay, R. and K. Hruska (1990). PTH receptor coupling to phospholipase C is an alternate pathway of signal transduction in bone and kidney. Am J Physiol **258**(2 Pt 2): F223-31.

Dvorak, M. M., A. Siddiqua, D. T. Ward, D. H. Carter, S. L. Dallas, E. F. Nemeth and D. Riccardi (2004). Physiological changes in extracellular calcium concentration directly control osteoblast function in the absence of

calciotropic hormones. Proc Natl Acad Sci U S A **101**(14): 5140-5.

Emerton, K. B., B. Hu, A. A. Woo, A. Sinofsky, C. Hernandez, R. J. Majeska, K. J. Jepsen and M. B. Schaffler (2010). Osteocyte apoptosis and control of bone resorption following ovariectomy in mice. Bone **46**(3): 577-83.

Erickson, K. L., J. A. Beutler, I. J. Cardellina and M. R. Boyd (1997). Salicylihalamides A and B, Novel Cytotoxic Macrolides from the Marine Sponge Haliclona sp. J Org Chem **62**(23): 8188-8192.

Eriksen, E. F. (1986). Normal and pathological remodeling of human trabecular bone: three dimensional reconstruction of the remodeling sequence in normals and in metabolic bone disease. Endocr Rev **7**(4): 379-408.

Eriksen, E. F., G. Z. Eghbali-Fatourechi and S. Khosla (2007). Remodeling and vascular spaces in bone. J Bone Miner Res **22**(1): 1-6.

Eriksen, E. F., B. Langdahl, A. Vesterby, J. Rungby and M. Kassem (1999). Hormone replacement therapy prevents osteoclastic hyperactivity: A histomorphometric study in early postmenopausal women. J Bone Miner Res **14**(7): 1217-21.

Eriksen, E. F., F. Melsen and L. Mosekilde (1984). Reconstruction of the resorptive site in iliac trabecular bone: a kinetic model for bone resorption in 20 normal individuals. Metab Bone Dis Relat Res **5**(5): 235-42.

Eser, P., A. Frotzler, Y. Zehnder, L. Wick, H. Knecht, J. Denoth and H. Schiessl (2004). Relationship between the duration of paralysis and bone structure: a pQCT study of spinal cord injured individuals. Bone **34**(5): 869-80.

Ettinger, B., D. M. Black, B. H. Mitlak, R. K. Knickerbocker, T. Nickelsen, H. K. Genant, C. Christiansen, P. D. Delmas, J. R. Zanchetta, J. Stakkestad, C. C. Gluer, K. Krueger, F. J. Cohen, S. Eckert, K. E. Ensrud, L. V. Avioli, P. Lips and S. R. Cummings (1999). Reduction of vertebral fracture risk in postmenopausal women with osteoporosis treated with raloxifene: results from a 3-year randomized clinical trial. Multiple Outcomes of Raloxifene Evaluation (MORE) Investigators. Jama **282**(7): 637-45.

Everts, V., J. M. Delaisse, W. Korper, D. C. Jansen, W. Tigchelaar-Gutter, P. Saftig and W. Beertsen (2002). The bone lining cell: its role in cleaning Howship's lacunae and initiating bone formation. J Bone Miner Res **17**(1): 77-90.

Evio, S., A. Tiitinen, K. Laitinen, O. Ylikorkala and M. J. Valimaki (2004). Effects of alendronate and hormone replacement therapy, alone and in combination, on bone mass and markers of bone turnover in elderly women with osteoporosis. J Clin Endocrinol Metab **89**(2): 626-31.

Farlay, D., G. Boivin, G. Panczer, A. Lalande and P. J. Meunier (2005). Long-term strontium ranelate administration in monkeys preserves characteristics of bone mineral crystals and degree of mineralization of bone. J Bone Miner Res **20**(9): 1569-78.

Finbow, M. E., T. E. Buultjens, N. J. Lane, J. Shuttleworth and J. D. Pitts (1984). Isolation and characterisation of arthropod gap junctions. Embo J **3**(10): 2271-8.

Finbow, M. E., S. John, E. Kam, D. K. Apps and J. D. Pitts (1993). Disposition and orientation of ductin (DCCD-reactive vacuolar H(+)-ATPase subunit) in mammalian membrane complexes. Exp Cell Res **207**(2): 261-70.

Finkelstein, J. S., S. E. Brockwell, V. Mehta, G. A. Greendale, M. R. Sowers, B. Ettinger, J. C. Lo, J. M. Johnston, J. A. Cauley, M. E. Danielson and R. M. Neer (2008). Bone mineral density changes during the menopause transition in a multiethnic cohort of women. J Clin Endocrinol Metab **93**(3): 861-8.

Finkelstein, J. S., J. J. Wyland, H. Lee and R. M. Neer (2010). Effects of teriparatide, alendronate, or both in women with postmenopausal osteoporosis. J Clin Endocrinol Metab **95**(4): 1838-45.

Fitzpatrick, L. A. (2002). Secondary causes of osteoporosis. Mayo Clin Proc **77**(5): 453-68.

Flannery, A. R., L. A. Graham and T. H. Stevens (2004). Topological characterization of the c, c', and c" subunits of the vacuolar ATPase from the yeast Saccharomyces cerevisiae. J Biol Chem **279**(38): 39856-62.

Forgac, M. (2007). Vacuolar ATPases: rotary proton pumps in physiology and pathophysiology. Nat Rev Mol Cell Biol **8**(11): 917-29.

Frattini, A., P. J. Orchard, C. Sobacchi, S. Giliani, M. Abinun, J. P. Mattsson, D. J. Keeling, A. K. Andersson, P. Wallbrandt, L. Zecca, L. D. Notarangelo, P. Vezzoni and A. Villa (2000). Defects in TCIRG1 subunit of the vacuolar proton pump are responsible for a subset of human autosomal recessive osteopetrosis. Nat Genet **25**(3): 343-6.

Frolik, C. A., E. C. Black, R. L. Cain, J. H. Satterwhite, P. L. Brown-Augsburger, M. Sato and J. M. Hock (2003). Anabolic and catabolic bone effects of human parathyroid hormone (1-34) are predicted by duration of hormone exposure. Bone **33**(3): 372-9.

Frost, H. M. (1987). Bone "mass" and the "mechanostat": a proposal. Anat Rec **219**(1): 1-9.

Gagliardi, S., P. A. Gatti, P. Belfiore, A. Zocchetti, G. D. Clarke and C. Farina (1998a). Synthesis and structure-activity relationships of bafilomycin A1 derivatives as inhibitors of vacuolar H+-ATPase. J Med Chem **41**(11): 1883-93.

Gagliardi, S., G. Nadler, E. Consolandi, C. Parini, M. Morvan, M. N. Legave, P. Belfiore, A. Zocchetti, G. D. Clarke, I. James, P. Nambi, M. Gowen and C. Farina (1998b). 5-(5,6-Dichloro-2-indolyl)-2-methoxy-2,4-pentadienamides: novel and selective inhibitors of the vacuolar H+-ATPase of osteoclasts with bone antiresorptive activity. J Med Chem **41**(10): 1568-73.

Getlawi, F., A. Laslop, H. Schagger, J. Ludwig, J. Haywood and D. Apps (1996). Chromaffin granule membrane glycoprotein IV is identical with Ac45, a membrane-integral subunit of the granule's H(+)-ATPase. Neurosci Lett **219**(1): 13-6.

Glimcher, M. J. (1984). Recent studies of the mineral phase in bone and its possible linkage to the organic matrix by protein-bound phosphate bonds. Philos Trans R Soc Lond B Biol Sci **304**(1121): 479-508.

Graves, A. R., P. K. Curran, C. L. Smith and J. A. Mindell (2008). The Cl-/H+ antiporter ClC-7 is the primary chloride permeation pathway in lysosomes. Nature **453**(7196): 788-92.

Greenspan, S. L., H. G. Bone, M. P. Ettinger, D. A. Hanley, R. Lindsay, J. R. Zanchetta, C. M. Blosch, A. L. Mathisen, S. A. Morris and T. B. Marriott (2007). Effect of recombinant human parathyroid hormone (1-84) on vertebral fracture and bone mineral density in postmenopausal women with osteoporosis: a randomized trial. Ann Intern Med **146**(5): 326-39.

Hall, G. E. and A. D. Kenny (1987). Role of carbonic anhydrase in bone resorption: effect of acetazolamide on basal and parathyroid hormone-induced bone metabolism. Calcif Tissue Int **40**(4): 212-8.

Harvey, N., E. Dennison and C. Cooper (2010). Osteoporosis: impact on health and economics. Nat Rev Rheumatol **6**(2): 99-105.

Hauge, E. M., D. Qvesel, E. F. Eriksen, L. Mosekilde and F. Melsen (2001). Cancellous bone remodeling occurs in specialized compartments lined by cells expressing osteoblastic markers. J Bone Miner Res **16**(9): 1575-82.

Hellman, J., S. M. Kakonen, M. T. Matikainen, M. Karp, T. Lovgren, H. K. Väänänen and K. Pettersson (1996). Epitope mapping of nine monoclonal antibodies against osteocalcin: combinations into two-site assays affect both assay specificity and sample stability. J Bone Miner Res **11**(8): 1165-75.

Hertzberg, E. L. (1984). A detergent-independent procedure for the isolation of gap junctions from rat liver. J Biol Chem **259**(15): 9936-43.

Hiesinger, P. R., A. Fayyazuddin, S. Q. Mehta, T. Rosenmund, K. L. Schulze, R. G. Zhai, P. Verstreken, Y. Cao, Y. Zhou, J. Kunz and H. J. Bellen (2005). The v-ATPase V0 subunit a1 is required for a late step in synaptic vesicle exocytosis in Drosophila. Cell **121**(4): 607-20.

Hirata, R., L. A. Graham, A. Takatsuki, T. H. Stevens and Y. Anraku (1997). VMA11 and VMA16 encode second and third proteolipid subunits of the Saccharomyces cerevisiae vacuolar membrane H+-ATPase. J Biol Chem **272**(8): 4795-803.

Hirata, T., A. Iwamoto-Kihara, G. H. Sun-Wada, T. Okajima, Y. Wada and M. Futai (2003). Subunit rotation of vacuolar-type proton pumping ATPase: relative rotation of the G and C subunits. J Biol Chem **278**(26): 23714-9.

Hodsman, A. B., D. A. Hanley, M. P. Ettinger, M. A. Bolognese, J. Fox, A. J. Metcalfe and R. Lindsay (2003). Efficacy and safety of human parathyroid hormone-(1-84) in increasing bone mineral density in postmenopausal osteoporosis. J Clin Endocrinol Metab **88**(11): 5212-20.

Hurtado-Lorenzo, A., M. Skinner, J. El Annan, M. Futai, G. H. Sun-Wada, S. Bourgoin, J. Casanova, A. Wildeman, S. Bechoua, D. A. Ausiello, D. Brown and V. Marshansky (2006). V-ATPase interacts with ARNO and Arf6 in early endosomes and regulates the protein degradative pathway. Nat Cell Biol **8**(2): 124-36.

Huss, M., F. Sasse, B. Kunze, R. Jansen, H. Steinmetz, G. Ingenhorst, A. Zeeck and H. Wieczorek (2005). Archazolid and apicularen: novel specific V-ATPase inhibitors. BMC Biochem **6**: 13.

Hwang, K., J. O. Hollinger, R. S. Chung and S. I. Lee (2000). Histomorphometry of parietal bones versus age and race. J Craniofac Surg **11**(1): 17-23.

Ikeda, T., M. Utsuyama and K. Hirokawa (2001). Expression profiles of receptor activator of nuclear factor kappaB ligand, receptor activator of nuclear factor kappaB, and osteoprotegerin messenger RNA in aged and ovariectomized rat bones. J Bone Miner Res **16**(8): 1416-25.

Imai-Senga, Y., G. H. Sun-Wada, Y. Wada and M. Futai (2002). A human gene, ATP6E1, encoding a testis-specific isoform of H(+)-ATPase subunit E. Gene **289**(1-2): 7-12.

Iwata, M., H. Imamura, E. Stambouli, C. Ikeda, M. Tamakoshi, K. Nagata, H. Makyio, B. Hankamer, J. Barber, M. Yoshida, K. Yokoyama and S. Iwata (2004). Crystal structure of a central stalk subunit C and reversible association/dissociation of vacuole-type ATPase. Proc Natl Acad Sci U S A **101**(1): 59-64.

Järvinen, T. L., H. Sievänen, K. M. Khan, A. Heinonen and P. Kannus (2008). Shifting the focus in fracture prevention from osteoporosis to falls. Bmj **336**(7636): 124-6.

Jefferies, K. C. and M. Forgac (2008). Subunit H of the vacuolar (H+) ATPase inhibits ATP hydrolysis by the free V1 domain by interaction with the rotary subunit F. J Biol Chem **283**(8): 4512-9.

Jilka, R. L., C. A. O'Brien, A. A. Ali, P. K. Roberson, R. S. Weinstein and S. C. Manolagas (2009). Intermittent PTH stimulates periosteal bone formation by actions on post-mitotic preosteoblasts. Bone **44**(2): 275-86.

Johnson, R. G., S. Carty and A. Scarpa (1982). A model of biogenic amine accumulation into chromaffin granules and ghosts based on coupling to the electrochemical proton gradient. Federation Proceedings **41**(11): 2746-54.

Jowsey, J. (1966). Studies of Haversian systems in man and some animals. J Anat **100**(Pt 4): 857-64.

Kane, P. M. (1995). Disassembly and reassembly of the yeast vacuolar H(+)-ATPase in vivo. J Biol Chem **270**(28): 17025-32.

Kanehisa, J., T. Yamanaka, S. Doi, K. Turksen, J. N. Heersche, J. E. Aubin and H. Takeuchi (1990). A band of F-actin containing podosomes is involved in bone resorption by osteoclasts. Bone **11**(4): 287-93.

Kanis, J. A., D. Black, C. Cooper, P. Dargent, B. Dawson-Hughes, C. De Laet, P. Delmas, J. Eisman, O. Johnell, B. Jonsson, L. Melton, A. Oden, S. Papapoulos, H. Pols, R. Rizzoli, A. Silman and A. Tenenhouse (2002a). A new approach to the development of assessment guidelines for osteoporosis. Osteoporos Int **13**(7): 527-36.

Kanis, J. A., O. Johnell, A. Oden, C. De Laet, B. Jonsson and A. Dawson (2002b). Ten-year risk of osteoporotic fracture and the effect of risk factors on screening strategies. Bone **30**(1): 251-8.

Karet, F. E., K. E. Finberg, R. D. Nelson, A. Nayir, H. Mocan, S. A. Sanjad, J. Rodriguez-Soriano, F. Santos, C. W. Cremers, A. Di Pietro, B. I. Hoffbrand, J. Winiarski, A. Bakkaloglu, S. Ozen, R. Dusunsel, P. Goodyer, S. A. Hulton, D. K. Wu, A. B. Skvorak, C. C. Morton, M. J. Cunningham, V. Jha and R. P. Lifton (1999). Mutations in the gene encoding B1 subunit

of H+-ATPase cause renal tubular acidosis with sensorineural deafness. Nat Genet **21**(1): 84-90.

Kariya, Y., M. Honma, A. Hanamura, S. Aoki, T. Ninomiya, Y. Nakamichi, N. Udagawa and H. Suzuki (2011). Rab27a and Rab27b are involved in stimulation-dependent RANKL release from secretory lysosomes in osteoblastic cells. J Bone Miner Res **26**(4):689-703

Karsdal, M. A., T. J. Martin, J. Bollerslev, C. Christiansen and K. Henriksen (2007). Are nonresorbing osteoclasts sources of bone anabolic activity? J Bone Miner Res **22**(4): 487-94.

Karsdal, M. A., A. V. Neutzsky-Wulff, M. H. Dziegiel, C. Christiansen and K. Henriksen (2008). Osteoclasts secrete non-bone derived signals that induce bone formation. Biochem Biophys Res Commun **366**(2): 483-8.

Kasper, D., R. Planells-Cases, J. C. Fuhrmann, O. Scheel, O. Zeitz, K. Ruether, A. Schmitt, M. Poet, R. Steinfeld, M. Schweizer, U. Kornak and T. J. Jentsch (2005). Loss of the chloride channel ClC-7 leads to lysosomal storage disease and neurodegeneration. Embo J **24**(5): 1079-91.

Kawasaki-Nishi, S., K. Bowers, T. Nishi, M. Forgac and T. H. Stevens (2001c). The amino-terminal domain of the vacuolar proton-translocating ATPase a subunit controls targeting and in vivo dissociation, and the carboxyl-terminal domain affects coupling of proton transport and ATP hydrolysis. J Biol Chem **276**(50): 47411-20.

Kawasaki-Nishi, S., T. Nishi and M. Forgac (2001a). Arg-735 of the 100-kDa subunit a of the yeast V-ATPase is essential for proton translocation. Proc Natl Acad Sci U S A **98**(22): 12397-402.

Kawasaki-Nishi, S., T. Nishi and M. Forgac (2001b). Yeast V-ATPase complexes containing different isoforms of the 100-kDa a-subunit differ in coupling efficiency and in vivo dissociation. J Biol Chem **276**(21): 17941-8.

Kawasaki-Nishi, S., T. Nishi and M. Forgac (2003). Interacting helical surfaces of the transmembrane segments of subunits a and

c' of the yeast V-ATPase defined by disulfide-mediated cross-linking. J Biol Chem **278**(43): 41908-13.

Kawasaki-Nishi, S., A. Yamaguchi, M. Forgac and T. Nishi (2007). Tissue specific expression of the splice variants of the mouse vacuolar proton-translocating ATPase a4 subunit. Biochem Biophys Res Commun **364**(4): 1032-6.

Keeling, D. J., M. Herslof, B. Ryberg, S. Sjogren and L. Solvell (1997). Vacuolar H(+)-ATPases. Targets for drug discovery? Ann N Y Acad Sci **834**: 600-8.

Keller, H. and M. Kneissel (2005). SOST is a target gene for PTH in bone. Bone **37**(2): 148-58.

Khan, S. A., J. A. Kanis, S. Vasikaran, W. F. Kline, B. K. Matuszewski, E. V. McCloskey, M. N. Beneton, B. J. Gertz, D. G. Sciberras, S. D. Holland, J. Orgee, G. M. Coombes, S. R. Rogers and A. G. Porras (1997). Elimination and biochemical responses to intravenous alendronate in postmenopausal osteoporosis. J Bone Miner Res **12**(10): 1700-7.

Kim, J. W., K. Shin-Ya, K. Furihata, Y. Hayakawa and H. Seto (1999). Oximidines I and II: Novel Antitumor Macrolides from Pseudomonas sp. J Org Chem **64**(1): 153-155.

Knothe Tate, M. L., P. Niederer and U. Knothe (1998). In vivo tracer transport through the lacunocanalicular system of rat bone in an environment devoid of mechanical loading. Bone **22**(2): 107-17.

Kornak, U., D. Kasper, M. R. Bosl, E. Kaiser, M. Schweizer, A. Schulz, W. Friedrich, G. Delling and T. J. Jentsch (2001). Loss of the ClC-7 chloride channel leads to osteopetrosis in mice and man. Cell **104**(2): 205-15.

Kornak, U., A. Schulz, W. Friedrich, S. Uhlhaas, B. Kremens, T. Voit, C. Hasan, U. Bode, T. J. Jentsch and C. Kubisch (2000). Mutations in the a3 subunit of the vacuolar H(+)-ATPase cause infantile malignant osteopetrosis. Hum Mol Genet **9**(13): 2059-63.

Kreja, L., R. E. Brenner, A. Tautzenberger, A. Liedert, B. Friemert, C. Ehrnthaller, M. Huber-Lang and A. Ignatius (2010). Non-

resorbing osteoclasts induce migration and osteogenic differentiation of mesenchymal stem cells. J Cell Biochem **109**(2): 347-55.

Kunze, B., R. Jansen, F. Sasse, G. Hofle and H. Reichenbach (1998). Apicularens A and B, new cytostatic macrolides from Chondromyces species (myxobacteria): production, physico-chemical and biological properties. J Antibiot (Tokyo) **51**(12): 1075-80.

Lafourcade, C., K. Sobo, S. Kieffer-Jaquinod, J. Garin and F. G. van der Goot (2008). Regulation of the V-ATPase along the endocytic pathway occurs through reversible subunit association and membrane localization. PLoS One **3**(7): e2758.

Larsson, L., G. Grimby and J. Karlsson (1979). Muscle strength and speed of movement in relation to age and muscle morphology. J Appl Physiol **46**(3): 451-6.

Lee, S. H., J. Rho, D. Jeong, J. Y. Sul, T. Kim, N. Kim, J. S. Kang, T. Miyamoto, T. Suda, S. K. Lee, R. J. Pignolo, B. Koczon-Jaremko, J. Lorenzo and Y. Choi (2006). v-ATPase V0 subunit d2-deficient mice exhibit impaired osteoclast fusion and increased bone formation. Nat Med **12**(12): 1403-9.

Leisle, L., C. F. Ludwig, F. A. Wagner, T. J. Jentsch and T. Stauber (2011). ClC7 is a slowly voltage-gated 2Cl-/1H+-exchanger and requires Ostm1 for transport activity. Embo j (in press).

Li, X., M. S. Ominsky, Q. T. Niu, N. Sun, B. Daugherty, D. D'Agostin, C. Kurahara, Y. Gao, J. Cao, J. Gong, F. Asuncion, M. Barrero, K. Warmington, D. Dwyer, M. Stolina, S. Morony, I. Sarosi, P. J. Kostenuik, D. L. Lacey, W. S. Simonet, H. Z. Ke and C. Paszty (2008). Targeted deletion of the sclerostin gene in mice results in increased bone formation and bone strength. J Bone Miner Res **23**(6): 860-9.

Lindsay, R., J. Nieves, C. Formica, E. Henneman, L. Woelfert, V. Shen, D. Dempster and F. Cosman (1997). Randomised controlled study of effect of parathyroid hormone on vertebral-bone mass and fracture incidence among postmenopausal women on oestrogen with osteoporosis. Lancet **350**(9077): 550-5.

Lindsay, R., J. Nieves, E. Henneman, V. Shen and F. Cosman (1993). Subcutaneous administration of the amino-terminal fragment of human parathyroid hormone-(1-34): kinetics and biochemical response in estrogenized osteoporotic patients. J Clin Endocrinol Metab **77**(6): 1535-9.

Lippman, M. E., S. R. Cummings, D. P. Disch, J. L. Mershon, S. A. Dowsett, J. A. Cauley and S. Martino (2006). Effect of raloxifene on the incidence of invasive breast cancer in postmenopausal women with osteoporosis categorized by breast cancer risk. Clin Cancer Res **12**(17): 5242-7.

Lips, P., P. Courpron and P. J. Meunier (1978). Mean wall thickness of trabecular bone packets in the human iliac crest: changes with age. Calcif Tissue Res **26**(1): 13-7.

Liu, Q., P. M. Kane, P. R. Newman and M. Forgac (1996). Site-directed mutagenesis of the yeast V-ATPase B subunit (Vma2p). J Biol Chem **271**(4): 2018-22.

Liu, Q., X. H. Leng, P. R. Newman, E. Vasilyeva, P. M. Kane and M. Forgac (1997). Site-directed mutagenesis of the yeast V-ATPase A subunit. J Biol Chem **272**(18): 11750-6.

Lu, M., D. Ammar, H. Ives, F. Albrecht and S. L. Gluck (2007). Physical interaction between aldolase and vacuolar H+-ATPase is essential for the assembly and activity of the proton pump. J Biol Chem **282**(34): 24495-503.

Ma, Y. L., R. L. Cain, D. L. Halladay, X. Yang, Q. Zeng, R. R. Miles, S. Chandrasekhar, T. J. Martin and J. E. Onyia (2001). Catabolic effects of continuous human PTH (1--38) in vivo is associated with sustained stimulation of RANKL and inhibition of osteoprotegerin and gene-associated bone formation. Endocrinology **142**(9): 4047-54.

MacLeod, K. J., E. Vasilyeva, J. D. Baleja and M. Forgac (1998). Mutational analysis of the nucleotide binding sites of the yeast vacuolar proton-translocating ATPase. J Biol Chem **273**(1): 150-6.

Mahamid, J., A. Sharir, D. Gur, E. Zelzer, L. Addadi and S. Weiner (2011). Bone mineralization proceeds through intracellular calcium phosphate loaded vesicles: A cryo-

electron microscopy study. J Struct Biol. (in press).

Mahon, M. J., T. M. Bonacci, P. Divieti and A. V. Smrcka (2006). A docking site for G protein betagamma subunits on the parathyroid hormone 1 receptor supports signaling through multiple pathways. Mol Endocrinol **20**(1): 136-46.

Majima, T., A. Shimatsu, Y. Komatsu, N. Satoh, A. Fukao, K. Ninomiya, T. Matsumura and K. Nakao (2008). Association between baseline values of bone turnover markers and bone mineral density and their response to raloxifene treatment in Japanese postmenopausal women with osteoporosis. Endocr J **55**(1): 41-8.

Mann, V., C. Huber, G. Kogianni, D. Jones and B. Noble (2006). The influence of mechanical stimulation on osteocyte apoptosis and bone viability in human trabecular bone. J Musculoskelet Neuronal Interact **6**(4): 408-17.

Manolson, M. F., B. Wu, D. Proteau, B. E. Taillon, B. T. Roberts, M. A. Hoyt and E. W. Jones (1994). STV1 gene encodes functional homologue of 95-kDa yeast vacuolar H(+)-ATPase subunit Vph1p. J Biol Chem **269**(19): 14064-74.

Manolson, M. F., H. Yu, W. Chen, Y. Yao, K. Li, R. L. Lees and J. N. Heersche (2003). The a3 isoform of the 100-kDa V-ATPase subunit is highly but differentially expressed in large (>or=10 nuclei) and small (<or= nuclei) osteoclasts. J Biol Chem **278**(49): 49271-8.

Marcus, R., L. Holloway, B. Wells, G. Greendale, M. K. James, C. Wasilauskas and J. Kelaghan (1999). The relationship of biochemical markers of bone turnover to bone density changes in postmenopausal women: results from the Postmenopausal Estrogen/Progestin Interventions (PEPI) trial. J Bone Miner Res **14**(9): 1583-95.

Marie, P. J. (2008). Transcription factors controlling osteoblastogenesis. Arch Biochem Biophys **473**(2): 98-105.

Martin, T. J. and N. A. Sims (2005). Osteoclast-derived activity in the coupling of bone formation to resorption. Trends Mol Med **11**(2): 76-81.

Mattsson, J. P. and D. J. Keeling (1996). [3H]Bafilomycin as a probe for the transmembrane proton channel of the osteoclast vacuolar H(+)-ATPase. Biochimica et Biophysica Acta **1280**(1): 98-106.

McHugh, K. P., K. Hodivala-Dilke, M. H. Zheng, N. Namba, J. Lam, D. Novack, X. Feng, F. P. Ross, R. O. Hynes and S. L. Teitelbaum (2000). Mice lacking beta3 integrins are osteosclerotic because of dysfunctional osteoclasts. J Clin Invest **105**(4): 433-40.

Menche, D., J. Hassfeld, H. Steinmetz, M. Huss, H. Wieczorek and F. Sasse (2007). The first hydroxylated archazolid from the myxobacterium Cystobacter violaceus: isolation, structural elucidation and V-ATPase inhibition. J Antibiot (Tokyo) **60**(5): 328-31.

Messalli, E. M., G. Mainini, C. Scaffa, A. Cafiero, P. L. Salzillo, A. Ragucci and L. Cobellis (2007). Raloxifene therapy interacts with serum osteoprotegerin in postmenopausal women. Maturitas **56**(1): 38-44.

Meunier, P. J., C. Roux, E. Seeman, S. Ortolani, J. E. Badurski, T. D. Spector, J. Cannata, A. Balogh, E. M. Lemmel, S. Pors-Nielsen, R. Rizzoli, H. K. Genant and J. Y. Reginster (2004). The effects of strontium ranelate on the risk of vertebral fracture in women with postmenopausal osteoporosis. N Engl J Med **350**(5): 459-68.

Milat, F. and K. W. Ng (2009). Is Wnt signalling the final common pathway leading to bone formation? Mol Cell Endocrinol **310**(1-2): 52-62.

Miller, P. D., M. A. Bolognese, E. M. Lewiecki, M. R. McClung, B. Ding, M. Austin, Y. Liu and J. San Martin (2008). Effect of denosumab on bone density and turnover in postmenopausal women with low bone mass after long-term continued, discontinued, and restarting of therapy: a randomized blinded phase 2 clinical trial. Bone **43**(2): 222-9.

Miller, R. L., P. Zhang, M. Smith, V. Beaulieu, T. G. Paunescu, D. Brown, S. Breton and R. D. Nelson (2005). V-ATPase B1-subunit promoter drives expression of EGFP in intercalated cells of kidney, clear cells of epididymis and airway cells of lung in

transgenic mice. Am J Physiol Cell Physiol **288**(5): C1134-44.

Mitchell, D. Y., W. H. Barr, R. A. Eusebio, K. A. Stevens, F. P. Duke, D. A. Russell, J. D. Nesbitt, J. H. Powell and G. A. Thompson (2001). Risedronate pharmacokinetics and intra- and inter-subject variability upon single-dose intravenous and oral administration. Pharm Res **18**(2): 166-70.

Morel, N., J. C. Dedieu and J. M. Philippe (2003). Specific sorting of the a1 isoform of the V-H+ATPase a subunit to nerve terminals where it associates with both synaptic vesicles and the presynaptic plasma membrane. J Cell Sci **116**(Pt 23): 4751-62.

Moustafa, A., T. Sugiyama, L. K. Saxon, G. Zaman, A. Sunters, V. J. Armstrong, B. Javaheri, L. E. Lanyon and J. S. Price (2009). The mouse fibula as a suitable bone for the study of functional adaptation to mechanical loading. Bone **44**(5): 930-5.

Mulari, M. T., Q. Qu, P. L. Harkonen and H. K. Väänänen (2004). Osteoblast-like cells complete osteoclastic bone resorption and form new mineralized bone matrix in vitro. Calcif Tissue Int **75**(3): 253-61.

Murata, T., I. Yamato, Y. Kakinuma, A. G. Leslie and J. E. Walker (2005). Structure of the rotor of the V-Type Na+-ATPase from Enterococcus hirae. Science **308**(5722): 654-9.

Murata, Y., G. H. Sun-Wada, T. Yoshimizu, A. Yamamoto, Y. Wada and M. Futai (2002). Differential localization of the vacuolar H+ pump with G subunit isoforms (G1 and G2) in mouse neurons. J Biol Chem **277**(39): 36296-303.

Murray, M. P., E. H. Duthie, Jr., S. R. Gambert, S. B. Sepic and L. A. Mollinger (1985). Age-related differences in knee muscle strength in normal women. J Gerontol **40**(3): 275-80.

Murray, M. P., G. M. Gardner, L. A. Mollinger and S. B. Sepic (1980). Strength of isometric and isokinetic contractions: knee muscles of men aged 20 to 86. Phys Ther **60**(4): 412-9.

Nadler, G., M. Morvan, I. Delimoge, P. Belfiore, A. Zocchetti, I. James, D.

Zembryki, E. Lee-Rycakzewski, C. Parini, E. Consolandi, S. Gagliardi and C. Farina (1998). (2Z,4E)-5-(5,6-dichloro-2-indolyl)-2-methoxy-N-(1,2,2,6,6-pentamethylpiperidin-4-yl)-2,4-pentadienamide, a novel, potent and selective inhibitor of the osteoclast V-ATPase. Bioorganic & Medicinal Chemistry Letters **8**(24): 3621-6.

Neer, R. M., C. D. Arnaud, J. R. Zanchetta, R. Prince, G. A. Gaich, J. Y. Reginster, A. B. Hodsman, E. F. Eriksen, S. Ish-Shalom, H. K. Genant, O. Wang and B. H. Mitlak (2001). Effect of parathyroid hormone (1-34) on fractures and bone mineral density in postmenopausal women with osteoporosis. N Engl J Med **344**(19): 1434-41.

Nelson, R. D., X. L. Guo, K. Masood, D. Brown, M. Kalkbrenner and S. Gluck (1992). Selectively amplified expression of an isoform of the vacuolar H(+)-ATPase 56-kilodalton subunit in renal intercalated cells. Proc Natl Acad Sci U S A **89**(8): 3541-5.

Nenonen, A., S. Cheng, K. K. Ivaska, S. L. Alatalo, T. Lehtimaki, H. Schmidt-Gayk, K. Uusi-Rasi, A. Heinonen, P. Kannus, H. Sievanen, I. Vuori, H. K. Väänänen and J. M. Halleen (2005). Serum TRACP 5b Is a Useful Marker for Monitoring Alendronate Treatment: Comparison With Other Markers of Bone Turnover. J Bone Miner Res **20**(8): 1804-1812.

Nielsen, R. H., M. A. Karsdal, M. G. Sorensen, M. H. Dziegiel and K. Henriksen (2007). Dissolution of the inorganic phase of bone leading to release of calcium regulates osteoclast survival. Biochem Biophys Res Commun **360**(4): 834-9.

Niikura, K., S. Nakajima, M. Takano and H. Yamazaki (2007). FR177995, a novel vacuolar ATPase inhibitor, exerts not only an inhibitory effect on bone destruction but also anti-immunoinflammatory effects in adjuvant-induced arthritic rats. Bone **40**(4): 888-94.

Niikura, K., M. Takano and M. Sawada (2004). A novel inhibitor of vacuolar ATPase, FR167356, which can discriminate between osteoclast vacuolar ATPase and lysosomal vacuolar ATPase. Br J Pharmacol **142**(3): 558-66.

Niikura, K., N. Takeshita and M. Takano (2005). A vacuolar ATPase inhibitor, FR167356, prevents bone resorption in ovariectomized rats with high potency and specificity: potential for clinical application. J Bone Miner Res **20**(9): 1579-88.

Nilsson, S. and K. F. Koehler (2005). Oestrogen receptors and selective oestrogen receptor modulators: molecular and cellular pharmacology. Basic Clin Pharmacol Toxicol **96**(1): 15-25.

Nishi, T. and M. Forgac (2000). Molecular cloning and expression of three isoforms of the 100-kDa a subunit of the mouse vacuolar proton-translocating ATPase. J Biol Chem **275**(10): 6824-30.

Nishi, T. and M. Forgac (2002). The vacuolar (H+)-ATPases--nature's most versatile proton pumps. Nature Reviews Molecular Cell Biology **3**(2): 94-103.

Nishi, T., S. Kawasaki-Nishi and M. Forgac (2003). Expression and function of the mouse V-ATPase d subunit isoforms. J Biol Chem **278**(47): 46396-402.

Orimo, H. (2010). The mechanism of mineralization and the role of alkaline phosphatase in health and disease. J Nippon Med Sch **77**(1): 4-12.

Ott, S. M., A. Oleksik, Y. Lu, K. Harper and P. Lips (2002). Bone histomorphometric and biochemical marker results of a 2-year placebo-controlled trial of raloxifene in postmenopausal women. J Bone Miner Res **17**(2): 341-8.

Pal, G. P. and R. V. Routal (1998). Architecture of the cancellous bone of the human talus. Anat Rec **252**(2): 185-93.

Pali, T., M. E. Finbow, A. Holzenburg, J. B. Findlay and D. Marsh (1995). Lipid-protein interactions and assembly of the 16-kDa channel polypeptide from Nephrops norvegicus. Studies with spin-label electron spin resonance spectroscopy and electron microscopy. Biochemistry **34**(28): 9211-8.

Palokangas, H., M. Mulari and H. K. Väänänen (1997). Endocytic pathway from the basal plasma membrane to the ruffled border membrane in bone-resorbing osteoclasts. J Cell Sci **110 (Pt 15)**: 1767-80.

Papapoulos, S. E., S. A. Quandt, U. A. Liberman, M. C. Hochberg and D. E. Thompson (2005). Meta-analysis of the efficacy of alendronate for the prevention of hip fractures in postmenopausal women. Osteoporos Int **16**(5): 468-74.

Parra, K. J., K. L. Keenan and P. M. Kane (2000). The H subunit (Vma13p) of the yeast V-ATPase inhibits the ATPase activity of cytosolic V1 complexes. J Biol Chem **275**(28): 21761-7.

Peng, S. B., X. Li, B. P. Crider, Z. Zhou, P. Andersen, S. J. Tsai, X. S. Xie and D. K. Stone (1999). Identification and reconstitution of an isoform of the 116-kDa subunit of the vacuolar proton translocating ATPase. J Biol Chem **274**(4): 2549-55.

Peri, F. and C. Nusslein-Volhard (2008). Live imaging of neuronal degradation by microglia reveals a role for v0-ATPase a1 in phagosomal fusion in vivo. Cell **133**(5): 916-27.

Perin, M. S., V. A. Fried, D. K. Stone, X. S. Xie and T. C. Sudhof (1991). Structure of the 116-kDa polypeptide of the clathrin-coated vesicle/synaptic vesicle proton pump. J Biol Chem **266**(6): 3877-81.

Peters, C., M. J. Bayer, S. Buhler, J. S. Andersen, M. Mann and A. Mayer (2001). Trans-complex formation by proteolipid channels in the terminal phase of membrane fusion. Nature **409**(6820): 581-8.

Poea-Guyon, S., M. Amar, P. Fossier and N. Morel (2006). Alternative splicing controls neuronal expression of v-ATPase subunit a1 and sorting to nerve terminals. J Biol Chem **281**(25): 17164-72.

Prestwood, K. M., C. C. Pilbeam, J. A. Burleson, F. N. Woodiel, P. D. Delmas, L. J. Deftos and L. G. Raisz (1994). The short-term effects of conjugated estrogen on bone turnover in older women. J Clin Endocrinol Metab **79**(2): 366-71.

Qi, J. and M. Forgac (2007). Cellular environment is important in controlling V-ATPase dissociation and its dependence on activity. J Biol Chem **282**(34): 24743-51.

Qiu, S., D. S. Rao, S. Palnitkar and A. M. Parfitt (2010). Dependence of bone yield (volume of bone formed per unit of cement surface area) on resorption cavity size during

osteonal remodeling in human rib: implications for osteoblast function and the pathogenesis of age-related bone loss. J Bone Miner Res **25**(2): 423-30.

Quandt, S. A., D. E. Thompson, D. L. Schneider, M. C. Nevitt and D. M. Black (2005). Effect of alendronate on vertebral fracture risk in women with bone mineral density T scores of-1.6 to -2.5 at the femoral neck: the Fracture Intervention Trial. Mayo Clin Proc **80**(3): 343-9.

Rautiala, T. J., A. M. Koskinen and H. K. Väänänen (1993). Purification of vacuolar ATPase with bafilomycin C1 affinity chromatography. Biochem Biophys Res Commun **194**(1): 50-6.

Recker, R., J. Lappe, K. M. Davies and R. Heaney (2004). Bone remodeling increases substantially in the years after menopause and remains increased in older osteoporosis patients. J Bone Miner Res **19**(10): 1628-33.

Recker, R. R., S. P. Bare, S. Y. Smith, A. Varela, M. A. Miller, S. A. Morris and J. Fox (2009). Cancellous and cortical bone architecture and turnover at the iliac crest of postmenopausal osteoporotic women treated with parathyroid hormone 1-84. Bone **44**(1): 113-9.

Reginster, J. Y., O. Bruyere, A. Sawicki, A. Roces-Varela, P. Fardellone, A. Roberts and J. P. Devogelaer (2009). Long-term treatment of postmenopausal osteoporosis with strontium ranelate: results at 8 years. Bone **45**(6): 1059-64.

Reginster, J. Y., E. Seeman, M. C. De Vernejoul, S. Adami, J. Compston, C. Phenekos, J. P. Devogelaer, M. D. Curiel, A. Sawicki, S. Goemaere, O. H. Sorensen, D. Felsenberg and P. J. Meunier (2005). Strontium ranelate reduces the risk of nonvertebral fractures in postmenopausal women with osteoporosis: Treatment of Peripheral Osteoporosis (TROPOS) study. J Clin Endocrinol Metab **90**(5): 2816-22.

Reid, I. R., P. D. Miller, J. P. Brown, D. L. Kendler, A. Fahrleitner-Pammer, I. Valter, K. Maasalu, M. A. Bolognese, G. Woodson, H. Bone, B. Ding, R. B. Wagman, J. San Martin, M. S. Ominsky and D. W. Dempster (2010). Effects of denosumab on bone histomorphometry:

the FREEDOM and STAND studies. J Bone Miner Res **25**(10): 2256-65.

Ren, S., H. Takano and K. Abe (2005). Two types of bone resorption lacunae in the mouse parietal bones as revealed by scanning electron microscopy and histochemistry. Arch Histol Cytol **68**(2): 103-13.

Rey, C., C. Combes, C. Drouet and M. J. Glimcher (2009). Bone mineral: update on chemical composition and structure. Osteoporos Int **20**(6): 1013-21.

Rizzo, V. F., U. Coskun, M. Radermacher, T. Ruiz, A. Armbruster and G. Gruber (2003). Resolution of the V1 ATPase from Manduca sexta into subcomplexes and visualization of an ATPase-active A3B3EG complex by electron microscopy. J Biol Chem **278**(1): 270-5.

Robling, A. G., P. J. Niziolek, L. A. Baldridge, K. W. Condon, M. R. Allen, I. Alam, S. M. Mantila, J. Gluhak-Heinrich, T. M. Bellido, S. E. Harris and C. H. Turner (2008). Mechanical stimulation of bone in vivo reduces osteocyte expression of Sost/sclerostin. J Biol Chem **283**(9): 5866-75.

Rodan, G., A. Reszka, E. Golub and R. Rizzoli (2004). Bone safety of long-term bisphosphonate treatment. Curr Med Res Opin **20**(8): 1291-300.

Roschger, P., I. Manjubala, N. Zoeger, F. Meirer, R. Simon, C. Li, N. Fratzl-Zelman, B. M. Misof, E. P. Paschalis, C. Streli, P. Fratzl and K. Klaushofer (2010). Bone material quality in transiliac bone biopsies of postmenopausal osteoporotic women after 3 years of strontium ranelate treatment. J Bone Miner Res **25**(4): 891-900.

Rossouw, J. E., G. L. Anderson, R. L. Prentice, A. Z. LaCroix, C. Kooperberg, M. L. Stefanick, R. D. Jackson, S. A. Beresford, B. V. Howard, K. C. Johnson, J. M. Kotchen and J. Ockene (2002). Risks and benefits of estrogen plus progestin in healthy postmenopausal women: principal results From the Women's Health Initiative randomized controlled trial. Jama **288**(3): 321-33.

Rubin, C. T. and L. E. Lanyon (1984). Dynamic strain similarity in vertebrates; an alternative

to allometric limb bone scaling. J Theor Biol **107**(2): 321-7.

Rubin, C. T. a. R. J. (1999). Biomechanics of bone. In Favus, M.J (ed) Primer on the metabolic bone diseases and disorders of mineral metabolism. American Society for Bone and Mineral Research, Washington, DC, USA, pp. 39-42.

Rubin, J., T. Murphy, M. S. Nanes and X. Fan (2000). Mechanical strain inhibits expression of osteoclast differentiation factor by murine stromal cells. Am J Physiol Cell Physiol **278**(6): C1126-32.

Sakai, E., H. Miyamoto, K. Okamoto, Y. Kato, K. Yamamoto and H. Sakai (2001). Characterization of phagosomal subpopulations along endocytic routes in osteoclasts and macrophages. J Biochem **130**(6): 823-31.

Sambade, M. and P. M. Kane (2004). The yeast vacuolar proton-translocating ATPase contains a subunit homologous to the Manduca sexta and bovine e subunits that is essential for function. J Biol Chem **279**(17): 17361-5.

Sanchez-Fernandez, M. A., A. Gallois, T. Riedl, P. Jurdic and B. Hoflack (2008). Osteoclasts control osteoblast chemotaxis via PDGF-BB/PDGF receptor beta signaling. PLoS One **3**(10): e3537.

Sarkar, S., J. Y. Reginster, G. G. Crans, A. Diez-Perez, K. V. Pinette and P. D. Delmas (2004). Relationship between changes in biochemical markers of bone turnover and BMD to predict vertebral fracture risk. J Bone Miner Res **19**(3): 394-401.

Sasse, F., H. Steinmetz, G. Hofle and H. Reichenbach (2003). Archazolids, new cytotoxic macrolactones from Archangium gephyra (Myxobacteria). Production, isolation, physico-chemical and biological properties. J Antibiot (Tokyo) **56**(6): 520-5.

Sautin, Y. Y., M. Lu, A. Gaugler, L. Zhang and S. L. Gluck (2005). Phosphatidylinositol 3-kinase-mediated effects of glucose on vacuolar H+-ATPase assembly, translocation, and acidification of intracellular compartments in renal epithelial cells. Mol Cell Biol **25**(2): 575-89.

Schindl, M. J., D. N. Redhead, K. C. Fearon, O. J. Garden and S. J. Wigmore (2005). The value of residual liver volume as a predictor of hepatic dysfunction and infection after major liver resection. Gut **54**(2): 289-96.

Schmidt, I. U., H. Dobnig and R. T. Turner (1995). Intermittent parathyroid hormone treatment increases osteoblast number, steady state messenger ribonucleic acid levels for osteocalcin, and bone formation in tibial metaphysis of hypophysectomized female rats. Endocrinology **136**(11): 5127-34.

Schwartz, Z., J. Sela, V. Ramirez, D. Amir and B. D. Boyan (1989). Changes in extracellular matrix vesicles during healing of rat tibial bone: a morphometric and biochemical study. Bone **10**(1): 53-60.

Scimeca, J. C., A. Franchi, C. Trojani, H. Parrinello, J. Grosgeorge, C. Robert, O. Jaillon, C. Poirier, P. Gaudray and G. F. Carle (2000). The gene encoding the mouse homologue of the human osteoclast-specific 116-kDa V-ATPase subunit bears a deletion in osteosclerotic (oc/oc) mutants. Bone **26**(3): 207-13.

Scimeca, J. C., D. Quincey, H. Parrinello, D. Romatet, J. Grosgeorge, P. Gaudray, N. Philip, A. Fischer and G. F. Carle (2003). Novel mutations in the TCIRG1 gene encoding the a3 subunit of the vacuolar proton pump in patients affected by infantile malignant osteopetrosis. Hum Mutat **21**(2): 151-7.

Seol, J. H., A. Shevchenko, A. Shevchenko and R. J. Deshaies (2001). Skp1 forms multiple protein complexes, including RAVE, a regulator of V-ATPase assembly. Nat Cell Biol **3**(4): 384-91.

Shane, E., D. Burr, P. R. Ebeling, B. Abrahamsen, R. A. Adler, T. D. Brown, A. M. Cheung, F. Cosman, J. R. Curtis, R. Dell, D. Dempster, T. A. Einhorn, H. K. Genant, P. Geusens, K. Klaushofer, K. Koval, J. M. Lane, F. McKiernan, R. McKinney, A. Ng, J. Nieves, R. O'Keefe, S. Papapoulos, H. T. Sen, M. C. van der Meulen, R. S. Weinstein and M. Whyte (2010). Atypical subtrochanteric and diaphyseal femoral fractures: report of a task force of the American Society for Bone and Mineral Research. J Bone Miner Res **25**(11): 2267-94.

Silva, M. J. (2007). Biomechanics of osteoporotic fractures. Injury **38** Suppl 3: S69-76.

Silverman, S. L., C. Christiansen, H. K. Genant, S. Vukicevic, J. R. Zanchetta, T. J. de Villiers, G. D. Constantine and A. A. Chines (2008). Efficacy of bazedoxifene in reducing new vertebral fracture risk in postmenopausal women with osteoporosis: results from a 3-year, randomized, placebo-, and active-controlled clinical trial. J Bone Miner Res **23**(12): 1923-34.

Silvestrini, G., P. Ballanti, F. Patacchioli, M. Leopizzi, N. Gualtieri, P. Monnazzi, E. Tremante, D. Sardella and E. Bonucci (2005). Detection of osteoprotegerin (OPG) and its ligand (RANKL) mRNA and protein in femur and tibia of the rat. J Mol Histol **36**(1-2): 59-67.

Siris, E. S., S. T. Harris, R. Eastell, J. R. Zanchetta, S. Goemaere, A. Diez-Perez, J. L. Stock, J. Song, Y. Qu, P. M. Kulkarni, S. R. Siddhanti, M. Wong and S. R. Cummings (2005). Skeletal effects of raloxifene after 8 years: results from the continuing outcomes relevant to Evista (CORE) study. J Bone Miner Res **20**(9): 1514-24.

Smith, A. N., K. E. Finberg, C. A. Wagner, R. P. Lifton, M. A. Devonald, Y. Su and F. E. Karet (2001). Molecular cloning and characterization of Atp6n1b: a novel fourth murine vacuolar H+-ATPase a-subunit gene. J Biol Chem **276**(45): 42382-8.

Smith, A. N., F. Jouret, S. Bord, K. J. Borthwick, R. S. Al-Lamki, C. A. Wagner, D. C. Ireland, V. Cormier-Daire, A. Frattini, A. Villa, U. Kornak, O. Devuyst and F. E. Karet (2005). Vacuolar H+-ATPase d2 subunit: molecular characterization, developmental regulation, and localization to specialized proton pumps in kidney and bone. J Am Soc Nephrol **16**(5): 1245-56.

Smith, A. N., J. Skaug, K. A. Choate, A. Nayir, A. Bakkaloglu, S. Ozen, S. A. Hulton, S. A. Sanjad, E. A. Al-Sabban, R. P. Lifton, S. W. Scherer and F. E. Karet (2000). Mutations in ATP6N1B, encoding a new kidney vacuolar proton pump 116-kD subunit, cause recessive distal renal tubular acidosis with preserved hearing. Nat Genet **26**(1): 71-5.

Sobacchi, C., A. Frattini, P. Orchard, O. Porras, I. Tezcan, M. Andolina, R. Babul-Hirji, I. Baric, N. Canham, D. Chitayat, S. Dupuis-Girod, I. Ellis, A. Etzioni, A. Fasth, A. Fisher, B. Gerritsen, V. Gulino, E. Horwitz, V. Klamroth, E. Lanino, M. Mirolo, A. Musio, G. Matthijs, S. Nonomaya, L. D. Notarangelo, H. D. Ochs, A. Superti Furga, J. Valiaho, J. L. van Hove, M. Vihinen, D. Vujic, P. Vezzoni and A. Villa (2001). The mutational spectrum of human malignant autosomal recessive osteopetrosis. Hum Mol Genet **10**(17): 1767-73.

Sorensen, M. G., K. Henriksen, A. V. Neutzsky-Wulff, M. H. Dziegiel and M. A. Karsdal (2007). Diphyllin, a novel and naturally potent V-ATPase inhibitor, abrogates acidification of the osteoclastic resorption lacunae and bone resorption. J Bone Miner Res **22**(10): 1640-8.

Sornay-Rendu, E., P. Garnero, F. Munoz, F. Duboeuf and P. D. Delmas (2003). Effect of withdrawal of hormone replacement therapy on bone mass and bone turnover: the OFELY study. Bone **33**(1): 159-66.

Stehberger, P. A., N. Schulz, K. E. Finberg, F. E. Karet, G. Giebisch, R. P. Lifton, J. P. Geibel and C. A. Wagner (2003). Localization and regulation of the ATP6V0A4 (a4) vacuolar H+-ATPase subunit defective in an inherited form of distal renal tubular acidosis. J Am Soc Nephrol **14**(12): 3027-38.

Steiniche, T., C. Hasling, P. Charles, E. F. Eriksen, L. Mosekilde and F. Melsen (1989). A randomized study on the effects of estrogen/gestagen or high dose oral calcium on trabecular bone remodeling in postmenopausal osteoporosis. Bone **10**(5): 313-20.

Stenbeck, G. (2002). Formation and function of the ruffled border in osteoclasts. Semin Cell Dev Biol **13**(4): 285-92.

Stroup, J. S., S. M. Rivers, A. M. Abu-Baker and M. P. Kane (2007). Two-year changes in bone mineral density and T scores in patients treated at a pharmacist-run teriparatide clinic. Pharmacotherapy **27**(6): 779-88.

Su, Y., K. G. Blake-Palmer, S. Sorrell, B. Javid, K. Bowers, A. Zhou, S. H. Chang, S. Qamar

and F. E. Karet (2008). Human H+ATPase a4 subunit mutations causing renal tubular acidosis reveal a role for interaction with phosphofructokinase-1. Am J Physiol Renal Physiol **295**(4): F950-8.

Sun-Wada, G. H., Y. Murata, M. Namba, A. Yamamoto, Y. Wada and M. Futai (2003a). Mouse proton pump ATPase C subunit isoforms (C2-a and C2-b) specifically expressed in kidney and lung. J Biol Chem **278**(45): 44843-51.

Sun-Wada, G. H., H. Tabata, N. Kawamura, M. Aoyama and Y. Wada (2009). Direct recruitment of H+-ATPase from lysosomes for phagosomal acidification. J Cell Sci **122**(Pt 14): 2504-13.

Sun-Wada, G. H., H. Tabata, N. Kawamura, M. Futai and Y. Wada (2007). Differential expression of a subunit isoforms of the vacuolar-type proton pump ATPase in mouse endocrine tissues. Cell Tissue Res **329**(2): 239-48.

Sun-Wada, G. H., T. Toyomura, Y. Murata, A. Yamamoto, M. Futai and Y. Wada (2006). The a3 isoform of V-ATPase regulates insulin secretion from pancreatic beta-cells. J Cell Sci **119**(Pt 21): 4531-40.

Sun-Wada, G. H., T. Yoshimizu, Y. Imai-Senga, Y. Wada and M. Futai (2003b). Diversity of mouse proton-translocating ATPase: presence of multiple isoforms of the C, d and G subunits. Gene **302**(1-2): 147-53.

Sundquist, K., P. Lakkakorpi, B. Wallmark and K. Väänänen (1990). Inhibition of osteoclast proton transport by bafilomycin A1 abolishes bone resorption. Biochem Biophys Res Commun **168**(1): 309-13.

Tan, S. D., A. D. Bakker, C. M. Semeins, A. M. Kuijpers-Jagtman and J. Klein-Nulend (2008). Inhibition of osteocyte apoptosis by fluid flow is mediated by nitric oxide. Biochem Biophys Res Commun **369**(4): 1150-4.

Taranta, A., S. Migliaccio, I. Recchia, M. Caniglia, M. Luciani, G. De Rossi, C. Dionisi-Vici, R. M. Pinto, P. Francalanci, R. Boldrini, E. Lanino, G. Dini, G. Morreale, S. H. Ralston, A. Villa, P. Vezzoni, D. Del Principe, F. Cassiani, G. Palumbo and A. Teti (2003). Genotype-phenotype relationship in human ATP6i-

dependent autosomal recessive osteopetrosis. Am J Pathol **162**(1): 57-68.

Taylor, A. F., M. M. Saunders, D. L. Shingle, J. M. Cimbala, Z. Zhou and H. J. Donahue (2007). Mechanically stimulated osteocytes regulate osteoblastic activity via gap junctions. Am J Physiol Cell Physiol **292**(1): C545-52.

Terland, O. and T. Flatmark (2000). Energy-dependent accumulation of calcium antagonists in catecholamine storage vesicles. Biochemical Pharmacology **59**(2): 123-9.

Tesch, W., T. Vandenbos, P. Roschgr, N. Fratzl-Zelman, K. Klaushofer, W. Beertsen and P. Fratzl (2003). Orientation of mineral crystallites and mineral density during skeletal development in mice deficient in tissue nonspecific alkaline phosphatase. J Bone Miner Res **18**(1): 117-25.

Teti, A., H. C. Blair, S. L. Teitelbaum, J. A. Kahn, A. Carano, M. Grano, G. Santacroce, P. Schlesinger and A. Zambonin Zallone (1989). Cytoplasmic pH is regulated in isolated avian osteoclasts by a Cl-/HCO3-exchanger. Boll Soc Ital Biol Sper **65**(7): 589-95.

Thomsen, J. S., E. N. Ebbesen and L. Mosekilde (2002). Static histomorphometry of human iliac crest and vertebral trabecular bone: a comparative study. Bone **30**(1): 267-74.

Tiemann, K. and J. J. Rossi (2009). RNAi-based therapeutics-current status, challenges and prospects. EMBO Mol Med **1**(3): 142-51.

Torres-Lagares, D., J. F. Tulasne, C. Pouget, A. Llorens, J. L. Saffar and P. Lesclous (2010). Structure and remodelling of the human parietal bone: an age and gender histomorphometric study. J Craniomaxillofac Surg **38**(5): 325-30.

Toyomura, T., Y. Murata, A. Yamamoto, T. Oka, G. H. Sun-Wada, Y. Wada and M. Futai (2003). From lysosomes to the plasma membrane: localization of vacuolar-type H+-ATPase with the a3 isoform during osteoclast differentiation. J Biol Chem **278**(24): 22023-30.

Travison, T. G., A. B. Araujo, G. R. Esche, T. J. Beck and J. B. McKinlay (2008). Lean mass and not fat mass is associated with male

proximal femur strength. J Bone Miner Res **23**(2): 189-98.

Uchida, E., Y. Ohsumi and Y. Anraku (1985). Purification and properties of H+-translocating, Mg2+-adenosine triphosphatase from vacuolar membranes of Saccharomyces cerevisiae. J Biol Chem **260**(2): 1090-5.

Wagermaier, W., H. S. Gupta, A. Gourrier, M. Burghammer, P. Roschger and P. Fratzl (2006). Spiral twisting of fiber orientation inside bone lamellae. Biointerphases **1**(1): 1.

Wagner, C. A., K. E. Finberg, S. Breton, V. Marshansky, D. Brown and J. P. Geibel (2004). Renal vacuolar H+-ATPase. Physiol Rev **84**(4): 1263-314.

Wang, Y., D. J. Cipriano and M. Forgac (2007). Arrangement of subunits in the proteolipid ring of the V-ATPase. J Biol Chem **282**(47): 34058-65.

Wang, Y., T. Inoue and M. Forgac (2005). Subunit a of the yeast V-ATPase participates in binding of bafilomycin. J Biol Chem **280**(49): 40481-8.

Vanhoenacker, F. M., W. Balemans, G. J. Tan, F. G. Dikkers, A. M. De Schepper, D. G. Mathysen, A. Bernaerts and W. V. Hul (2003). Van Buchem disease: lifetime evolution of radioclinical features. Skeletal Radiol **32**(12): 708-18.

Vasilyeva, E., Q. Liu, K. J. MacLeod, J. D. Baleja and M. Forgac (2000). Cysteine scanning mutagenesis of the noncatalytic nucleotide binding site of the yeast V-ATPase. J Biol Chem **275**(1): 255-60.

Vedi, S., J. R. Tighe and J. E. Compston (1984). Measurement of total resorption surface in iliac crest trabecular bone in man. Metab Bone Dis Relat Res **5**(6): 275-80.

Weinstein, R. S., A. M. Parfitt, R. Marcus, M. Greenwald, G. Crans and D. B. Muchmore (2003). Effects of raloxifene, hormone replacement therapy, and placebo on bone turnover in postmenopausal women. Osteoporos Int **14**(10): 814-22.

Weinstein, R. S., P. K. Roberson and S. C. Manolagas (2009). Giant osteoclast formation and long-term oral bisphosphonate therapy. N Engl J Med **360**(1): 53-62.

Veis, A. and A. Perry (1967). The phosphoprotein of the dentin matrix. Biochemistry **6**(8): 2409-16.

Wergedal, J. E., K. Veskovic, M. Hellan, C. Nyght, W. Balemans, C. Libanati, F. M. Vanhoenacker, J. Tan, D. J. Baylink and W. Van Hul (2003). Patients with Van Buchem disease, an osteosclerotic genetic disease, have elevated bone formation markers, higher bone density, and greater derived polar moment of inertia than normal. J Clin Endocrinol Metab **88**(12): 5778-83.

Whyteside, G., P. J. Meek, S. K. Ball, N. Dixon, M. E. Finbow, T. P. Kee, J. B. Findlay and M. A. Harrison (2005). Concanamycin and indolyl pentadieneamide inhibitors of the vacuolar H+-ATPase bind with high affinity to the purified proteolipid subunit of the membrane domain. Biochemistry **44**(45): 15024-31.

Villa, A., M. M. Guerrini, B. Cassani, A. Pangrazio and C. Sobacchi (2009). Infantile malignant, autosomal recessive osteopetrosis: the rich and the poor. Calcif Tissue Int **84**(1): 1-12.

Williamson, W. R., D. Wang, A. S. Haberman and P. R. Hiesinger (2010). A dual function of V0-ATPase a1 provides an endolysosomal degradation mechanism in Drosophila melanogaster photoreceptors. J Cell Biol **189**(5): 885-99.

Visentin, L., R. A. Dodds, M. Valente, P. Misiano, J. N. Bradbeer, S. Oneta, X. Liang, M. Gowen and C. Farina (2000). A selective inhibitor of the osteoclastic V-H(+)-ATPase prevents bone loss in both thyroparathyroidectomized and ovariectomized rats. J Clin Invest **106**(2): 309-18.

Wittich, A., C. A. Mautalen, M. B. Oliveri, A. Bagur, F. Somoza and E. Rotemberg (1998). Professional football (soccer) players have a markedly greater skeletal mineral content, density and size than age- and BMI-matched controls. Calcif Tissue Int **63**(2): 112-7.

Voss, M., O. Vitavska, B. Walz, H. Wieczorek and O. Baumann (2007). Stimulus-induced phosphorylation of vacuolar H(+)-ATPase by protein kinase A. J Biol Chem **282**(46): 33735-42.

Väänänen, H. K., N. D. Carter and S. J. Dodgson (1991). Immunocytochemical localization of mitochondrial carbonic anhydrase in rat tissues. J Histochem Cytochem **39**(4): 451-9.

Väänänen, H. K., E. K. Karhukorpi, K. Sundquist, B. Wallmark, I. Roininen, T. Hentunen, J. Tuukkanen and P. Lakkakorpi (1990). Evidence for the presence of a proton pump of the vacuolar H(+)-ATPase type in the ruffled borders of osteoclasts. J Cell Biol **111**(3): 1305-11.

Väänänen, H. K., D. C. Morris and H. C. Anderson (1983). Calcification of cartilage matrix in chondrocyte cultures derived from rachitic rat growth plate cartilage. Metab Bone Dis Relat Res **5**(2): 87-92.

Väänänen, H. K. and E. K. Parvinen (1983). High active isoenzyme of carbonic anhydrase in rat calvaria osteoclasts. Immunohistochemical study. Histochemistry **78**(4): 481-5.

Xie, X. S., D. Padron, X. Liao, J. Wang, M. G. Roth and J. K. De Brabander (2004). Salicylihalamide A inhibits the V0 sector of the V-ATPase through a mechanism distinct from bafilomycin A1. J Biol Chem **279**(19): 19755-63.

Xu, T. and M. Forgac (2001). Microtubules are involved in glucose-dependent dissociation of the yeast vacuolar [H+]-ATPase in vivo. J Biol Chem **276**(27): 24855-61.

Yamaguchi, T. (2008). The calcium-sensing receptor in bone. J Bone Miner Metab **26**(4): 301-11.

Yokoyama, K., M. Nakano, H. Imamura, M. Yoshida and M. Tamakoshi (2003). Rotation of the proteolipid ring in the V-ATPase. J Biol Chem **278**(27): 24255-8.

Youm, T., K. J. Koval, F. J. Kummer and J. D. Zuckerman (1999). Do all hip fractures result from a fall? Am J Orthop (Belle Mead NJ) **28**(3): 190-4.

Young, A., M. Stokes and M. Crowe (1984). Size and strength of the quadriceps muscles of old and young women. Eur J Clin Invest **14**(4): 282-7.

Young, A., M. Stokes and M. Crowe (1985). The size and strength of the quadriceps muscles of old and young men. Clin Physiol **5**(2): 145-54.

Zanchetta, J. R., C. E. Bogado, C. Cisari, S. Aslanidis, H. Greisen, J. Fox and W. Lems (2010). Treatment of postmenopausal women with osteoporosis with PTH(1-84) for 36 months: treatment extension study. Curr Med Res Opin **26**(11): 2627-33.

Zanchetta, J. R., C. E. Bogado, J. L. Ferretti, O. Wang, M. G. Wilson, M. Sato, G. A. Gaich, G. P. Dalsky and S. L. Myers (2003). Effects of teriparatide [recombinant human parathyroid hormone (1-34)] on cortical bone in postmenopausal women with osteoporosis. J Bone Miner Res **18**(3): 539-43.